building 4.0 crc

PROJECT #24: NEXT GENERATION OF ROBUST AND FIRE-RESILIENT LIGHT GAUGE STEEL SYSTEMS FOR MID-RISE BUILDINGS

SUB-PROJECT 2: FIRE RESISTANCE OF LIGHT GAUGE STEEL (LGS) FLOOR SYSTEMS

FINAL REPORT

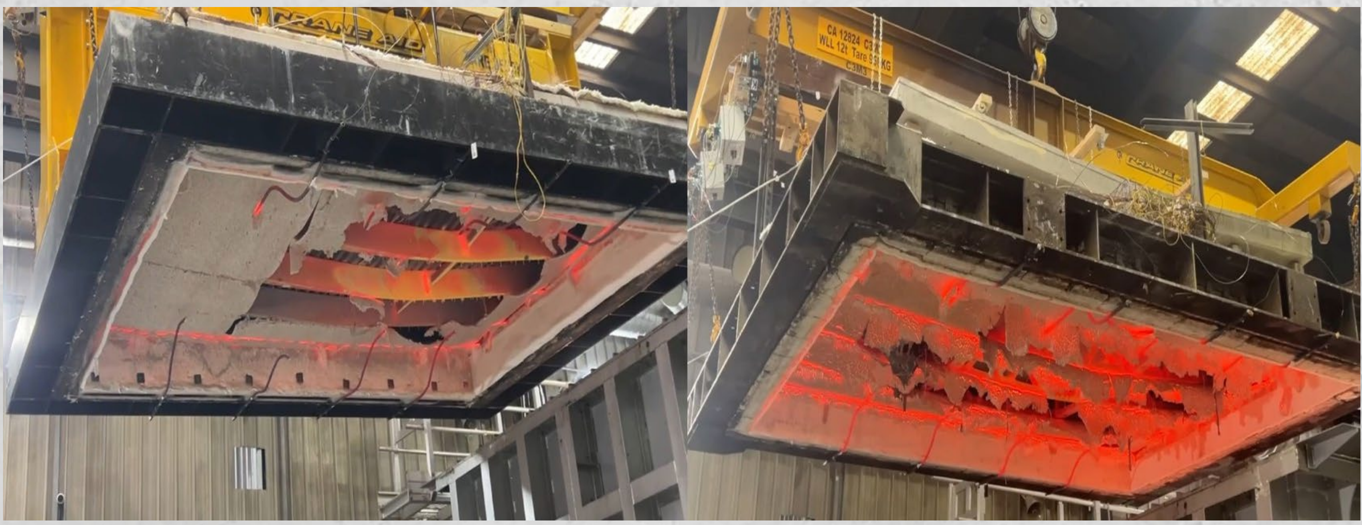

BlueScope
NASH NATIONAL ASSOCIATION OF STEEL-FRAMED HOUSING INC.
QUT
THE UNIVERSITY OF MELBOURNE

Australian Government
Department of Industry, Science and Resources
Cooperative Research Centres Program

CONTENTS

LIST OF TABLES

LIST OF FIGURES

CONFIDENTIAL:	☐ Yes X No
Author/s of this report:	Mahen Mahendran, Anthony Ariyanayagam, Gihan Ranasinghe, Fatheen Hisham, Son Tung Vy
Date of this report:	31/08/2025
Project completion date:	31/07/2025
Program Leader reviewer:	Mahen Mahendran
Project title:	**Project #24: Next Generation of Robust and Fire-resilient Light Gauge Steel Systems for Mid-Rise Buildings** **Sub-project 2 – Fire resistance of light gauge steel (LGS) framed floor systems**
Project duration:	3 years
Partners:	• BlueScope • NASH National Association of Steel Framed Housing • Queensland University of Technology
Project team members:	• Queensland University of Technology: Mahen Mahendran, Anthony Ariyanayagam, Fatheen Hisham, Gihan Ranasinghe, Son Tung Vy
Ethics approval details (if relevant)	Not applicable
Acknowledgements:	We thank the significant contributions in the form of technical advice, supply of test materials, assembly of full-scale test specimens and deliveries to testing laboratories provided by the following: Ken Watson (NASH), Dr Ian Bennetts and Mike Kelly from NASH, Trevor Clayton, Brett Taylor and Ian Thow from BlueScope Steel, Dr Thanuja Ranawaka, Alex Glivinskiy & Dr Hari Magarabooshanam from Scottsdale Construction Systems, Peter Blythe from Dynamic Frame, Ashley Baxter from Bendigo Building Products, Adrian Brown from ICCONS, Ashika Sharma from Fielders, Randall West from Apex Steel, Ben Wright from Siniat and Susie Jaber from James Hardie Building Systems, Dr Imran Ahamed from Halliwel and Dr Yomal Dias from GHD.

1 EXECUTIVE SUMMARY

The use of Light gauge steel wall and floor systems is a modern Cold-Formed Steel (CFS) construction technology with significantly increased adoption in both low- and mid-rise buildings due to their high strength-to-weight ratio, durability, non-combustibility, prefabrication and construction advantages. The conventional light gauge steel (LGS) framed floor systems comprise a single row of thin (<3.0 mm), high strength (450-550MPa) CFS lipped channel section joists or C-section or top hat trusses connected to flooring made of timber boards or fibre cement boards, protected by one or two layers of fire-rated gypsum plasterboard on the ceiling side with or without cavity insulation. However, fire can rapidly deteriorate the strength and stiffness of light steel members when gypsum plasterboard ceiling is compromised during a fire event, which can lead to a catastrophic failure. Suitable ceiling, flooring, and insulation configurations are needed to keep the temperature rise in both the joist/truss and the unexposed flooring side within accepted safe limits during fires, and thus delay structural, integrity and insulation failures and provide the required Fire Resistance Levels (FRL) of floors, e.g. 120/120/120 min for office buildings. However, there have been very limited studies on the behaviour and design of high strength LGS floor systems under ambient and fire conditions specially in an Australian context. Fire design of LGS floors is critical, however, currently the FRLs are based on limited fire test data obtained for LGS floors made of low strength steels and proprietary boards and/or expert opinions. This is inadequate considering the many potential applications of LGS floor systems in mid-rise buildings. The critical problem in LGS floors is the board fall-off from the ceiling, which affects the FRL significantly.

To address these specific industry problems and research gaps, two extensive experimental and numerical studies were conducted on the performance of LGS joist and truss floor systems under ambient and fire conditions to enhance the current knowledge and understanding of these floor systems. Each study consisted of material property tests at ambient and elevated temperatures, ambient temperature and standard fire tests (short-span and full-scale), and advanced heat transfer and structural finite-element (FE) modelling to obtain practical insights and accurate FRLs of LGS floor systems.

Further, robustness of LGS buildings in fire also needs to be assessed when non-fire rated floor/roof systems are used with fire-rated load-bearing wall systems or when unprotected combustible electrical sockets and service pipes are used within wall systems. In this case (third study), fire tests of small-scale wall assemblies and numerical studies were conducted to investigate the effects of using non-fire rated floor/roof to wall connections and combustible electrical sockets and service pipes on the fire behaviour and FRLs of load-bearing LGS walls.

Key findings from each study are summarised next.

LGS floor systems made of CFS lipped channel joists

This study examined the fire behaviour of high strength lipped channel joist floors sheathed with fibre cement board flooring and fire rated gypsum plasterboard ceiling.

- *Material property tests:* Two common non-combustible fibre cement board floor panels were tested for ambient and elevated temperature thermal properties. James Hardie Secura fibre cement board was chosen based on its overall superior properties (higher specific heat, lower thermal conductivity, less mass loss). Tensile tests on C20024 joists formed the baseline steel mechanical properties for the numerical analysis under ambient and fire conditions.

- *Short-span floor tests:* One ambient temperature load test and six standard fire tests were performed on 1.67 m span floors made of two joists with varying ceiling configurations (two or three layers of 13 mm or 16 mm fire rated gypsum plasterboard). All the tests utilised a non-combustible fibre cement board flooring. The FRLs of five typical configurations showed that short-span results were in good agreement with limited full-scale test data in the literature, confirming that short-span fire test setup can be used cost-effectively to determine the FRLs. According to this study, adding gypsum plasterboard layers significantly increased the FRL: for example, 2×13 mm gypsum boards gave 60 min, while 3×16 mm gypsum boards gave 120 min. Plasterboard joints were critical as it impacted the FRLs. Temperature measurements indicated that the cold (top) flange temperature governed the joist failure. Cavity insulation had minor effect on the FRL for a given ceiling configuration.

- *FE modelling of short-span floor systems*: Structural FE models (initially unsheathed single joists, then with sheathing) accurately captured ambient and fire behaviour. Innovative heat transfer models that included plasterboard fall-off and cavity convection were developed and validated with fire test results, which reliably predicted temperature rise, and together with sequentially coupled structural models predicted reliable FRLs. These models showed that the selection of flooring material (plywood versus fibre cement) had negligible impact on FRL.

- *Full-scale floor tests*: Two ambient temperature and three standard fire tests were conducted on full-scale floor assemblies not previously tested, ie. channel joist and truss floor systems with varying ceiling and floor configurations. Full-scale fire tests showed similar trends observed in short-span fire tests, where adding a third 16 mm gypsum plasterboard to a two-layer system increased the FRL by ~66%, and substituting a steel-concrete composite deck for the standard fibre cement floor improved the FRL by ~32%. Comparison with Australian plasterboard manufacturers' manuals showed that some of the FRLs included were unconservative, underscoring the need for updated results. Short-span fire tests gave slightly conservative FRLs compared to full-scale fire tests for the same ceiling configurations. Detailed measurements of plasterboard fall-off were recorded to support the development of numerical models.

- *FE modelling of full-scale floor systems*: Numerical models were developed for the tested full-scale ambient temperature and fire tests and verified. Incorporating flooring board into the structural models, captured the composite action between the joist and flooring. Heat transfer and sequentially coupled models developed were able to predict the fire behaviour and failure times (FRLs). The developed models offer a robust tool for comprehensive parametric investigations, to establish the FRL data for LGS floor systems, eliminating the need for extensive full-scale fire testing.

- *Fall-off behaviour of gypsum plasterboards*: Six full-scale fire tests in this study plus analysis of 50 previously conducted fire tests were considered to investigate the plasterboard fall-off behaviour. In cavity insulated assemblies, plasterboard fell-off quickly, but the failure was delayed due to the heat being blocked by cavity insulation. Assemblies without cavity insulation structurally failed soon after fall-off. Average times from fall-off to failure were established for insulated versus uninsulated assemblies. Four empirical methods for predicting the plasterboard fall-off were evaluated, and a suitable method was recommended for researchers, while a simpler method was suggested for designers. These methods provide suitable formulae to estimate the FRL for given ceiling plasterboard configurations.

- *Parametric numerical studies*: Using the verified heat transfer and structural models, FRLs were determined for 378 combinations of 18 joist sections and three ceiling configurations (2×13 mm, 2×16 mm, 3×16 mm gypsum plasterboards). Analysis of the results showed that the load ratio (applied load during fire/ambient temperature capacity) increased, the failure time decreased. In contrast, joist section type had minimal effect on FRL. Substituting plywood for fibre cement boards did not significantly change the FRLs with a maximum difference of 4 min. Noggings, point versus distributed loads, and using resilient ceiling channels made negligible difference under the same load ratio. Resilient channels spaced similarly to joists provided minimal additional failure time, while reducing channel spacing improved the FRL.

LGS floor systems made of CFS Trusses

The second study focused on short-span and full-scale floor systems made of CFS top hat and C-section minor axis trusses.

- *Material property tests:* Mechanical property tests at room and elevated temperature showed that fibre cement board flooring and gypsum plasterboards lose stiffness and strength above ~200 °C, transitioning to brittle failure. Notably, gypsum paper liners are essential to board strength under fire conditions.

- *Ambient temperature structural tests:* Eight short-span (two trusses with 1.67 m span) truss floors were tested under ambient conditions. Investigated variables included support conditions, truss geometry, and connections. Results showed that adding nylon spacers and extra screws at web-to-chord connections significantly increased the strength by reducing eccentricity. Increasing the number of web members delayed local buckling, but overall capacity was governed more by section thickness and connection type than diagonal web member layout. The Direct Strength Method (DSM) design calculations tended to overestimate the truss capacity unless the combined effect of bending and axial compression loads in web members was explicitly included in the design calculations.

- *FE modelling of short-span floor systems*: Advanced structural FE models were developed, including geometric imperfections, nonlinear material behaviour, and sheathing (floor and ceiling boards). These sheathed truss models accurately captured the load–deflection behaviour and failure modes observed in the tests. A parametric study using the validated model provided further design insight and underscored the need for the use of such detailed models in practice.

- *Short-span fire tests*: Three fire tests were carried out on 1.67 m span trusses made of two top-hat or minor axis C-sections with two or three layers of 16 mm fire rated plasterboard ceilings and fibre-cement flooring. Results showed that a two-layer ceiling achieved an FRL of 90/90/90 min (structural/insulation/integrity), while adding a third board raised the FRL to 120/120/120 min. Cavity insulation caused plasterboard to fall-off slightly earlier by trapping heat, but also slowed heating of the truss hence FRL was similar with or without cavity insulation. Importantly, these short-span tests produced conservative but comparable failure times and FRLs when compared to full-scale truss test results.

- *Full-scale fire tests*: Two 4.1 m length truss floor assemblies with six trusses spaced at 600 mm were tested under standard fire conditions (0.4 load ratio). Configurations included two versus three 16 mm plasterboard layers, with cavity insulation. Again, two 16 mm thick plasterboard ceiling provided 90 min FRL and three 16 mm boards gave 120 min FRL, consistent with the short-span fire tests. Adding the third layer extended FRL by ~45%. In all cases, plasterboard fall-off was the governing event: once the gypsum plasterboard ceiling fell-off, critical chord temperatures were reached quickly, leading to truss failure.

- *FE modelling of short-span and full-scale floor systems*: Heat-transfer FE models incorporating plasterboard fall-off, joint fall-off and cavity convection and sequentially coupled structural models closely matched the measured temperature and deflection profiles and truss failure times (FRLs). Structural models of full-scale trusses (with and without blocking) confirmed that blocking trusses had little effect on capacity. Code-based truss capacity checks (AS/NZS 4600) were found to be conservative for ambient temperature conditions and reasonably accurate in fire. This shows the effectiveness of using verified numerical models and design approach to obtain reliable FRLs of LGS truss floors while reducing the need for full-scale fire testing.

- Parametric numerical studies: Using the verified heat transfer and structural models, FRLs were determined for 504 combinations of truss floor systems with varying geometry, plasterboard thickness and number of gypsum plasterboard layers, cavity insulation, and flooring material. This expanded FRL database identifies critical factors and provides design recommendations (e.g. emphasising ceiling protection and connection detailing) for fire-resistant LGS truss floors.

Effects of unprotected combustible electrical sockets and service pipes, and non-fire rated floor/roof to wall connections

The third study investigated the effects of using non-fire rated floor/roof to wall connections and combustible electrical sockets and service pipes on the behaviour and FRLs of load-bearing LGS walls.

- Unprotected combustible electrical sockets*:* Fire behaviour of LGS walls with unprotected combustible electrical sockets was assessed using two fire tests. The fire test results showed that combustible electrical sockets and service openings allowed hot gasses to penetrate the wall cavities, but mostly led to localised higher temperatures on plasterboard and stud surfaces near the service openings. Their effects on the insulation and structural adequacy based FRLs of LGS walls were determined. However, such reductions were shown to be small due to localised detrimental effects around the service opening.

- Combustible service pipes: Fire behaviour of LGS walls with service pipe openings was investigated using two fire tests. The fire test results revealed that service openings caused large differences in the temperatures of wall studs and plasterboards, with localised high temperatures only in the regions (including studs) near the service pipe opening. Although the integrity and insulation criteria based FRLs were not satisfied or inadequate, their structural adequacy-based FRLs were estimated as reasonable.

- Non-fire rated floor/roof-to-wall cleat connections: Fire behaviour of LGS walls with non-fire rated floor/roof-to-wall cleat connections was investigated using one fire test and thermal and sequentially coupled structural FE analyses. Although the results showed that it led to localised high temperatures on stud hot and cold flanges near the floor-to-wall connections depending on the cleat thickness, the FRLs of LGS walls with connections using 1.0 mm or 1.9 mm thick cleats were nearly the same as for walls without such connections. The FRLs of cavity insulated LGS walls with non-fire rated floor-to-wall cleat connections can still be reasonable (not less than about 60 min).

- Non-fire rated floor/roof-to-wall connections using steel bearers and cleats: Fire behaviour of LGS walls with these connections was investigated using one fire test and thermal and sequentially coupled structural FE analyses. The results showed that it led to considerable localised high temperatures on the flanges of top stud segment when cleats were located near the studs. However, their effects on the FRLs of the walls were insignificant with the reduction to the FRL being less than 17% and were negligible in many cases.

Main Findings and Design Recommendations

Overall, the first two studies deepen the knowledge and understanding of the behaviour of LGS floor and wall systems under ambient and fire conditions, and suggest practical design guidance. Similarly, the third study has provided new knowledge and understanding of the fire resistance of load-bearing LGS wall systems when they (1) are attached to floor/roof systems using non-fire rated cleat or bearer and cleat connections or (2) inadvertently include unprotected combustible electrical sockets or service pipes. Main findings and recommendations are given next.

- Ceiling protection is paramount. Using multiple layers of fire-rated gypsum plasterboard in the ceiling is the most effective way to meet FRL requirements. For example, two layers of 16 mm gypsum plasterboard board typically achieve about 90 min FRL, while adding a third raises it to ~120 min.

- Plasterboard fall-off governs failure. The time when the ceiling fall-off is critical. After fall-off, unprotected steel joists/trusses heat up rapidly. Insulation in the cavity mainly delays floor failure in insulated cases. Empirical formulae developed in this study allow prediction of fall-off time (and hence FRL) based on ceiling configuration.

- Type of joist/truss or flooring material (plywood or fibre cement board) has negligible impact on FRLs. This implies that the FRL is independent of the type of joist and conventional flooring material for a given ceiling configuration.

- Short-span fire tests are an effective way of determining the FRLs as the test results were comparable (though slightly conservative) to full-scale tests. Thus, it is recommended that short-span fire tests can be utilised to obtain the FRLs of LGS floor systems.

- Advanced FE models of LGS floor systems were validated against test results. This study developed heat-transfer and structural FE models under ambient and fire conditions (including imperfections and plasterboard fall-off behaviour). Verified models enabled large-scale parametric studies. By using these tools, engineers can predict the FRLs of new floor configurations with confidence, reducing reliance on testing. For design, it is recommended that analysis includes the thermo-mechanical degradation of LGS floor components and plasterboard fall-off mechanism.

- CFS design standards such as AS/NZS 4600 provide conservative capacity and FRL predictions for LGS floor systems.

- Plasterboard manufacturer-provided FRLs do not consider the critical parameters identified in this study, such as the load ratio, truss configuration, depth variations, flooring types, and cavity insulation. Furthermore, manufacturer recommendations for two and three layers of 16 mm plasterboard were significantly more conservative compared to the study's findings with respect to joist/truss spacing (450 mm to 600 mm) and FRLs (60 min to 90 min).

- Effects of unprotected combustible electrical sockets and service pipes and non-fire rated floor/roof-to-wall connections were shown to be mainly localised high temperatures in the regions near where they were located. In general, they were shown to have minimal impact on the FRLs of load-bearing LGS walls, demonstrating the robustness of LGS construction. However, reassessment of their FRLs and the need for protecting them are recommended.

- Overall, the findings from this study not only enable fire safety designers to optimise LGS floor system designs but also contribute to the National Construction Code (NCC), particularly Part 1, Section C. The comprehensive findings and recommendations of FRLs provided by this research can now be effectively employed to ensure compliance and enhance structural safety across various building classes employing LGS floor systems. Our previous research conducted on the fire behaviour of LGS wall systems was reviewed and the essential FRL data and design methods have also been summarised. They will all be utilised by our industry partners, National Association of Steel Framed Housing (NASH) and BlueScope Steel, in preparing and publishing the proposed Fire Design Handbook for use by fire design engineers of LGS buildings. Our advanced fire research studies have enabled efficient utilisation of light steel floor systems in mid-rise buildings.

2 PROJECT OVERVIEW

2.1 Introduction

LGS framed floor systems made of channel joists and trusses have become increasingly popular in modern buildings due to their strength, lightweight, durability, appealing appearance, and cost-effectiveness. However, these thin-walled lightweight structural steel systems have a significant drawback as they lose strength and stiffness when exposed to fire. One critical safety issue is the fall-off of gypsum plasterboard ceiling during a fire. This puts building occupants at risk and can lead to the collapse of the building, causing extensive building damage and loss of lives.

To prevent these dangerous situations, it is crucial to design LGS joist and truss floors that can resist fire effectively. However, the current knowledge and understanding of how these LGS floor systems behave during fires is limited, especially for floor configurations commonly used in Australia, such as those using fibre cement boards for flooring and gypsum plasterboards for ceiling. Most previous fire tests are either outdated, conducted in other countries, or did not cover these specific Australian floor configurations. The existing studies also mainly tested small specimens without simulating actual load conditions, making their results less reliable for real-life situations.

Since conducting full-scale fire tests is costly and time-consuming, researchers have turned to numerical simulations to predict how LGS floor and wall systems behave in fires. However, most such simulations oversimplify them by not considering the interaction between the joists/truss and the flooring. Additionally, accurately simulating how heat affects these floors and predicting when plasterboards will fall-off have been challenging tasks. So far, no reliable method has been developed to predict this plasterboard fall-off accurately.

To improve the safety and reliability of LGS floors in fire, it is necessary to develop better numerical models that include how gypsum plasterboards behave under heat and when exactly they fall-off. Previous methods used to predict plasterboard fall-off are outdated and overly conservative, meaning they predict failures earlier than they actually occur. This approach results in designs that are safe but overly expensive and inefficient. Furthermore, these methods do not account for the difference in insulation and how thicker plasterboards, while more protective, can fall-off sooner due to their increased weight. Current Australian standards do not fully address all possible failure modes of LGS floors under fire conditions, such as specific types of buckling (local and distortional buckling). There is also a lack of clear guidelines even under ambient conditions for certain LGS truss floor types and configurations used in Australia.

Given these gaps, comprehensive research is urgently needed to better understand and improve the fire performance of Australian LGS joist and truss floor systems. Factors such as the type and spacing of channel joists or trusses, the number and thickness of plasterboard layers, insulation, and screw positions of ceiling can influence the fire resistance levels. More detailed full-scale experimental studies and accurate numerical simulations, supported by short-span fire tests, will help identify how each factor affects the overall fire safety of LGS joist and truss floor systems.

Further, robustness of LGS buildings in fire also need to be assessed when non-fire rated floor/roof systems are used with fire-rated load-bearing wall systems or when unprotected combustible electrical sockets and service pipes are used within wall systems, for which detailed experimental and numerical studies are needed. Ultimately, the findings from this research will provide clearer guidelines for safely designing and building LGS floor and wall systems, ensuring they protect occupants and buildings during fires effectively.

2.2 Research Aims

This research project includes three studies. The aim of the first two studies is to investigate how LGS channel joist and truss floor systems behave thermally and structurally during ambient and fire conditions. Through detailed experimental and numerical studies, they will focus on understanding (1) why gypsum plasterboards, which protect these steel floors, fall-off when exposed to fire and identify the key factors affecting this process (2) how flooring, insulation and ceiling materials and steel joists and trusses lose their strength and stiffness in fire (3) the heat transfer across the floor when exposed to increasing fire intensity with time and (4) the structural behaviour of light steel joists and trusses in fire. The overall goal is to reliably understand and predict how these LGS channel joist and truss floor systems behave under ambient and fire conditions and establish their fire resistance levels (FRLs).

Using the findings from the first two studies, recommendations for design guidelines are provided to enhance the safety of LGS floor systems. Additionally, practical criteria to accurately predict the timing of plasterboard fall-off are introduced, which will support numerical modelling and help in designing safer LGS floor configurations. The research has developed a comprehensive database of fire resistance data specifically tailored for floor configurations commonly used in Australia. To successfully achieve the aim, a series of experimental and numerical studies was conducted.

Experimental studies included the following tasks, and were followed by developing a suitable criterion for plasterboard fall-off using the test data from this study and past literature.

- Mechanical and thermal property tests of flooring and ceiling materials
- Short span and full-scale ambient temperature tests to determine the failure loads/capacities.
- Short-span fire tests and full-scale standard fire tests to investigate the FRL of different LGS joist and truss floor configurations (two layers of 13 mm, two layers of 16 mm and three layers of 16 mm fire-rated gypsum plasterboard (Pb); with and without cavity insulation).
- Develop correlations between short-span and full-scale fire tests and importantly evaluate the use of short-span fire tests.

Numerical studies included the following tasks.

- Develop heat transfer and structural FE models for ambient temperature and fire tests and validate them using test results.
- Use validated heat transfer models in a parametric study to obtain the time-temperature profiles for different LGS joist and truss floor configurations, and structural models to obtain ambient temperature capacities and FRLs versus Load ratio curves.
- Investigate how plasterboard fall-off criterion can be used in modelling and fire design.
- Review the existing fire design rules for LGS floors and propose improved fire design rules for the FRLs of different LGS channel joist and truss floor configurations.

The aim of the third study is to investigate the behaviour and FRL of load-bearing LGS wall systems in fire when non-fire rated floor/roof systems are used with these wall systems or when unprotected combustible electrical sockets and service pipes are used within these wall systems. The results will allow the assessment of the robustness of LGS buildings in fire. To achieve this aim, a series of experimental and numerical studies was conducted. These studies included the following tasks:

- Small-scale fire tests of non-load bearing LGS walls with non-fire rated floor/roof to wall connections (steel cleats or bearers and cleats) or when unprotected combustible electrical sockets and service pipes to investigate their effects on the heat transfer behaviour and FRLs of LGS walls.
- Develop heat transfer FE models and validate them using test results, and extend them to simulate full-scale wall conditions and conduct a parametric study.
- Develop sequentially coupled structural FE models, validate them against available full-scale test results, conduct a parametric study and assess the effects on the structural behaviour and FRLs of LGS walls.
- Assess the robustness of LGS walls and make recommendations in relation to the use of non-fire rated floor/roof to wall connections and unprotected combustible electrical sockets and service pipes and the need for any protection.

3 LITERATURE REVIEW

3.1 Introduction

This chapter provides a summary of the previous research findings and existing knowledge regarding LGS floor systems. It outlines LGS floor system components and materials, testing methods, thermal and mechanical properties, previous experimental and numerical studies on LGS floor systems (full- and small-scale) and current design provisions, finally research gaps. The intent of this chapter is to synthesise existing findings of LGS floor-ceiling assemblies comprising both LGS joist and truss systems, highlight the research gaps, and outline research problems.

3.2 Components and Materials in LGS Floor Systems

LGS floors commonly use cold-formed steel (CFS) members (e.g. lipped channel joists or trusses) with flooring (plywood or fibre-cement) and gypsum plasterboard ceiling. CFS and hot-rolled steel (HRS) differ by fabrication route, with CFS increasingly used for lightweight, efficient structures. Trusses are typically fabricated using lipped channel or top-hat sections with chords and web members connected by rivets or bolts with screws (Figure 1).

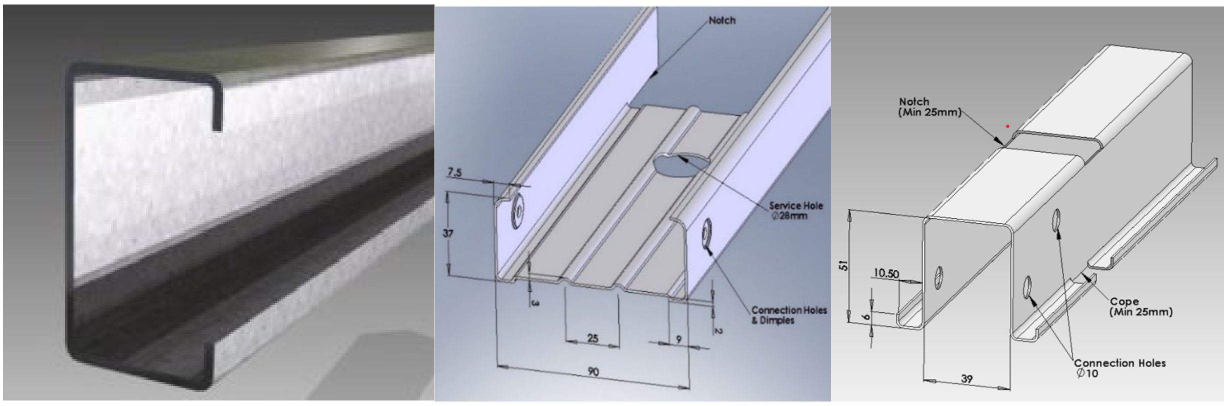

(a) *(b)* *(c)*

Figure 1. (a) Lipped channel joist section (b) Lipped channel (c) Top hat section used in trusses (Scottsdale Construction Systems)

Gypsum plasterboard (drywall) is the most common ceiling lining for LGS floors due to its excellent fire protection characteristics and ready availability. A standard gypsum board consists of a core of gypsum (calcium sulfate dihydrate, $CaSO_4{\cdot}2H_2O$) sandwiched between paper liners. Boards used in fire-rated assemblies typically have additives like glass fibres, vermiculite, or perlite to improve their fire performance. These additives reduce thermal conductivity and help the board retain integrity at high temperatures – for instance, glass fibres hold the calcined gypsum together after the paper facing burns off, delaying crack formation. Gypsum boards generally have a density of 600–850 kg/m³ and thickness of 10–16 mm in floor/ceiling applications. Crucially, about 20% of the weight of gypsum drywall is chemically bound water within the gypsum crystal structure. When exposed to fire, this water is heated to ~100–150°C and then undergoes an endothermic reaction to evaporate (gypsum calcination), absorbing a large amount of heat in the process. Thus, plasterboard linings act as a thermal barrier: they delay heat penetration through the floor-ceiling system until the gypsum is fully dehydrated, and the board eventually loses strength. The low thermal conductivity of the gypsum core further keeps the unexposed side relatively cool during a fire. Because of these properties, a fire-rated plasterboard ceiling significantly increases the fire resistance of LGS floors compared to an unprotected or combustible ceiling finish. Studies by Sultan et al. (1998) at NRC Canada showed that using two layers of Type X gypsum boards can dramatically increase the fire endurance of steel-joist floors compared to a single layer. In one series of tests, doubling the ceiling boards (from one 12.7 mm layer to two) increased the time to failure by about 73%. Conversely, early plasterboard fall-off – when ceiling boards detach and fall during a fire – exposes the steel joists/trusses and usually marks the beginning of rapid temperature rise in the assembly. Plasterboard fall-off tends to occur sooner in horizontal floor assemblies than in walls due to gravity, once their fixity is lost. Sultan (2015) found that floor (horizontal) assemblies experienced gypsum board fall-off at much lower temperatures than wall assemblies of similar construction, meaning floor joists are exposed to flames earlier. To mitigate this, proper screw fastening patterns and resilient channels are used to support the ceiling boards. Closer screw spacing and keeping fasteners away from board edges have been shown to delay fall-off and improve fire resistance. For example, placing screws 38 mm from board edges instead of 10 mm improved the time to fall-off (and hence fire resistance) by 50% in one study. Overall, the integrity of the plasterboard ceiling and its attachment is critical for maintaining the protection of the steel floor joists/trusses in fire.

LGS floors are typically constructed with either timber-based or cement-based floorboards. Traditionally, structural plywood or oriented strand board (OSB) sheets are used as the floor over joists/trusses due to their strength and stiffness under ambient conditions. However, wood-based panels are combustible and contribute fuel in a fire. Research indicates that plywood ignites and decomposes at relatively low temperatures (around 230 °C), which can compromise the fire performance of the floor system. During fire tests on insulated floor assemblies, the presence of a plywood deck led to high temperatures (exceeding 230 °C) at the flooring layer and vigorous burning once ignition occurred. In fact, adding a second layer of plasterboard in a plywood floor was found to raise the plywood's temperature (by trapping heat), accelerating its burning rate. For these reasons, non-combustible fiber cement sheets are often recommended as an alternative flooring material in fire-rated LGS floor systems. Fiber cement boards have much better fire endurance as they possess higher specific heat and do not ignite, resulting in lower heat release and mass loss than plywood. A study by Steau and Mahendran (2021b) showed that substituting plywood with fibre cement board in LGS floor assemblies markedly improved fire performance, and the authors advise using fiber cement boards in lieu of plywood for enhanced fire safety. In practice, many LGS joist/truss floor manufacturers prefer fiber cement floor panels because they are non-combustible, moisture resistant, and dimensionally stable under heat. Overall, the choice of flooring can influence the fire outcome: timber-based sheathing may lead to earlier fire involvement of the floor, whereas non-combustible boards like fibre cement board help preserve the structural floor until steel failure.

Glass fibre *Rock wool fibre* *Cellulose fibre*

Figure 2. Commonly used insulation materials in LGS floors

Thermal/acoustic insulation is often installed in the floor cavity between joists/trusses to improve energy efficiency and sound insulation. Common insulation types in LGS floors include glass fibre batts, rockwool (stone wool), and cellulose fibre (recycled paper) insulation. They all have good thermal resistance under ambient conditions, but their behavior in fire can vary. Glass and mineral wool insulations are non-combustible and can withstand high temperatures, whereas cellulose (being organic) will char or burn if exposed, although it is usually treated with fire retardants. The net effect of cavity insulation on floor fire performance is somewhat complex and has been a topic of research. On one hand, insulation in the cavity slows the heat transfer upward: it keeps the floor's upper layers cooler and can delay the heating of the steel joists' top flange. For example, Ye et al. (2017) observed that adding rockwool insulation between floor joists helped delay the temperature rise in the steel joists, thereby improving the assembly's fire resistance in some tests. On the other hand, insulation also means heat is trapped near the ceiling, causing the gypsum board to heat up faster from the fire side. This can lead to earlier failure of the ceiling (insulation and integrity criteria) even if the steel joists are somewhat protected. Baleshan and Mahendran (2016) found that inserting cavity insulation in short-span floors reduced the fire resistance since the insulated floors underwent larger deflections due to thermal bowing. Similarly, these fire tests showed that a filled cavity raises the gypsum board and bottom flange temperatures, contributing to early plasterboard fall-off and hence quicker loss of protection for the joists. The type of insulation can also influence the final outcomes: Sultan (2015) reported that in wood truss floors, cellulose insulation gave better fire resistance than glass fibre or rockwool, improving the fire endurance by 28–43%. Overall, while insulation is critical for thermal efficiency, its inclusion in LGS floors for fire resistance must be considered carefully. It can either enhance the fire resistance by delaying steel joist heating or degrade it by causing faster plasterboard failure, depending on the floor assembly. Figure 2 shows the commonly used insulation materials in LGS floor systems.

3.3 Fire Resistance Testing and Standards

In Australia, the fire performance of floor systems is evaluated in terms of Fire Resistance Level (FRL), defined by the *National Construction Code (NCC,* 2022) under three criteria: structural adequacy, integrity, and insulation. Structural adequacy is the ability to carry load without collapse for a specified time, integrity is preventing flames/hot gases from passing through, and insulation is limiting temperature rise on the unexposed face. For floors separating occupancies or fire compartments, the NCC mandates minimum FRL ratings (in min) for each criterion depending on building class. Standard fire tests are conducted in accordance with AS 1530.4 (2014) or similar standards to determine these ratings. In a full-scale floor furnace test, a specimen (typically about 4 m by 3 m) is exposed from below to the standard fire curve (ISO 834/AS1530 time-temperature curve) under a constant load until a failure criterion is met. The time at which the floor can no longer support the load is taken as failure time in structural adequacy; the time when cracks/openings allow flames is integrity failure time; and the time when the top surface temperature rise exceeds 140°C (average) or 180°C (peak) above ambient temperature is insulation failure time. These times determine the FRL designation (e.g. 60/60/60 means 60 min each for structural/integrity/insulation).

Full-scale floor fire tests are expensive and complex, so only limited experiments are reported in literature relative to walls. Hence small-scale testing and numerical analysis are often used to predict their fire performance. AS 1530.4 (2018) allows some scaling, but generally a full-size assembly is needed to determine FRL. In research studies, alternative orientations have been attempted: for example, some floor assemblies were tested “vertically” in a wall furnace to simulate the fire exposure with load applied horizontally. Jatheeshan (2015) and Baleshan (2012) used this approach in their studies of LGS floors. However, differences like plasterboard fall-off behaviour between horizontal and vertical orientations must be considered when interpreting such results.

The Australian standard AS/NZS 4600 (2018) provides design rules for CFS structures at ambient temperature, and includes some guidance for fire design. However, its elevated-temperature design provisions currently cover traditional floor assemblies with CFS lipped channel joists and LGS wall panels, but not for truss floor systems. The design of CFS truss floors (with top-hat or minor-axis C-sections) under fire is not directly addressed in the current CFS standards and thus typically requires either full-scale fire testing or advanced analysis to demonstrate compliance. Building design manuals such as the AISI Truss Design Guide (2012) provides methods for ambient design of CFS trusses, but their applicability to fire conditions remains unverified.

3.4 Thermal and Mechanical Properties of LGS Floor Components at Elevated Temperatures

Accurate knowledge of material properties at elevated temperatures is essential for predicting LGS floor behaviour in fire. The key thermal properties are thermal conductivity, specific heat (heat capacity), and thermal diffusivity of each component, which govern heat transfer through the floor assembly. Despite broad coverage of flooring and ceiling materials, the thermal properties of fibre-cement board used in Australian context are yet to be determined and are addressed in this project. These data allow more accurate thermal simulation of floor assemblies under fire exposure.

The mechanical properties of CFS degrade significantly as temperature rises. Experiments on high-strength CFS (grades G550, G450, etc.) by Ranawaka and Mahendran (2009) and Kankanamge and Mahendran (2011) quantified the reduction in yield stress, tensile strength, and Young's modulus at elevated temperatures. For example, thin G550 steel loses a large fraction of its strength by 500°C and essentially has no structural capacity above ~600°C. Based on these tests, predictive equations for strength reduction factors were formulated. Rokilan and Mahendran (2020) later confirmed those yield strength and stiffness reduction formulae and proposed new correlations for ultimate strength and proportional limit reductions. These correlations are in line with Eurocode 3 and other international standards, which also provide reduction factors for steel. In design, a critical failure temperature for steel joists is often defined (commonly around 500–600°C for CFS), beyond which the steel joists can no longer sustain loads – this often governs the structural failure time in fire.

For gypsum plasterboard, mechanical properties at high temperature are equally important, especially to predict when the boards will crack or fall-off. Plasterboard retains little strength once it has fully dehydrated (typically above 300°C in the core). While some studies have measured plasterboard strength at ambient temperature (Dodangoda et al., 2019, Abeysiriwardena & Mahendran, 2022), there is a lack of data for its high-temperature mechanical properties in Australia. Generally, it has been found that once the gypsum is calcinated and paper layer is burnt out, the board loses integrity. Similarly, fibre cement board properties in fire have not been investigated; these boards are expected to retain strength longer than plywood, but their exact thermal-mechanical behaviour (e.g. strength retention, cracking point) needs further investigation and this project has investigated the thermo-mechanical properties of gypsum plasterboard and fibre cement boards. Overall, reliable numerical modelling and design of LGS floors in fire requires incorporating these temperature-dependent properties for all the floor components: steel channel joists/trusses, plasterboard, insulation, and ceiling and flooring boards.

3.5 Experimental Studies of LGS Floor Systems under Fire Conditions

3.5.1 Full-scale fire tests

Compared to walls, relatively few full-scale fire tests on LGS floor assemblies have been reported. One of the most extensive series was by Sultan (2008); Sultan et al. (1998) at NRC Canada, who tested 19 floor assemblies with CFS joists (203 mm deep) under standard fire. The floors measured roughly 4.8 m by 4 m, supported a design live load, and were finished with different ceiling and flooring configurations, which are not used in Australian context. More recently, Ye et al. (2017) carried out full-scale fire tests on five LGS floor assemblies (4.8 m × 3.6 m each) to study various parameters. The assemblies used seven CFS joists (255 mm deep, 1.5 mm thick) spaced at 600 mm, with unlipped channel section tracks at the ends and blocking between joists for bridging. The floors had a composite concrete slab on steel deck as the subfloor. For the ceiling, some tests used two layers of 12 mm fire-rated gypsum board, while others used a combination of gypsum and magnesium oxide board layers. One test included rockwool cavity insulation to examine its impact. They found that floor assemblies generally achieved lower fire resistance times than comparable wall assemblies, primarily due to earlier plasterboard fall-off in the floors. Even with the same load ratio and ceiling setup, the horizontal orientation meant gravity caused the ceiling boards to fall-off sooner, exposing the joists. Also insulated specimen demonstrated that adding rockwool can delay the heating of steel joists (since the insulation kept the joist's cold flange cooler for longer), thereby improving structural adequacy time. Indeed, placing insulation between joists tends to keep the compression (top) flange cool, which can mitigate thermal bowing and extend time to structural failure. However, if the insulation causes the ceiling to fail first, that benefit may be offset. Overall, full-scale fire tests confirm that maintaining ceiling integrity (preventing board fall-off) and managing thermal gradients in the joists (to reduce bowing) are essential to achieving higher FRL in LGS floors.

Another notable series of tests was conducted in Australia by Baleshan (2012) and Jatheeshan and Mahendran (2015). They tested a number of LGS floor assemblies using standard fire exposure, but in a vertical furnace configuration. The specimens were smaller (about 2.4 m x 2.1 m) and were loaded horizontally during the fire to simulate floor bending. In these tests, both the flooring and ceiling were lined with plasterboard (i.e. gypsum on both sides of the cavity) to avoid the use of combustible plywood. Rock-fibre insulation was used in some cases. The findings were that a double-layer plasterboard floor (uninsulated) had a higher FRL than a similar floor with a single-layer ceiling – consistent with other studies that more gypsum boards delay failure. However, when cavity insulation was added to a floor with double plasterboards, the FRL surprisingly dropped compared to the uninsulated case. This was attributed to excessive deflections from thermal bowing: the insulation kept the top cooler, exacerbating the differential expansion between top and bottom of the joists, which led to earlier structural failure (even though the insulation criterion itself wasn't compromised yet). This result underscores that insulation can be critical depending on whether structural deformation or heat penetration governs failure. These Australian tests also highlighted that using plasterboard as the flooring (instead of plywood) can eliminate the combustion issue, but it is not a practical flooring in real buildings – it was done only to isolate the effect of other parameters.

3.5.2 Short-span fire tests

Steau and Mahendran (2020a) conducted a series of short-span fire tests on floor specimens about 1.2 m square. Each specimen had two CFS joists (Grade G500, 200 mm deep lipped channels at 450 mm spacing) with a 16 mm fire-rated plasterboard ceiling and plywood flooring on top. The specimens were subjected to the standard ISO 834 fire curve in a small furnace (1.0×1.0 m opening) from below, without any applied load, evaluating only thermal and insulation performance. Two configurations were compared: one had the exposed plasterboard directly as the ceiling, and the other had an additional thin steel sheathing layer beneath the plasterboard as extra protection. Since no load was applied, both ultimately failed by the insulation criterion (excessive temperature rise on the unexposed side) rather than structural collapse. Their research suggested that for insulation performance, the key factor is the overall assembly configuration (number of ceiling boards, insulation presence, etc.) rather than the exact joist shape.

Short-span fire tests are useful to observe qualitative effects and to calibrate thermal models. Interestingly, comparisons of small-scale versus full-scale tests on LGS walls conducted by Magarabooshanam (2020) have shown that temperature profiles are comparable, though failure times may differ if load is applied. However, the current literature has no evidence of load-bearing short-span fire tests on joists and trusses, indicating a research gap addressed by this project.

3.6 Numerical Modelling of LGS Floor Systems

Given the cost and complexity of fire tests, numerical modelling is used to study most of the untested specimens in fire. A typical modelling approach is to conduct a thermal analysis of the floor assembly under the standard fire exposure to predict the temperature–time profiles in each component and then use them in a structural analysis to simulate deflection, stress, and failure over time. Such models must account for heat transfer through conduction, convection, and radiation in the cavity, and the degradation of material properties with temperature as discussed earlier. One challenge in modelling LGS floors is capturing plasterboard fall-off, since the sudden loss of the ceiling board greatly accelerates heating of the joists. This aspect has been meticulously addressed in this project.

Prior studies have focused on ambient-temperature modelling of LGS floor systems, providing a foundation for extending to fire scenarios. Kyvelou et al. (2018) modelled composite action between steel joists and wood-based flooring and introduced initial geometric imperfections (0.1t and 0.3t for local and distortional buckling modes, where t is steel thickness) in the finite element models of LGS floors. Several researchers have simulated CFS trusses under ambient conditions (Dizdar et al., 2019; Güldür et al., 2021; Tian et al., 2015; Tian et al., 2019), but they mainly considered trusses without flooring. A few have included floor sheathing in the models (de Seixas Leal & de Miranda Batista, 2020; Güldür et al., 2021; Tian et al., 2019), but even they did not consider top-hat chord trusses or cases with fibre cement board flooring. No published numerical models address the fire performance of LGS floor truss systems, which is an identified gap. Hence, this project developed finite element models for CFS truss floor–ceiling systems under fire and validated against test data.

For conventional LGS floors with channel joists, some numerical studies exist for fire conditions. Sultan et al. (2008) have modelled joist floors to study the effect of insulation and screw spacing on plasterboard fall-off. Steau and Mahendran (2020b) developed detailed finite element simulations of non-load bearing LGS floors, incorporating the thermal properties and degradation of materials.

These models can reasonably predict the time-temperature profiles of joists and deflections, though capturing the plasterboard joint and pieces fall-off remains unaddressed. Generally, a sequentially coupled thermal-structural analysis is performed: first, a heat transfer analysis provides the temperature distribution in all members over time; next, those temperatures are applied to a structural model where the steel's stiffness and strength are reduced accordingly, and load is applied to see when collapse occurs. The critical failure criterion is usually when the joist or truss can no longer support the load (structural adequacy). In a model, this might manifest as excessive mid-span deflection or a sudden drop in applied load at a certain time-step. Researchers often calibrate their model by comparing the predicted steel temperatures and deflection-time curve with fire test results.

Overall numerical modelling is a powerful tool to extrapolate beyond the limited fire tests. However, careful validation is needed. Important considerations for modelling LGS floor systems in fire include: the consideration of plasterboard fall-off (time or temperature threshold), inclusion of realistic imperfections and connections, accurate mechanical and thermal properties (especially for insulation, gypsum board and CFS), and the criteria for structural failure. The literature shows that while modelling techniques for CFS structures at ambient temperature are well established, their extension to fire scenarios for complex systems like trusses is still evolving. The lack of prior models for LGS truss floor systems in fire is a current research gap that this project aims to address.

3.7 Design Considerations and Research Gaps

Current CFS design standards provide only limited guidance for LGS floor assemblies in fire. The Australian CFS design standard AS/NZS 4600:2018 includes some prescriptive methods for designing traditional joist floors in fire, but these are largely based on standard configurations (e.g. joists with specific cross-sections and protection). For systems like CFS truss floors with different section profiles (top-hat chords, etc.), engineers must rely on proof testing or advanced analysis since the equations in the Standard have not been validated for these cases. The AISI Truss Design Guide (2012) and similar manuals help in ambient temperature design of CFS trusses (providing equations for axial capacities of chord and web members, for example), but studies have shown that directly applying those to newer truss configurations can be unreliable. Lim (2025) found that using the Direct Strength Method (DSM) formulae and assuming pure axial members and pinned joints did not accurately predict the ultimate capacity of tested CFS trusses, underscoring the need for refined design methods or calibration for truss floors. Moreover, the presence of flooring and eccentric screw-fastened connections in floor trusses complicates the design calculations; these factors are not fully accounted for in simple design equations.

From the literature review, several gaps and needs are evident. First, while extensive research exists on CFS wall systems in fire, there have been far fewer studies on CFS floor systems, especially those incorporating modern trusses. The behaviour of LGS truss floor–ceiling assemblies in fire has not been previously investigated, either experimentally or numerically. This means there is no published data on how such systems behave, what their typical failure modes and FRLs are, or how parameters like chord size, panel type, or connections affect their performance in fire. Consequently, designers of these systems must extrapolate from conventional joist floor data or run full-scale fire tests for each new configuration, which is not economical.

Another gap is in material property data: although some thermal property data have been proposed for relevant materials (CFS, plasterboard, insulation), there is a lack of high-temperature mechanical properties for components like plasterboard and fibre-cement flooring. Knowing when and how these materials lose strength or fail would greatly improve modelling accuracy and design confidence.

The complex interplay of cavity insulation and multiple layers on fire performance also calls for more research. Prior studies have shown conflicting outcomes (insulation sometimes beneficial, sometimes detrimental) depending on the configuration. No studies so far have investigated the effect of insulation in truss floors. This project addressed the aforementioned research problems.

Finally, robustness of LGS buildings also need to be assessed when non-fire rated floor/roof systems are used with fire-rated wall systems or when combustible electric sockets & service pipes are used within wall systems as they may significantly impact the load-bearing capacity and FRLs of walls.

4 MECHANICAL AND THERMAL PROPERTIES OF SHEATHING MATERIALS

4.1 Introduction

The performance of LGS floor systems under fire conditions depends critically on the thermal and mechanical properties of their constituent materials, especially as temperature rises. Key thermal properties include the specific heat capacity (C_p), density (ρ), and thermal conductivity (λ) of materials, which together govern heat transfer in the assembly. Equally important are the mechanical properties of sheathing materials and how they deteriorate with elevated temperature. In a typical LGS floor, CFS trusses/joists provide structural support, gypsum plasterboard ceiling offers fire protection, and flooring (often timber or fibre-cement board) completes the assembly. Timber-based flooring is combustible and poses significant fire risk, so this research utilised non-combustible fibre cement flooring boards. Fibre cement boards had not been extensively fire-tested in LGS floor systems before, presenting an opportunity to investigate their performance.

To enable accurate modelling of an LGS floor in fire, the relevant material properties at ambient and elevated temperatures must be established. This research therefore conducted an experimental evaluation of both mechanical and thermal properties for the materials in the floor system. Firstly, a series of bending tests was performed to characterise the flexural (bending) properties – modulus of elasticity (MOE) and modulus of rupture (MOR) of the selected fibre cement board flooring and gypsum plasterboard ceiling at ambient and elevated temperatures. Next, thermal property tests were carried out on multiple fibre cement board products to measure their temperature-dependent thermal properties (C_p, ρ, λ). Based on these results, the most suitable fibre cement board was chosen for use in the LGS floor, and its thermal property data were prepared for input into finite element fire models. The following sections outline the test procedures and key findings.

4.2 Mechanical Properties of Fibre Cement Board and Gypsum Plasterboard at Ambient and Elevated Temperatures

The bending strength and stiffness of the floor and ceiling boards were evaluated through flexural tests at various temperatures. In these tests, rectangular simply supported specimens were subjected to three-point bending until failure, both at ambient conditions and after heating to elevated set-point temperatures in a furnace. Figure 3 shows the three-point bending test arrangement inside an electric furnace, which was used for both fibre cement floor panels and gypsum plasterboard ceiling specimens. The aim was to determine the MOR (equivalent to bending strength) and MOE values for each material as temperature increases, since these properties are needed to numerically simulate deflection and failure of the LGS floor-ceiling systems in fire.

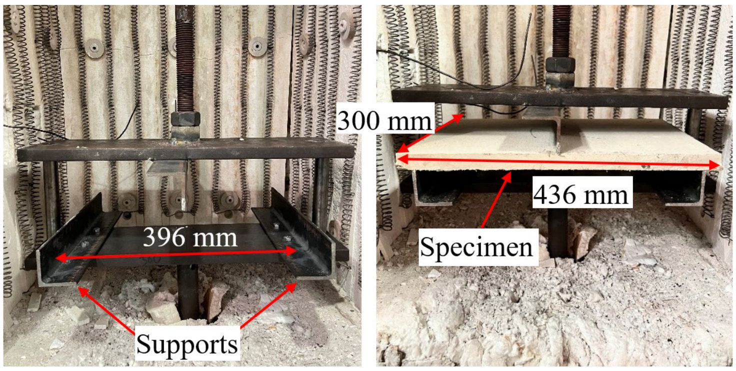

Figure 3. Three-point bending test set-up

4.2.1 Fibre cement board

For the flooring, fibre cement boards were tested in bending at ambient and elevated temperatures based on the standard for fibre cement sheet products, AS/NZS 2908.2 (2020). The tested boards (James Hardie Scyon™ Secura™ 22 mm thick internal flooring) are classified as Type B (for internal use) and Category 2, meaning they are required to have a minimum bending strength (MOR) of 7 MPa. The electric furnace allowed heating the specimens to target temperatures while the supports and loading ram connected to a 10 kN hydraulic actuator extended into the heating chamber. Load was applied under displacement control such that failure occurred within 10–30 s at ambient temperature. At elevated temperatures, a slower loading rate was used to capture post-yield behaviour, since the expected failure loads were lower due to thermal degradation. Thermocouples on the top and bottom surfaces of each sample monitored the specimen temperature.

The bending tests for fibre cement board were conducted at a range of temperatures: 23 °C (ambient), 100 °C, 200 °C, 300 °C, 400 °C, 500 °C, 700 °C, 800 °C, and 900 °C. An initial thermal analysis indicated that holding a specimen at the target temperature for about 20 min was sufficient to achieve a uniform through-thickness temperature (i.e. the core reached the target) before loading. Thus, for each test, the furnace was pre-heated to the desired temperature, the specimen was soaked at that temperature (~20 min) to ensure thermal steady-state, and then the bending load was applied until failure. The resulting load–deflection data were used to compute the MOE and MOR of the board at that temperature. The MOE was calculated from the initial slope of the load–deflection curve (elastic range) using standard beam formulae (e.g. the equation derived by Ardanuy et al. (2015) for mid-span deflection of a simply supported beam). The MOR was determined from the maximum load at failure using the simple bending theory formula given in AS/NZS 2908.2.

Table 1. Average MOE and MOR of tested fibre cement boards

Test	Temperature (°C)	Average MOE (MPa)	COV (%)	Average MOR (MPa)	COV (%)
1	Ambient (23)	4400	9.40	12.45	6.85
2	100	3788	7.09	10.20	8.25
3	200	3491	14.35	6.50	15.37
4	300	1589	11.60	1.96	9.08
5	400	1457	12.70	1.84	11.14
6	500	1546	11.38	2.18	9.86
7	700	598	9.47	2.20	7.94
8	800	533	12.36	2.10	10.47
9	900	124	10.45	1.80	11.90

Table 1 presents the average measured MOE and MOR of the fibre cement board at each test temperature. At ambient conditions (23 °C), the fibre cement board showed an MOR of about 12.45 MPa and an MOE around 4400 MPa. This ambient bending strength exceeds the 7 MPa minimum requirement for its product category, indicating the material met the expected quality. As temperature increased, the fibre cement board's strength and stiffness progressively degraded. A slight increase in bending strength was observed at 100 °C (MOR rose marginally above its room-temperature value), which is attributed to the drying out of free/bound moisture in the fibre cement board that temporarily enhances its strength. Beyond 100 °C, however, mechanical properties deteriorated markedly. The MOR dropped rapidly between ambient and 300 °C, falling to roughly 2 MPa by 300 °C (only ~15% of its original strength). Interestingly, beyond about 300 °C, the MOR did not decrease much further with increasing temperature, remaining within 1.8–2.2 MPa up to 900 °C. In contrast, the stiffness (MOE) exhibited a more gradual initial decline: the MOE reduced to ~3500 MPa at 200 °C and then dropped sharply by 300 °C to ~1600 MPa, about one-third of ambient. Between 300 °C and 500 °C, the MOE plateaued (1500–1600 MPa range), but at higher temperatures a further dramatic loss of stiffness occurred with the MOE only a few hundred MPa by 700–800 °C, and at 900 °C it was only ~124 MPa, effectively indicating near-zero residual stiffness.

The fibre cement boards failed at ambient temperature in a relatively ductile manner with a clear flexural crack at mid-span (bottom face). At elevated temperatures, the behaviour transitioned to a brittle failure mode. After about 300–500 °C, the specimens showed signs of thermal damage such as hairline cracks and a discoloured, embrittled core upon failure. The usual single wide crack seen at ambient temperature was less obvious at high temperatures – cracks were smaller or difficult to detect visually beyond 500 °C, likely because the of the lost ductility and did not exhibit large crack openings. Instead, specimens tended to bend and fracture with shallow cracks and significant stiffness loss. The degradation of the fibre cement board's mechanical properties with temperature is mainly due to thermo-chemical processes in the material. These include the evaporation of physically bound water and dehydration of cement hydrates, build-up of pore pressure, and the decomposition of constituents like calcium-silicate-hydrate (C–S–H), calcium hydroxide, and any cellulose fibres in the board. By ~200–300 °C, much of the free moisture and some chemically bound water have been driven off, and any polymer or fibre components begin to char, causing a transition from a pseudo-ductile to a brittle behaviour. Continued heating to 500 °C and above leads to further decomposition of cementitious binders (e.g. conversion of $Ca(OH)_2$ and carbonates), leaving behind a more fragile, porous matrix. These factors collectively explain the substantial reductions in both MOR and MOE at high temperatures. Figure 4 illustrates the post-test condition of a specimen.

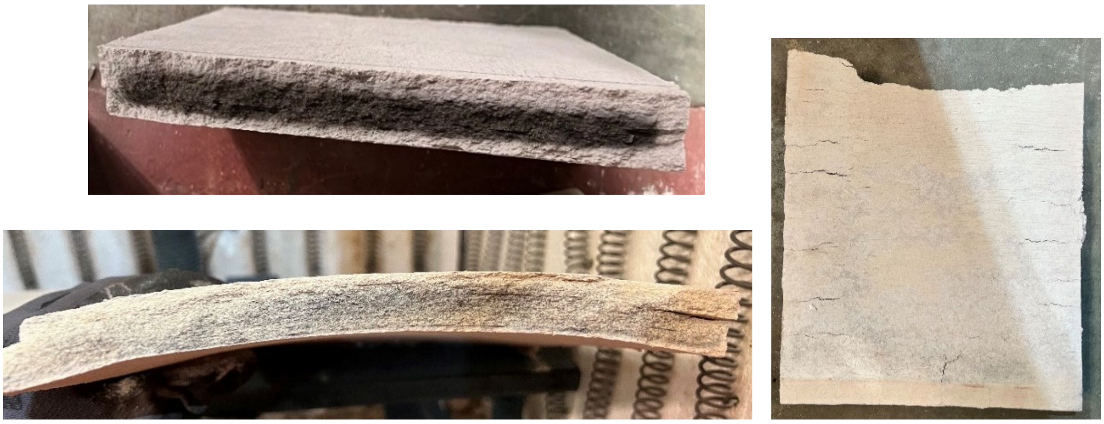

(a) (b)

Figure 4. a) Burnt cross-section and bent specimen at failure at elevated temperatures (b) thermal cracks on the surface.

4.2.2 Gypsum plasterboard

For the ceiling layer, gypsum plasterboards (Siniat FireShield plasterboard of 13 mm and 16 mm thicknesses) were tested under similar three-point bending conditions to determine their flexural strength and stiffness at ambient and elevated temperatures. Gypsum plasterboard is typically used in LGS floor-ceiling systems for its fire-protective properties, and the selected FireShield boards are rated to provide up to 240 min of fire resistance according to the manufacturer. The bending tests were conducted in accordance with AS/NZS 2588 (2017), which specifies quality requirements for gypsum plasterboard products. This standard ensures that boards have sufficient strength to resist cracking or breaking under their own weight during handling and service.

The experimental setup for plasterboards utilised the same furnace and loading apparatus as for the fibre cement board tests. Each plasterboard specimen (400 mm × 300 mm) was supported over a span of 356 mm (supports at that spacing per AS/NZS 2588) and loaded at mid-span until failure. Two specimens were tested at each temperature and average MOE and MOR were obtained. The tested temperatures for the plasterboard series were 23 °C (ambient), 50 °C, 100 °C, 150 °C, 200 °C, 250 °C, and 400 °C. Compared to the fibre cement boards, plasterboards were not tested beyond 400 °C because gypsum undergoes complete calcination and loses most of its strength by around that temperature under fire conditions. In preliminary tests, it was observed that above ~250 °C the protective paper facing on the plasterboard would char and could damage the furnace elements. Therefore, for tests above 200 °C, the paper lining was removed from some specimens to investigate the intrinsic strength of the calcined gypsum core without the paper reinforcement.

The test results showed that gypsum boards retain much of their strength up to a point, after which there is a precipitous decline due to gypsum dehydration (calcination) and loss of the paper's tensile reinforcement. At ambient temperature, the plasterboards exhibited bending strengths in line with expectations: for instance, the 16 mm board failed at an average load of about 380 N with the paper layer intact, exceeding the minimum 280 N (parallel to edge) specified by the standard. The presence of the paper significantly increased the load capacity in our ambient tests, a 16 mm specimen without the paper layer failed at only ~198 N, roughly half the load of an equivalent specimen with the paper layer (386 N). This highlights that the paper lining contributes substantially to the board's flexural strength under normal conditions, acting like a thin reinforcement on the tension face.

Interestingly, when the boards were heated to mild temperatures (around 50–100 °C), a slight increase in bending strength was observed, similar to the fibre cement boards. For example, at 50 °C the 16 mm board with paper showed a marginally higher failure load than at 23 °C. At 100 °C, the MOR of the 13 mm board also increased slightly above its ambient value. This increase is attributed to the drying of residual moisture in the gypsum – the evaporation of water within the board can lead to a temporary strengthening of the gypsum core, as the material becomes more rigid once free moisture is removed. However, this effect is temporary. Once temperatures exceed about 100 °C and especially after 150 °C, gypsum calcination begins, and the mechanical properties deteriorate rapidly. Calcination is the chemical dehydration of gypsum (calcium sulfate dihydrate) into hemihydrate and eventually anhydrous forms, which results in a loss of bonded water and the formation of a weaker, porous structure. Correspondingly, the MOR dropped significantly after 150 °C. By 250 °C, the bending strength of the 13 mm board was only a small fraction of its original value. At the highest test temperature of 400 °C, the MOR was nearly zero.

The stiffness (MOE) of gypsum plasterboard followed a similar degradation trend. Starting from an ambient MOE value in the order of 2500–3800 MPa (13 mm versus 16 mm boards), the boards showed a moderate drop in stiffness by 100 °C and then a very pronounced reduction beyond 200 °C. By 400 °C, the effective MOE had fallen to nearly zero, indicating an almost complete loss of rigidity. The loss of stiffness corresponds to the progressive breakdown of the gypsum's crystalline structure as water is driven off and micro-cracks form in the calcined core.

An important observation was the role of the paper facing at elevated temperatures. Up to about 150–200 °C, the paper remains intact and continues to provide reinforcing effect. At 200 °C, for example, a 16 mm specimen with the paper still attached sustained ~350 N before failure, whereas a similar specimen without paper failed at only ~93 N. This stark difference (~4× strength) at 200 °C underscores that the paper helps hold the calcining gypsum together, carrying tension even as the core weakens. However, beyond 200 °C the paper itself begins to char and lose strength. By around 250 °C, any paper present has mostly burnt, and the gypsum core, now largely dehydrated, is left without reinforcement. Consequently, plasterboard specimens without paper showed a dramatic drop in load capacity after 200 °C – for instance, the failure load for a 16 mm board without paper fell to ~88 N at 250–300 °C. Without the paper, the 16 mm board's strength at 250 °C was nearly the same as at 400 °C, indicating the core alone has very little strength. Figure 5 and Figure 6. illustrate the degradation of bending strength (MOR) and stiffness (MOE) with temperature for the gypsum plasterboards of thicknesses 13 mm and 16 mm, respectively. It is evident that beyond about 150 °C, both MOR and MOE decrease steeply, approaching zero bending strength by 400 °C. The 16 mm thick boards showed slightly higher strength and stiffness at ambient temperature (about 50% higher MOR and 20% higher MOE than 13 mm due to the increased thickness), but under fire conditions this advantage diminishes. By 300–400 °C, the residual strength and stiffness of both 13 mm and 16 mm boards were comparably low, as the dominant factors became the extent of gypsum calcination and absence of paper layer. In summary, the gypsum plasterboard maintains integrity up to moderate temperatures (helped by its paper facings and moisture content), but once the bound water is driven out and the paper chars, its mechanical properties rapidly reduce.

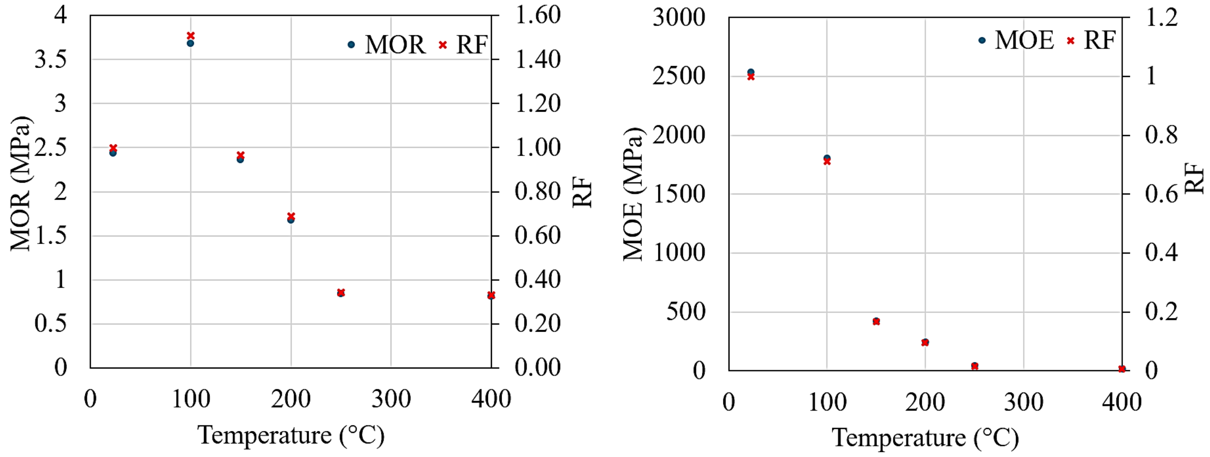

(a) (b)

Figure 5. (a) MOR and reduction factors (RF) (b) MOE and reduction factors (RF) of 13 mm plasterboards at elevated temperatures

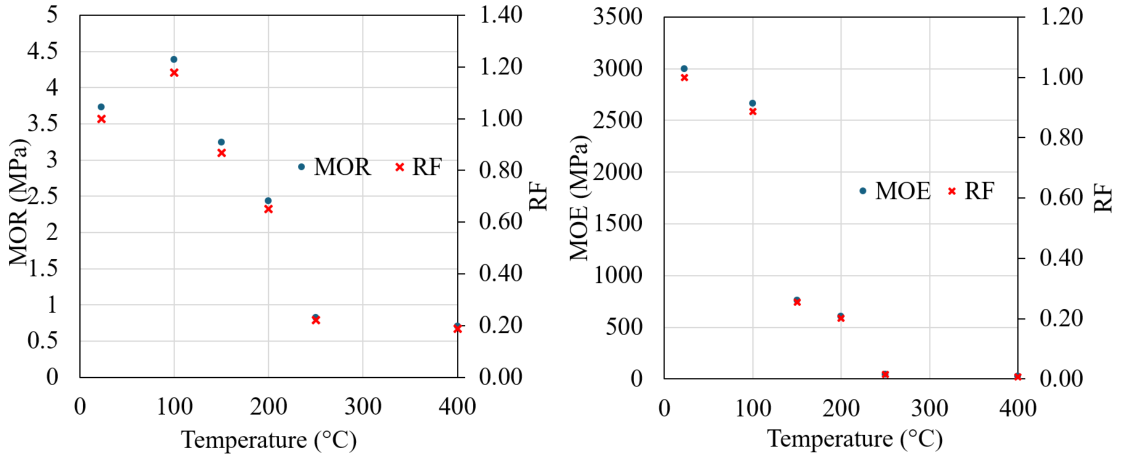

(a) (b)

Figure 6. (a) MOR and reduction factors (RF) (b) MOE and reduction factors (RF) of 16 mm plasterboards at elevated temperatures

4.3 Thermal Properties of Fibre Cement Board at Ambient and Elevated Temperatures

A comprehensive series of thermal property tests was undertaken to characterise the temperature-dependent thermal properties of various fibre cement boards. Since LGS floor performance in fire is highly sensitive to the thermal behaviour of the floor panel, it was necessary to obtain accurate thermal properties such as specific heat capacity, density, and thermal conductivity of the flooring boards at elevated temperatures. Four different fibre cement board products were evaluated: two types from Manufacturer A (James Hardie) and two from Manufacturer B (Cemintel), which included both standard and high-density variants. The aim was to compare their thermal responses and ultimately select the board with the most favourable properties for fire resistance.

Figure 7. Thermal Analysis Instruments (a) NETZSCH STA 449 F3 Jupiter (b) NETZSCH LFA 457 HyperFlash

To measure specific heat capacity (C_p) and mass loss (for computing density) as functions of temperature, simultaneous thermal analysis (STA) was employed. The STA apparatus (NETZSCH STA 449 F3 Jupiter, Figure 7) combines thermogravimetric analysis (TGA) and differential scanning calorimetry (DSC) on the same sample. Small powdered samples (~20 mg) of each fibre cement board were prepared for these tests. Each sample was placed in a tiny platinum crucible (with an inert alumina liner and a perforated lid) alongside an empty reference crucible. The STA furnace temperature was programmed from 25 to 1200 °C at 20 °C/min heating rate, with short isothermal holds at 25 °C and 1200 °C to stabilise readings. The tests were conducted in an inert nitrogen atmosphere (50 mL/min flow) to avoid combustion of the sample. During an STA run, the TGA component records the sample's weight change, while the DSC component measures the heat flow into the sample relative to the reference. Using the ASTM E1269-2018 procedure, the specific heat capacity $C_p(T)$ was determined from the DSC signal, with calibration to a known reference (a sapphire standard). In these tests, the raw ASTM E1269 calculation was further refined to account for the sample's mass loss as temperature increased, ensuring that the derived C_p reflected the actual material present at each temperature. The STA provided two key outputs for each board: a C_p–temperature curve and a mass–temperature curve (from which relative density at temperature can be inferred, since initial density is known).

In addition to STA, laser flash analysis (LFA) was used to measure the boards' thermal diffusivity (α) at elevated temperatures. Thermal diffusivity relates to how quickly a material conducts heat relative to how much heat it can store, and is linked to thermal conductivity by $\lambda = \alpha \cdot \rho \cdot C_p$. The LFA tests were performed on a NETZSCH LFA 467 HyperFlash apparatus. Small solid disk specimens (~10 mm diameter × 2 mm thick) were cut from each board and coated with a thin layer of graphite to ensure uniform heat absorption. In an LFA test, the specimen is subjected to a short laser pulse on its front face, and an infrared detector records the temperature rise on the back face over time. From this, the thermal diffusivity α(T) at the chosen test temperature was calculated. In our tests, specimens were tested at temperature intervals of 20 °C from 30 to 500 °C in a controlled nitrogen atmosphere. At each set-point temperature, the sample was equilibrated, then three laser shots were performed and averaged for accuracy. The result was a series of α values for each material across the 30–500 °C range. By combining the LFA results (α) with the STA results (C_p and mass/ρ), the thermal conductivity λ as a function of temperature was calculated for each board.

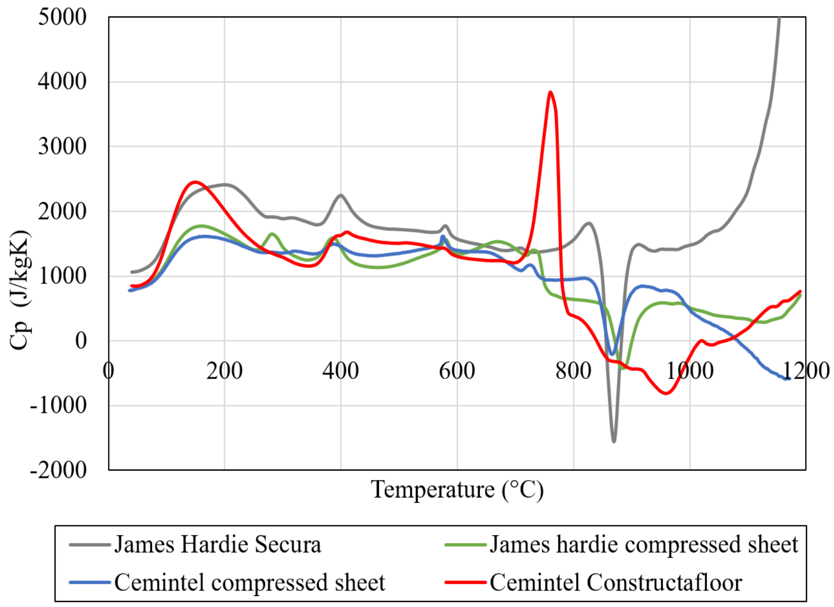

Figure 8. Variation of specific heat with temperature for the tested boards

After processing the experimental data, curves of specific heat (C_p), mass retention (or conversely, mass loss), thermal diffusivity, and derived thermal conductivity (λ) were obtained for each of the four fibre cement boards. These are the primary thermal properties that influence a board's fire performance. The comparative results revealed some key differences among the products, as shown in Figure 8. which plots the measured specific heat capacity versus temperature for all four boards (Boards 1 and 2 from Manufacturer A, Boards 3 and 4 from Manufacturer B). At ambient temperature (25 °C), the boards' specific heats were in the range of about 0.77–1.06 kJ/(kg·K). All boards exhibited an increase in C_p as temperature rose above room temperature, reaching a first peak in the 150–200 °C range. This peak corresponds to endothermic reactions such as the dehydroxylation of cementitious components and evaporation of bound water. Notably, different boards peaked at different temperatures: for example, Board 1 (James Hardie Scyon Secura) reached a C_p of ~2410 J/kg·K at around 200 °C, whereas Board 4 (Cemintel Constructafloor) peaked at ~2449 J/kg·K near 150 °C. Boards 2 and 3 had more modest peaks (around 1600–1770 J/kg·K) at roughly 160–166 °C. Following these initial peaks, the C_p of each board dropped off, and a significant specific heat reduction occurred in the high-temperature range around 800 °C for all boards. This drop is likely associated with major decomposition reactions completing (e.g. decomposition of carbonates or other fillers). Interestingly, after this dip, most boards showed a secondary rise in C_p at very high temperatures (>800–900 °C). For instance, Boards 1 to 3 exhibited a slight C_p increase after about 870 °C, whereas Board 4's specific heat continued to decrease until ~970 °C before increasing again. These high-temperature thermal phenomena reflect the complex makeup of the boards (each containing cement, fillers, fibres, etc., which contribute to heat capacity in different ways as they transform or degrade).

The mass loss curves (from TGA) complemented the C_p results. All boards gradually lost mass as temperature increased due to the loss of moisture and combustion of any combustible constituents. By 1200 °C, Boards 1–3 had each lost between 17 and 19% of their original mass, whereas Board 4 (Constructafloor) suffered a higher total mass loss of about 28%. Board 4 consistently showed the highest mass loss rate across the temperature range, indicating it had more volatile or decomposable content (possibly a higher fibre or binder content). The mass loss was most rapid between ~100 °C and 500 °C for all samples, which coincides with the dehydration of cement hydrates and burning of cellulose fibres if present. The increased mass loss of Board 4 suggests it may contain more organic material or a different formulation that makes it less stable at high temperatures.

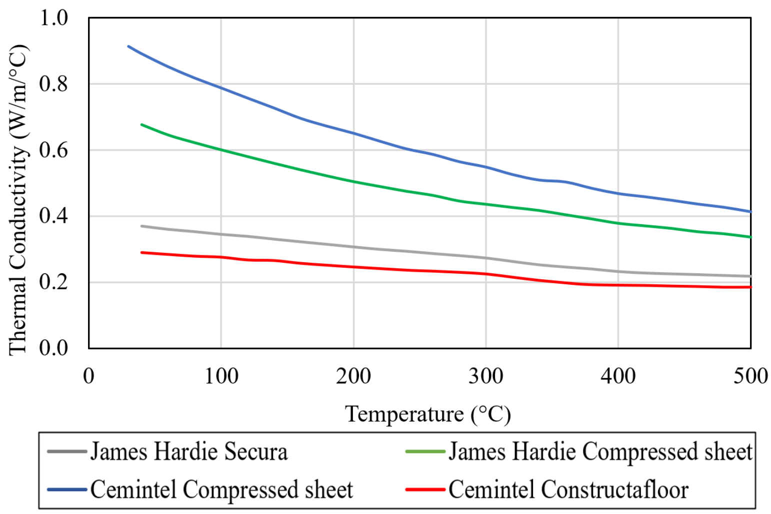

Figure 9. Variation of thermal conductivity with temperature for the tested boards.

The thermal conductivity (λ) was evaluated over the 30–500 °C range (beyond 500 °C, direct LFA measurements were not available, but trends can be extrapolated). At ambient temperature, the boards' thermal conductivities ranged from about 0.29 W/m·K (Board 4) to 0.91 W/m·K (Board 2). The two high-density compressed sheets (Board 2 and Board 3) exhibited the highest thermal conductivity among the group, which is expected because higher density generally means more solid material to conduct heat. In contrast, the lighter-weight boards (Board 1 Scyon and Board 4 Constructafloor) had lower initial conductivities (0.37 and 0.29 W/m·K, respectively). As temperature increased, all boards showed a decrease in thermal conductivity. This is a common behaviour as materials heat up – increased lattice vibrations can impede heat flow, and in these boards, the progressive loss of mass (creating porosity) also reduces their ability to conduct heat. By around

400–500 °C, the conductivities of all boards had declined substantially from their ambient values. Notably, the rank order remained: the compressed fibre cement boards retained higher λ values across temperatures (due to their higher ρ), whereas the lighter boards maintained lower λ. For example, even at elevated temperature, the compressed sheets (Boards 2 and 3) were less thermally insulative compared to Boards 1 and 4. Figure 9 illustrates the variation of thermal conductivity with temperature for the different boards tested. It can be seen that Board 4 (Constructafloor) and Board 1 (Scyon) have the lowest thermal conductivity curves, while Board 2 and Board 3 (both compressed sheets) have higher conductivity at all temperatures.

In summary, the ideal characteristics for a fire-resistant floor panel are high heat capacity, low thermal conductivity, and minimal mass loss at elevated temperatures, so that it can absorb a lot of heat, slow down heat transfer, and remain dimensionally stable (not weaken or shrink excessively). Among the boards tested, none excelled in every category, but James Hardie Scyon Secura (Board 1) emerged as the most balanced choice. It had one of the higher specific heat capacities (especially in the crucial 100–300 °C range), one of the lowest thermal conductivities, and only moderate mass loss (≈19%) up to 1200 °C. The Cemintel Constructafloor (Board 4) showed very low thermal conductivity and high specific heat as well, but its higher mass loss (28%) is a disadvantage for fire endurance. The compressed-sheet boards (Boards 2 and 3) were denser and thus had higher thermal conductivity (undesirable), despite having relatively low mass loss; their specific heat was also lower than that of Board 1 at many temperatures. Therefore, Scyon Secura (Board 1) was selected as the flooring material for the fire tests and subsequent finite element modelling. The comprehensive thermal property data obtained for this board – its $C_p(T)$, ρ(T), and λ(T) curves – will be used in the heat transfer analysis in the fire simulations. Combined with the ambient temperature mechanical properties of the steel and the known degradation relationships for steel strength at high temperatures, these thermal properties enable a robust predictive model for the LGS floor system's performance in fire. The experimental findings in this chapter thus provide a crucial foundation for understanding and improving the fire resistance of LGS floor assemblies.

5 EXPERIMENTAL STUDIES OF SHORT-SPAN LGS FLOOR SYSTEMS UNDER AMBIENT AND FIRE CONDITIONS

5.1 Lipped Channel Joist Floor Systems – Ambient Temperature

In Australia, typical LGS floor systems use CFS lipped channel joists, sheathed with plywood or fibre cement boards as flooring and one or more layers of fire-rated gypsum plasterboard as ceiling (Figure 10). To determine the ambient temperature capacity, which will later be used in short-span fire tests, a short-span floor specimen (1.67 m span) with two CFS channel joists (back-to-back) was tested under four-point bending (Figure 11). The joists had a depth of 203 mm with 76 mm flanges and 21 mm lips and were braced with steel end tracks and nogging cleats to simulate a typical floor frame. This test specimen failed when each hydraulic jack applied about 110.8 kN (total ~221 kN). As shown in Figure 12., the two channel joists ultimately failed by distortional buckling in their top (compression) flanges, the dominant failure mode at ambient temperature. No connection or sheathing failure was observed indicating that the floor's strength was governed by the joist capacity.

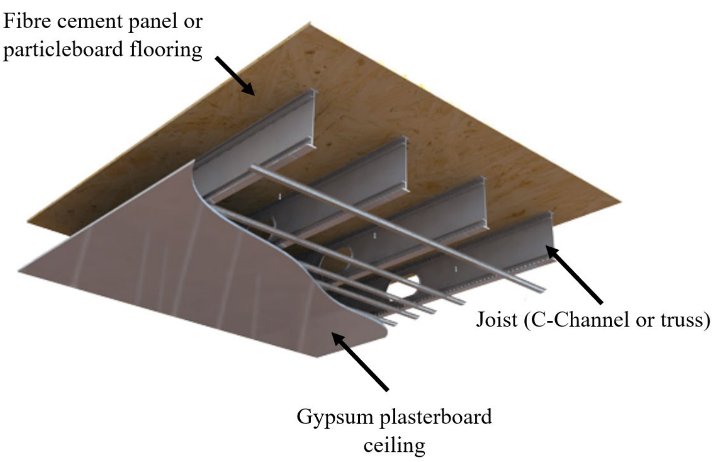

Figure 10. LGS floor systems commonly used in Australia.

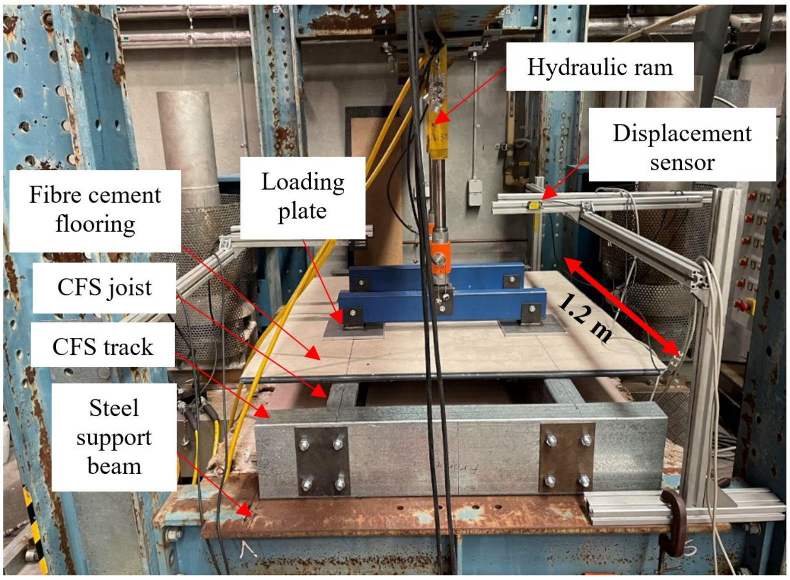

Figure 11. Ambient temperature test set-up

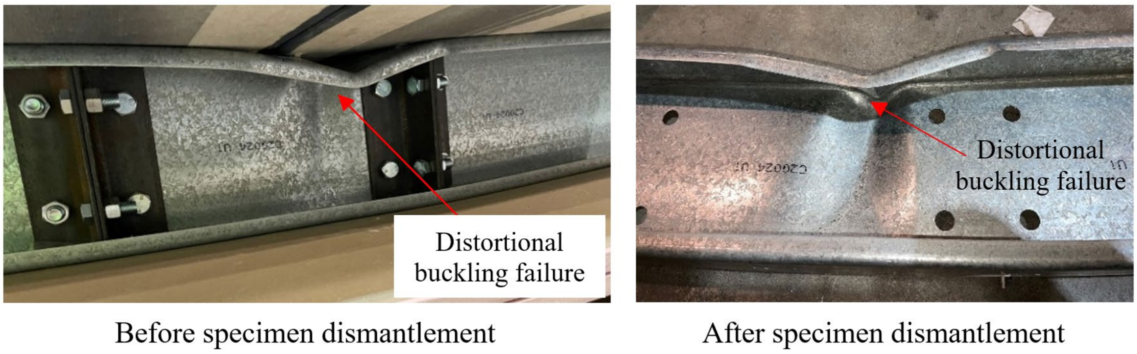

Figure 12. Failure of the CFS joists

5.2 Truss Floor Systems Made of Top Hat and C-sections – Ambient Temperature

Short-span LGS floors can also be constructed with trusses instead of lipped channel joists. Truss floor systems use top-hat or C-section CFS sections for chords and web members, offering a lightweight alternative to joists. Eight short-span truss floor-ceiling specimens (1.67 m length, 1200 mm square floor area) were tested to investigate their structural behaviour at ambient temperature. The trusses composed of high-strength G550 steel top-hat sections (60 mm-wide bottom flange, 39 mm-wide top flange, 51 mm web, six mm lips) in two thicknesses (0.75 mm and 0.95 mm). Key parameters studied included the truss web configuration (eight web members versus expanded ten web members), the end support conditions (simple versus idealised), and the web-to-chord connection details (standard bolted joints, use of nylon spacer sleeves, and addition of self-drilling Tek screws). In the initial truss tests (0.75 mm thick chords, eight-web configuration) with simple bolt connections, the floor truss exhibited early buckling of its slender web diagonals. The outer diagonal web members buckled locally at about half of the ultimate load (~6–7 kN per loading point), followed by buckling of the inner web members at around 10–12 kN, and the ultimate failure was reached when the top chord itself buckled at approximately 11–13 kN total load. This progressive failure sequence of web buckling leading to chord failure is characteristic of short-span trusses, where fewer web members carry higher forces and can fail early.

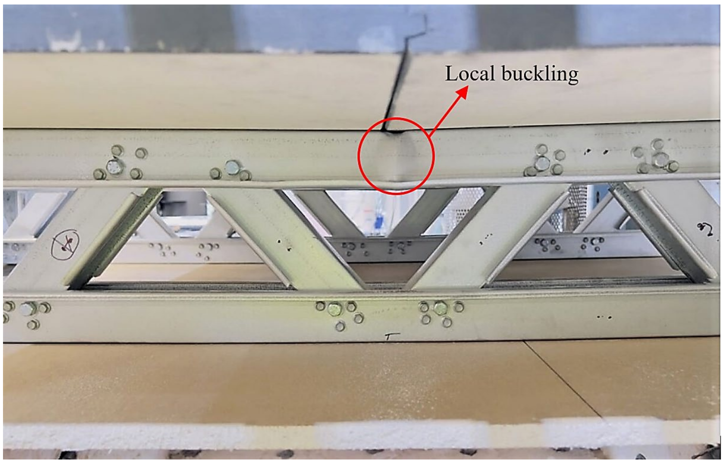

Figure 13. Top chord failure of Specimen with Tek screws

Several engineering improvements were found to significantly enhance the ambient temperature performance of the truss systems. Introducing a 50 mm long nylon spacer sleeve around the bolt at each web-to-chord connection helped stabilise the cut-out ends of the web members and delayed the onset of early web member buckling. With these spacers in place, the trusses sustained higher loads before the first buckling occurred. However, buckling was not entirely eliminated; thus, in the configuration used for fire tests, four Tek screws were additionally inserted through each connection (two on either side of the bolt) to further stiffen the web-chord connection. This final configuration of 0.95 mm thick top hat chords, 10 web members, bolted connections with nylon spacers plus Tek screws achieved about double the load capacity of the unmodified truss (Figure 13). The ultimate failure load increased from ~12 kN in the basic truss to about 25.7 kN in the best-performing specimen, which failed by top chord buckling. The use of thicker steel chords (0.95 mm vs 0.75 mm) also contributed to greater strength, but the primary gains came from preventing early web instability. All truss floor specimens ultimately failed by local buckling of the top chord in the mid-span region (Figure 13) (once the webs could carry no further load), similar to the failure in the joist tests. These ambient test results revealed that short-span LGS trusses can carry higher loads through relatively simple connection modifications (spacers and screws) without changing the overall truss layout (Ranasinghe, 2025). Table 2 shows a summary of the short-span ambient temperature tests using lipped channel joists (Hisham, 2024) and trusses.

Table 2. Summary of short-span ambient temperature tests and results

Test	Joist type	Thickness (mm)	Channel joist / Truss Orientation	Noggings/ Blockings	Ultimate failure Load per Joist (kN)
A1	Channel joist	2.4	Same direction	No	42
A2	Channel joist	2.4	Back to back	Yes	110
A3	Top hat truss	0.75	-	No	12.9
A4	Top hat truss	0.75	-	No	11.2
A5	Top hat truss	0.75	Flipped	No	11.8
A6	Top hat truss	0.75	-	No	11.7
A7	Top hat truss	0.75	-	No	10.5
A8	Top hat truss	0.75	-	No	9.8
A9	Top hat truss	0.95	-	No	16.8
A10	Top hat truss	0.95	-	No	25.7
A11	C-section minor axis truss	0.95	-	No	27.4

5.3 Lipped Channel Joist Floor Systems – Fire Conditions

Fire safety is critical for LGS floor systems, as the steel joists lose strength at high temperatures and the protective ceiling can fall-off, leading to rapid failure. In LGS floors, the plasterboard ceiling provides fire protection, but if it falls-off during a fire, the exposed steel joists heat up much faster. To evaluate this behaviour, a series of fire tests was conducted on short-span floor specimens (1.67 m span with two CFS channel joists, identical to the ambient test design). Each specimen was subjected to a standard fire curve (AS/NZS 1530.4 furnace exposure) while carrying a constant bending load equal to 40% of its ambient temperature capacity. This load level was intended to simulate a realistic service load and ensure failure would occur within a practical time frame (not too quickly, allowing observation of fire endurance). The floor specimens had various ceiling configurations: two layers of gypsum plasterboard (either 2×13 mm or 2×16 mm thick boards, with joints either absent or present between sheets), and three layers of 16 mm boards. In addition, certain tests included a layer of glass-fibre insulation in the floor cavity to examine its effect on fire resistance. Table 3 shows the details of the tested short-span specimens made of channel joists.

Table 3. Details of short-span fire test specimens made of lipped channel joists

Specimen	Configuration	Cavity insulation	Plasterboard ceiling configuration	Load ratio
SS2 (fire test)	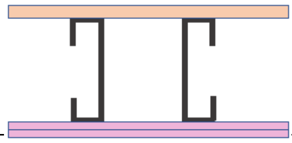	No	Two layers of 13 mm thick plasterboards (without joints)	0.40
SS3 (fire test)	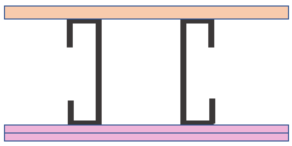	No	Two layers of 13 mm thick plasterboards (with joints)	0.40
SS4 (fire test)	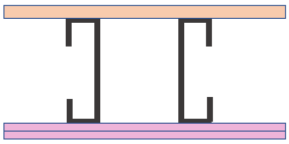	No	Two layers of 16 mm thick plasterboards (with joints)	0.40
SS5 (fire test)	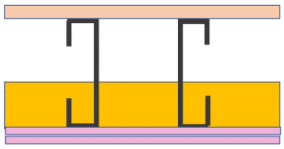	Yes	Two layers of 16 mm thick plasterboards (with joints)	0.40
SS6 (fire test)	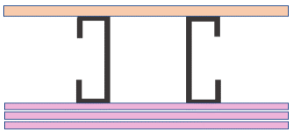	No	Three layers of 16 mm thick plasterboards (with joints)	0.40
SS7 (fire test)	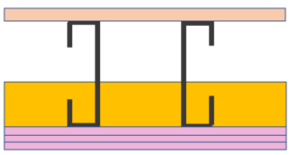	Yes	Three layers of 16 mm thick plasterboards (with joints)	0.40

The fire test outcomes revealed clear trends in the floor system's fire resistance levels (FRLs). With a two-layer 13 mm plasterboard ceiling (no board joints) and no insulation, the short-span floor survived about 60 to 70 min. The first test in this configuration (Specimen SS2) reached around 85 min before structural collapse, but this failure time was overconservative due to the absence of any plasterboard joints. A similar floor with plasterboard joints introduced (Specimen SS3) failed slightly earlier (about 67 min), corresponding to an FRL of 60/60/60 where the joints allowed hot gases to penetrate sooner, speeding the fire's impact. When thicker 16 mm plasterboards were used (two layers, with staggered joints), the floor's fire resistance increased substantially. In one test with 2×16 mm boards (Specimen SS4), the floor did not fail until about 90 min, achieving an FRL of 90 min for all criteria (structural adequacy, integrity and insulation). Generally, the two-layer ceiling configurations provided about one hour of fire resistance with 13 mm boards, and up to 90 min with 16 mm boards, assuming the load level was 40% of ultimate joist capacity.

Tests were also conducted with a three-layer plasterboard ceiling. Floors with 3×16 mm gypsum boards showed no failure even after 120 min of fire exposure. These specimens easily exceeded the 120 min mark, corresponding to FRLs of 120/120/120 (a two-hour fire rating). In fact, the fire was stopped after 120 min with the floor still intact, meaning the true time to collapse was beyond 120 min in those cases. Introducing cavity insulation (lightweight glass fibre) had a relatively modest effect compared to adding extra boards. The insulation helped slow the heating of the joists slightly, mainly by reducing heat transfer through the floor cavity. For example, an insulated floor with 2×16 mm boards (Specimen SS5) achieved around the same 90 min FRL as the uninsulated specimen, and with 3×16 mm boards (Specimen SS7) it likewise reached 120 min. This indicates that the number of fire-rated plasterboard layers was the dominant factor in fire resistance, while insulation provided an incremental benefit in terms of lower steel temperatures. Table 4 illustrates the test results.

Table 4. Short-span fire test results for channel joist floors

Test	Gypsum plasterboards	Load Ratio	Insulation	Applied Load (kN)	FRL (min)	Max HF Temp (°C)	Max CF Temp (°C)	Face Layer fall-off (min)	Base Layer fall-off (min)
SS1	Two 16 mm	-	No	110	-	-	-	-	-
SS2	Two 13 mm	0.40	No	44	85	585	493	70	--
SS3	Two 13 mm	0.40	No	44	67	645	500	42	-
SS4	Two 16 mm	0.40	No	44	83	625	526	58	-
SS5	Two 16 mm	0.40	Yes	44	90	737	538	49	81
SS6	Three 16 mm	0.40	No	44	132	540	506	91	-
SS7	Three 16 mm	0.40	Yes	44	124	609	511	75	113

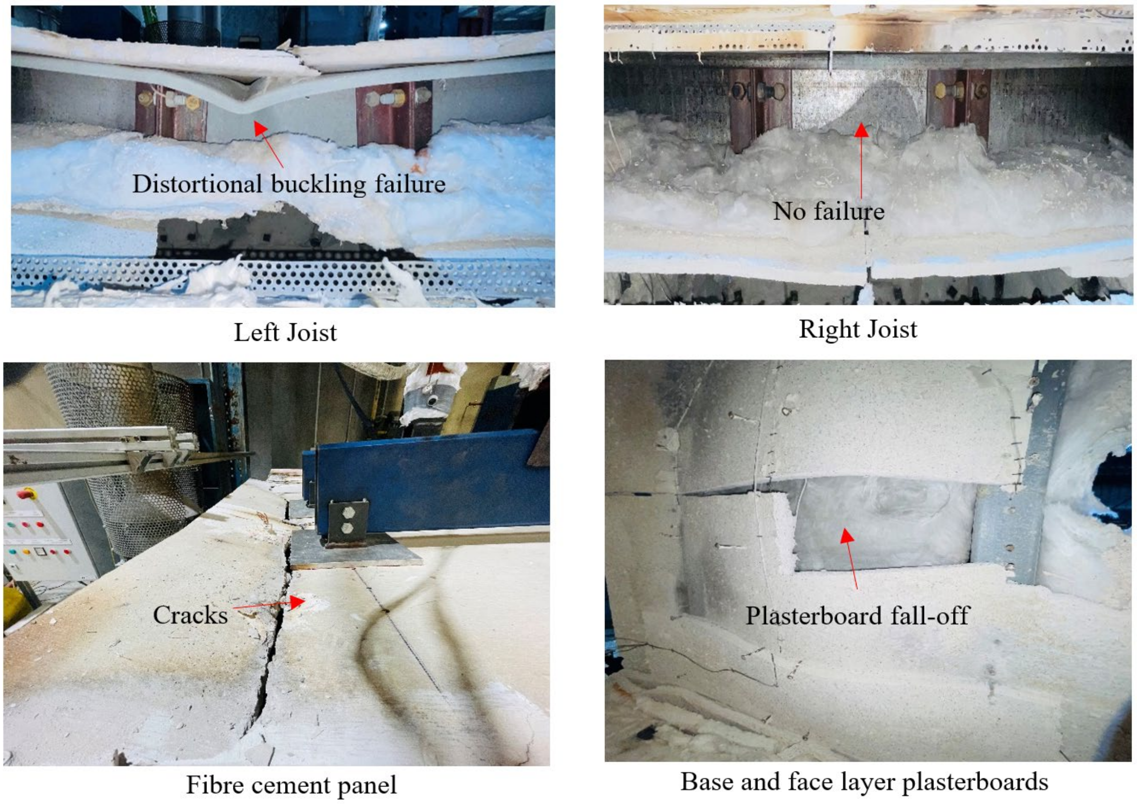

Figure 14. Post-failure observations of Specimen SS7

All short-span floor tests under fire conditions ultimately failed by distortional buckling of the channel joists, mirroring the ambient temperature failure mode but occurring at elevated temperature (Figure 14). The CFS joists would fail once they were sufficiently weakened by heat and the ceiling protection was largely lost. Notably, the timing of plasterboard fall-off had a critical influence on when this failure happened. In each test, the gypsum ceiling boards gradually heated and eventually began to crack and fall. The face layer (the first, exposed ceiling layer) typically fell-off partway through the test (e.g. after ~50–70 min, depending on board thickness and presence of joints), after which the joists' temperatures rose much more rapidly (Figure 14). The remaining base layer of plasterboard often stayed attached longer, but once the face layer had fallen-off, the floor's thermal barrier was greatly reduced. In tests where plasterboard joints were present, cracks formed sooner at the board seams and the face layer fell-off about 8–10 min earlier than in equivalent no-joint tests. This earlier fall-off led to an approximate 18 min reduction in the floor's failure time (SS3 versus SS2). Overall, the fire tests showed that a robust, uninterrupted ceiling (with thicker or multiple boards) delays heat penetration and thereby prolongs the floor's structural endurance in fire. All specimens were also evaluated against fire integrity and insulation criteria – integrity (no flaming or hot gases through the floor) and insulation (temperature rise on the unexposed side). In most cases, integrity was maintained until or just after the moment of structural collapse, and the insulation criterion was not met (the floor's top surface temperature stayed below the limit of +140 °C average) until failure. This meant that structural failure governed the FRL in these short-span floors, as the joists buckled and the floor deflected excessively once the fire protection was lost.

Importantly, the short-span fire tests were compared against previous full-scale floor fire tests, and the results were found to be comparable. Despite the much smaller span and specimen size, the temperature profiles and failure times in the 1.67 m span tests aligned well with those from full-length floor assemblies. For instance, the times recorded for plasterboard fall-off and joist failure in the short-span tests were in a similar range to those observed in full-scale experiments by Sultan et al. (1998, 2005) and others. This suggests that a carefully designed short-span test can accurately replicate the fire behaviour of a real floor system, making it a fast and economical way to determine the fire resistance of new LGS floor configurations. The findings from these tests were used to inform design guidelines, ensuring that LGS floors have adequate fire safety margins by accounting for the observed failure modes (distortional buckling) and the critical role of ceiling systems in fire protection.

5.4 Truss Floor Systems Made of Top Hat and C-sections – Fire Conditions

In parallel with the channel joist floor tests, fire tests were also performed on short-span truss floor systems. These tests used the same specimen dimensions (1.67 m span, ~1.2 m×1.2 m floor area) but the floor trusses were made of top-hat and minor axis C-sections (as described earlier). The truss floor specimens were subjected to the standard AS 1530.4 fire curve from below using a propane furnace (1 m×1 m internal chamber) with the floor loaded to 40% of its ambient temperature capacity. Three truss-based configurations were tested in fire, designated F1, F2, and F3. Specimen F1 was a floor with top-hat trusses (the same type tested under ambient conditions) and a two-layer 16 mm plasterboard ceiling (no insulation). Specimen F2 consisted of a similar floor type as in Specimen F1 but with minor axis C-section trusses for comparison, again with 2×16 mm boards. Specimen F3 was similar to F1, but included cavity insulation. All these tests had plasterboard joints in the ceiling layers to represent realistic construction joints.

Table 5. Details of short-span fire test specimens made of trusses

Specimen	CFS truss type	Cavity insulation	Load ratio
F1	Top hat	No	0.4
F2	Minor axis C-section	No	0.4
F3	Top hat	Yes	0.4

Specimen F1 exhibited a performance roughly equivalent to the channel joist floors. Under a constant load of ~10.3 kN (which was 40% of the ~25.7 kN ambient capacity of the truss floor), the assembly survived for an extended period before collapsing. Following early observations of smoke (2 min) and water droplets (9–10 min) typical early fire test observations, the first significant event was the plasterboard joint compound cracking at about 11 min, indicating the onset of plasterboard distress. As the fire progressed, the gypsum ceiling layers protected the trusses until just past the one-hour mark. At about 68 min, sections of the face-layer plasterboard began to fall-off the truss floor (earlier than in the channel joist floor, likely due to the joints and high heat). By about 85 min, the entire face layer had fallen-off, leaving only the second (base) layer of plasterboard attached in some areas. The increased heat input after face layer loss led to a steady rise in truss temperature.

The floor ultimately failed structurally at ~90 min, when the top chord of one of the trusses buckled at mid-span and collapsed as shown in Figure 15 (the left truss, which had the highest recorded temperature). Notably, the other truss did not buckle at that moment because it remained slightly cooler (insulated by the still-attached plasterboard in that area), illustrating how non-uniform heating can lead to one truss failing before the other.

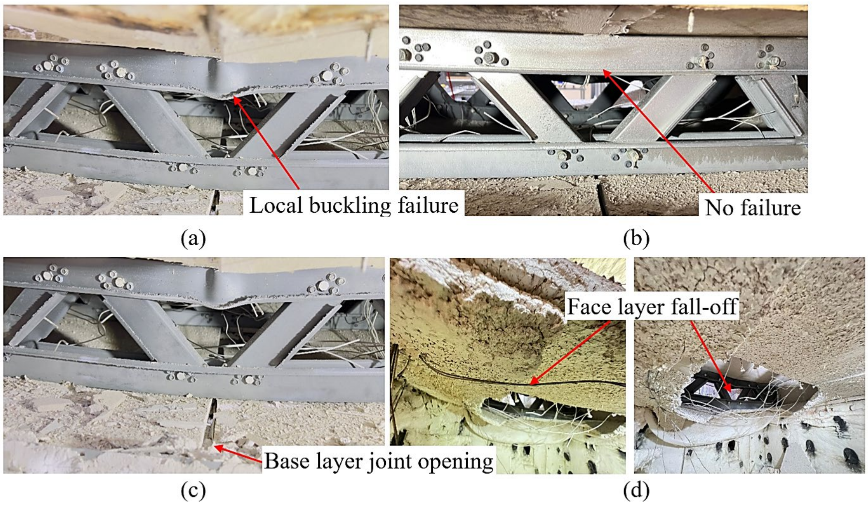

Figure 15. Post-failure observations of Specimen F1 (a) locally buckled left truss (b) no failure of right truss (c) base layer joint opening (d) face layer plasterboard fall-off

At the time of collapse, the floor system had not yet failed by the insulation criterion – the top surface temperature of the flooring was around 140 °C (below the 180 °C maximum limit). Integrity failure was observed (a crack in the fibre cement flooring) just after the truss failure. Thus, for Specimen F1 the governing fire resistance was 90 min based on structural adequacy (with integrity and insulation effectively also reaching 90 min). This result is on par with the 2×16 mm channel joist floor test (SS4) which also achieved ~90 min FRL, demonstrating that a LGS floor system can deliver equivalent fire performance when protected by a similar ceiling irrespective of the type of joist/truss..

The comparative test using minor axis C-section trusses (Specimen F2) provided insight into any differences in failure times for different truss types in fire by comparing with Specimen F1. Specimen F2 had an almost identical configuration (2×16 mm ceiling, no insulation, same load ratio) but with two C-section trusses. In Specimen F2, the plasterboard degradation happened somewhat faster so the joint opened and face-layer boards began falling about 10 min earlier than in Specimen F1 (major fall-off by ~58 min in F2 vs ~68 min in F1). This led to the trusses in F2 heating more quickly. As a result, F2's left truss reached the critical temperature and locally buckled at 80 min, ending the test about 10 min sooner than Specimen 1. The slightly shorter time to failure in F2 was attributed to the more pronounced thermal bowing and earlier plasterboard loss, rather than an inherent weakness in the C-section truss. However, if the plasterboard performance had been equal, the C-section truss floor would have also reached ~90 min before failing. Therefore, this shows that a truss made of top hat sections or C-section minor axis offers comparable fire resistance given the same ceiling configuration (their measured 80–90 min times fall in the same 90 min FRL category, considering the variability in board fall-off timing). The findings also revealed that the FRL is independent of the type of joist for a particular ceiling configuration and load ratio. This finding is significant because it indicates that replacing lipped channel joists with lightweight trusses does not negatively impact the fire resistance of an LGS floor system, as long as the ceiling system is equivalent.

In the third test, Specimen F3, the top-hat truss floor was equipped with a 75 mm thick cavity insulation to understand its impact on fire resistance. A thin layer of glass fibre insulation was placed between the trusses on top of the base plasterboard layer of the ceiling. Intuitively, insulation can delay heat reaching the floor cavity and steel members. In Specimen F3, the overall outcome was still a 90-min failure time, very similar to Specimen F1 (which had no insulation). The face-layer plasterboard in Specimen F3 fell-off slightly earlier (around 56 min) than in the uninsulated case, possibly because the insulation kept more heat in the plasterboard layer, causing it to degrade faster.

However, the insulation helped keep the trusses' top chord (cold-flange) temperatures lower, which may explain why despite early face layer fall-off, the trusses held on until 90 min. The base-layer plasterboard in Specimen F3 remained in place until 82 min, after which the steel temperatures rose rapidly. Structural failure again occurred by top-chord buckling at about 90 min. Thus, adding a modest amount of insulation did not dramatically extend the fire resistance beyond the ~90 min achieved by the two-layer ceiling alone; it mainly reduced the peak steel temperatures slightly at a given time. These results reinforce that the thickness of the ceiling system (number of plasterboard layers) is the primary factor in determining the floor's FRL, whereas cavity insulation plays a secondary role. Table 6 shows the test results along with failure temperatures and fall-off times.

Table 6. Short-span fire test results for truss floors

Test	Truss	Load (kN)	Failure time (min)	MTC temp °C	ATC temp °C	MBC temp °C	ABC temp °C	FL fall-off (min)	BL fall-off (min)
A1	Top hat	25.70	-	-		-		-	-
A2	C-section	27.35	-	-		-		-	-
F1	Top hat	10.28	90	583	525	632	614	68	-
F2	C-section	10.94	80	470	466	648	641	58	-
F3*	Top hat	10.28	90	578	484	737	669	56	82
			Average	544	492	672	641		
			COV%	9.6	5.0	6.9	3.5		

MTC: Maximum Top Chord, ATC: Average Top Chord, MBC: Maximum Bottom Chord, ABC: Average bottom chord, FL: face layer, BL: Base layer, * - with cavity insulation.

Overall, the short-span truss floor fire tests demonstrated that a properly protected LGS truss system can achieve fire resistance of the order of 60–90 min with standard floor-ceiling configurations, and up to 120 min with three layers of 16 mm fire-rated gypsum plasterboards. The failure mode was consistent with that observed in the joist floors: the CFS joist/truss members ultimately buckled once the fire protection was depleted and the steel reached critical temperatures (around 600 °C in the hottest portion). There was no evidence of connection failure or shear failure – the limit state was bending capacity of the truss chords in fire. The tests also highlighted that short-span tests in a 1 m×1 m furnace can reliably capture the structural fire behaviour of LGS floor systems. The comparison of temperature-time curves demonstrated that these curves reflecting the thermal behaviour are independent of the type of truss/joist used in the floor system. Instead, they are influenced by the presence or absence of cavity insulation for a particular ceiling configuration. The study also revealed that cavity insulation does not significantly affect the failure times of the floor system. Overall, these are valuable findings for researchers and designers, as it means innovative floor system designs (including those using new truss configurations or materials) can be evaluated under fire conditions using short-span fire tests without the need for full-scale fire tests, provided the critical features like plasterboard layers and joints and load ratios are properly represented.

6 EXPERIMENTAL STUDIES OF FULL-SCALE LGS FLOOR SYSTEMS UNDER AMBIENT AND FIRE CONDITIONS

6.1 Introduction

To evaluate the structural performance of LGS floor systems under ambient conditions, full-scale four point bending tests were conducted on representative floor assemblies using both conventional joists and truss-type joists. A typical LGS floor system in Australia consists of CFS channel joists or trusses, sheathed with fibre cement board or plywood flooring and a fire-rated gypsum plasterboard ceiling. These components provide the floor's strength at ambient temperature and its fire protection. The ambient temperature tests were conducted first to obtain the load capacities for use in subsequent full-scale fire tests conducted to investigate the fire resistance of joist and truss floor systems. Details of both ambient and fire tests and the results are given next.

6.2 Lipped Channel Joist Floor systems – Ambient Temperature

Full-scale ambient temperature tests on LGS joist floor systems were performed under four-point bending to determine their bending capacity. Each test specimen comprised two 203 mm deep CFS lipped-channel joists (4.2 m span) with a spacing of 600 mm connected by end tracks and nogging bracing, representing the critical joist spacing within a typical floor bay. The floor truss specimens also included fibre cement flooring boards. The joist floors were tested in two configurations: (1) both joists oriented in the same direction (with their open flanges facing in the same direction) with steel angle noggings between them for torsional restraint, and (2) joists placed in a symmetric back-to-back orientation (i.e. web-to-web, lips outward) without mid-span connection. In both setups, a pair of hydraulic actuators applied equal point loads at one-third spans as shown in Figure 16.

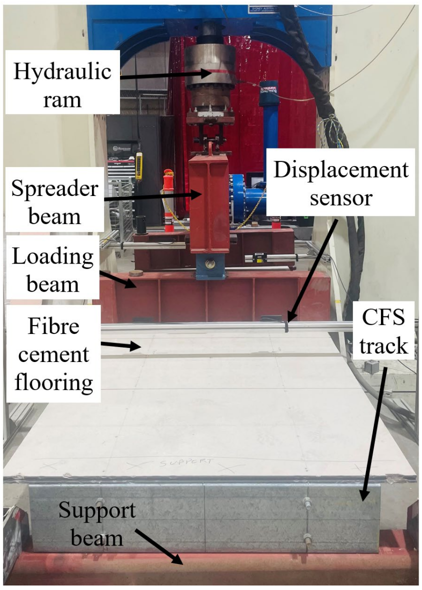

Figure 16. Ambient temperature test set-up of channel joist floors

Both LGS joist assemblies sustained substantial loads before failure, with ultimate loads of the order of 92–100 kN (total, across both joists). The joist orientation had a noticeable effect on behaviour: the same-direction joist specimen (Specimen FS1) experienced significant twisting during loading, leading to asymmetric bending and a slightly lower failure load. The top flange of one joist in Specimen FS1 twisted and buckled locally near a loading point (see Figure 17), indicating some loss of lateral stability. In contrast, the back-to-back (symmetric) joist specimen (FS2) exhibited no twisting and failed at about 8% higher load – approximately 50 kN per joist versus 46 kN in Specimen FS1. Failure in Specimen FS2 was governed by distortional buckling of the CFS joist webs at mid-span without any lateral deflection or twisting (Figure 18). These tests demonstrated that providing a symmetric joist orientation (or sufficient bracing) prevents twisting and slightly increases the load capacity. Overall, the ambient flexural capacity of the 4.2 m span joist floor system was about 35 kNm per joist. This capacity was used to define the load in subsequent fire tests (0.40 load ratio).

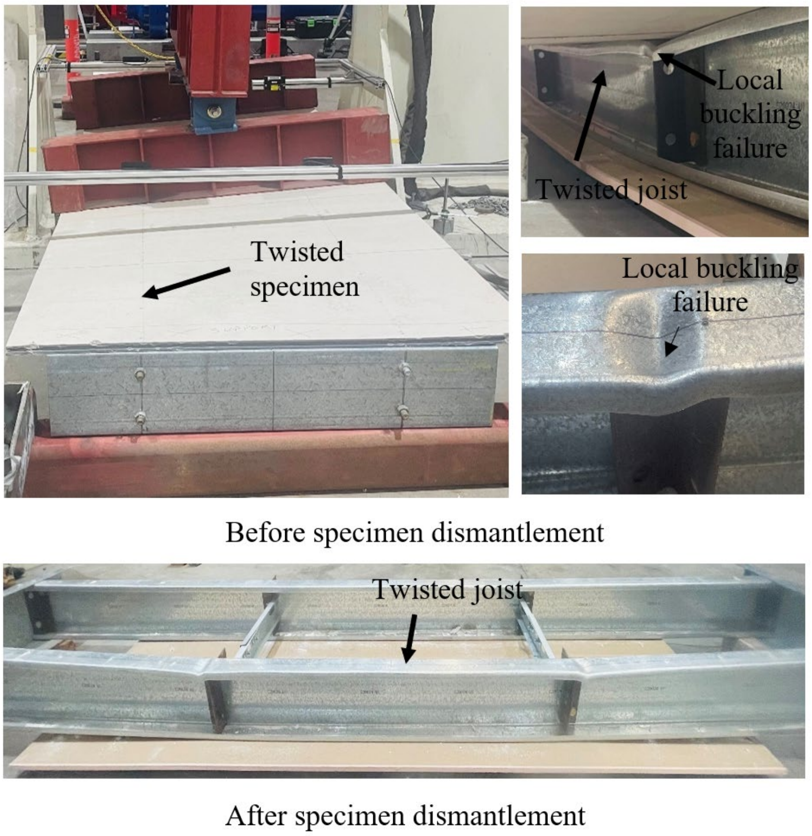

Figure 17. Failure of the channel joists in Specimen FS1

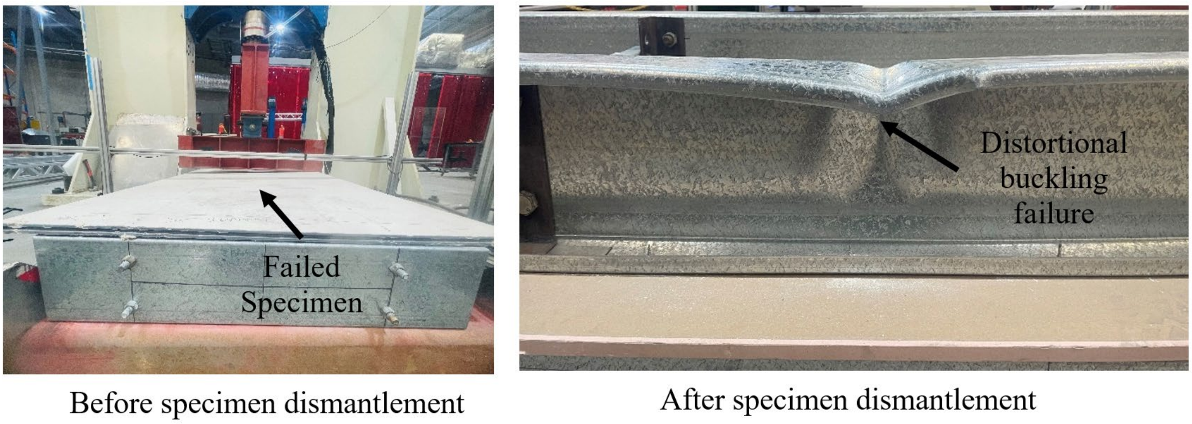

Figure 18. Failure of the channel joists in Specimen FS2

Notably, the steel nogging/blocking provided in Specimen FS1 remained intact and did not prevent the observed twist, whereas the symmetric arrangement of Specimen FS2 inherently stabilised the joists. In a real floor with multiple joists and continuous decking, even the same-direction joists would receive lateral restraint from the attached floorboards. In fact, it was observed that in the two-joist tests the floor sheathing acted as a diaphragm, and in the multi-joist floor used later for fire tests, joist twisting was unlikely to occur due to the stronger composite action of the sheathing.

6.3 Truss Floor Systems – Ambient Temperature

Ambient temperature bending tests were also conducted on full-scale floor assemblies made of C-section minor axis trusses of 200 mm depth. Two such trusses (200 mm depth with approximately 4.1 m span) were tested under four-point bending, simulating the primary load-bearing elements of a floor bay (see Figure 19). One truss specimen (Specimen FS1) was built with a mid-span blocking truss installed (as per standard practice for spans >3.5 m), while the other specimen was identical except without the mid-span blocking truss (Specimen FS2). Both had identical cross-sections and were tested with the same loading scheme (two-point loads at third spans). The floor trusses also included fibre cement flooring boards, similar to a real floor system.

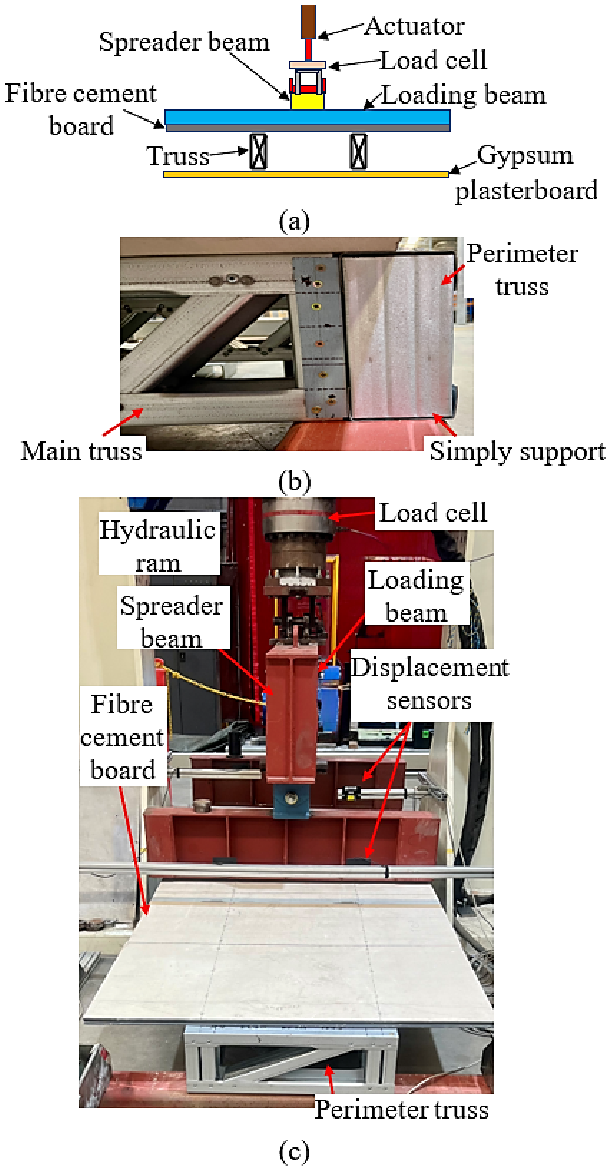

Figure 19. Ambient temperature test set-up (a) cross-section view (b) simply supported conditions (c) overall view

The truss floor assemblies exhibited comparable behaviour up to failure, with both specimens with and without blocking trusses reaching comparable ultimate loads (the difference in failure load was under 2%). In each test, failure was governed by local buckling of the top chord of the truss (compression chord) at mid-span (Figure 20). Importantly, no excessive lateral and/or twisting deformations occurred in either case – even the specimen without mid-span blocking did not twist, because the continuous fibre cement board flooring provided sufficient lateral restraint to the truss chords. The mid-span blocking truss in the first specimen remained in tact and did not significantly contribute to the load-bearing capacity. These ambient temperature tests indicated that additional mid-span blocking is not necessary for truss floors from a pure strength standpoint, as the floor deck and inherent truss stiffness prevented instability. Both configurations achieved comparable flexural capacities (on the order of 6.5–7 kN per truss in a two-truss test). Thus, similar to the channel joist floors, the bending capacity of the truss floors was controlled by the individual truss member buckling capacity, and not significantly by the presence of blocking. These ambient temperature capacities were later used to set the target load levels for the fire tests of truss floor assemblies.

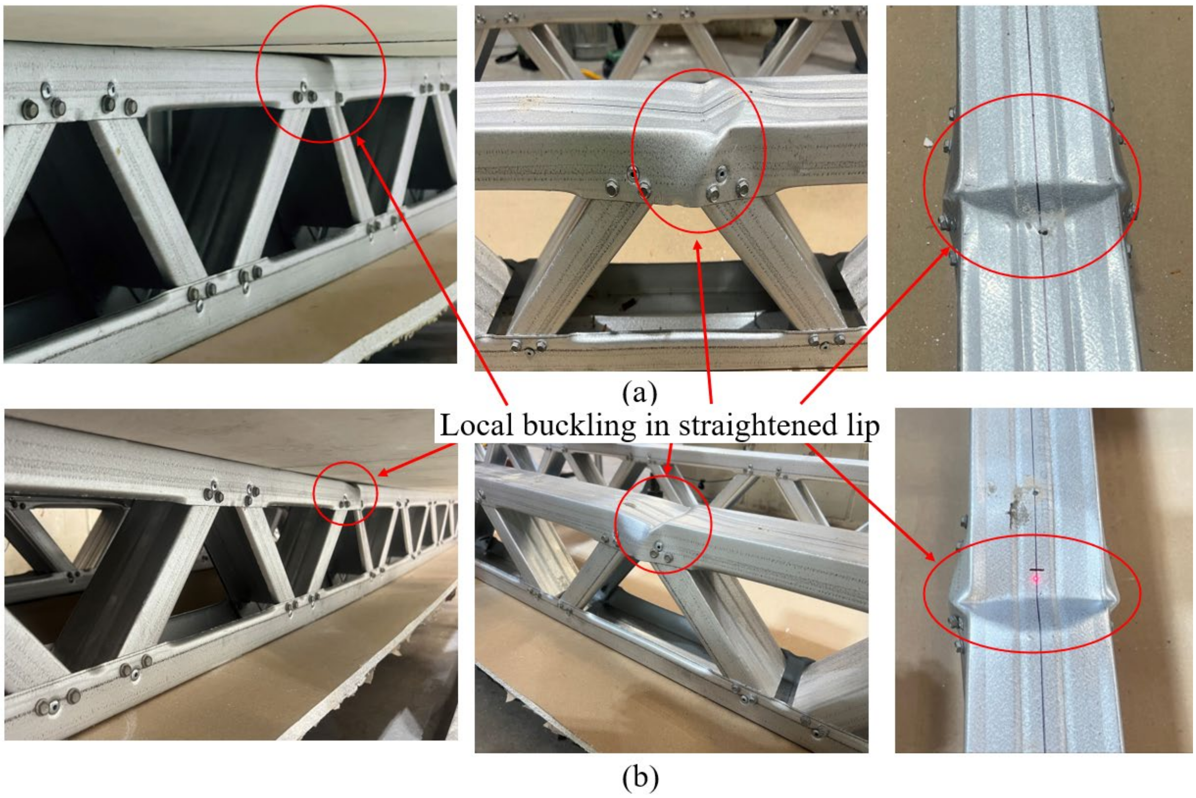

Figure 20. Local buckling failure of top chord of the truss at the unfolded lip in Specimens (a) FS1 (b) FS2

6.4 Lipped Channel Joist Floor Systems – Fire Conditions

Following the ambient temperature tests, a series of full-scale fire tests were carried out to investigate the fire resistance of LGS floor systems under standard fire exposure. All fire tests were conducted at an accredited fire testing facility (Jensen Hughes) in accordance with AS/NZS 1530.4 (2014), which prescribes the standard for fire resistance testing. Each floor specimen was loaded to approximately 40% of its ambient temperature capacity throughout the fire test duration, representing a realistic load level. The FRL of each floor system was determined by observing the times to reach failure under the three criteria defined in AS/NZS 1530.4: Structural Adequacy, Integrity, and Insulation. Structural adequacy failure corresponds to collapse or excessive deflection of the floor (criteria: deflection > $L^2/400d$ or rate > $L^2/9000d$, where L is span). Integrity failure is the passage of flames or hot gases through the floor, and insulation failure is when the average or peak temperature rise on the unexposed side exceeds 140 °C or 180 °C, respectively

Three full-scale fire tests were conducted on LGS floors framed with conventional CFS channel joists. Each floor specimen was a 4.0 m × 3.0 m assembly consisting of six parallel joists (203 mm deep lipped channels at 600 mm spacing) attached to perimeter tracks, with a typical flooring and ceiling. The joists were laterally braced with steel bridging (noggings) at mid-span to prevent twist during the tests. The tested configurations reflected common Australian floor systems and explored the effect of different flooring types and ceiling thicknesses on fire resistance.

Test Specimen FS3 (2-layer plasterboard ceiling): Floor with fibre-cement board flooring (22 mm thick panels) and a ceiling of two layers of 16 mm fire-rated gypsum plasterboard (no cavity insulation). This represents a standard LGS floor assembly.

Test Specimen FS4 (3-layer plasterboard ceiling): Same floor framing and flooring as FS3, but with a thicker ceiling consisting of three layers of 16 mm fire-rated gypsum plasterboard.

Test Specimen FS5 (Concrete slab floor): Floor with a composite steel deck + concrete slab (replacing fibre cement boards) and two layers of 16 mm fire-rated gypsum plasterboard ceiling. This heavier floor system was included to examine the benefit of a concrete topping on fire performance.

Table 7. Details of full-scale fire test specimens made of lipped channel joists

Specimen	Configuration	Flooring	Plasterboard ceiling configuration	Load ratio
FS3 (fire test)	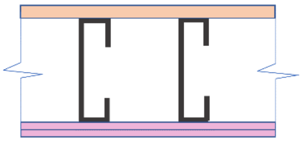	Fibre cement panel	Two layers of 16 mm thick plasterboards	0.40
FS4 (fire test)	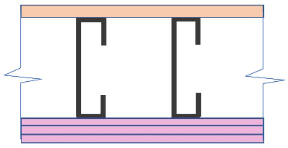	Fibre cement panel	Three layers of 16 mm thick plasterboards	0.40
FS5 (fire test)	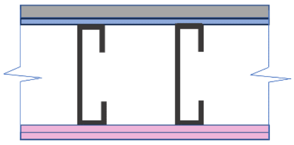	Corrugated sheet + Concrete	Two layers of 16 mm thick plasterboards	0.40

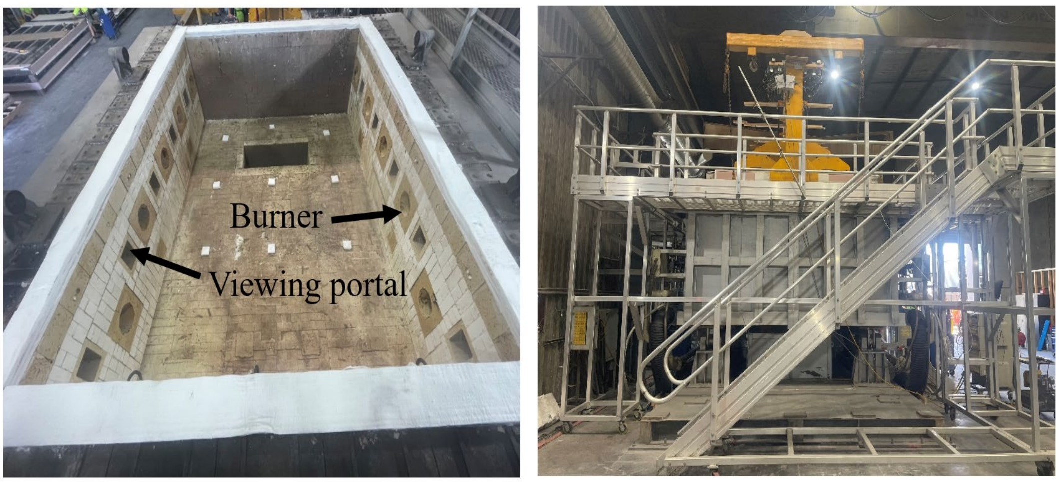

Figure 21. Gas furnace (dimensions: 4 m × 3 m) (a) interior (b) front view.

All three floor specimens were subjected to the standard fire from beneath while sustaining a uniformly distributed load (simulated by an array of hydraulic jacks or loading pads over the floor area) equivalent to 10.6 kPa on the floor. During the tests, deflections, temperatures, and failure events were closely monitored. Table 7 summarises the key parameters of these specimens, and Figure 21 and Figure 22 illustrate the gas furnace and test setup (floor specimen simply supported on all sides above a gas fire chamber, with load applied by numerous actuators), respectively.

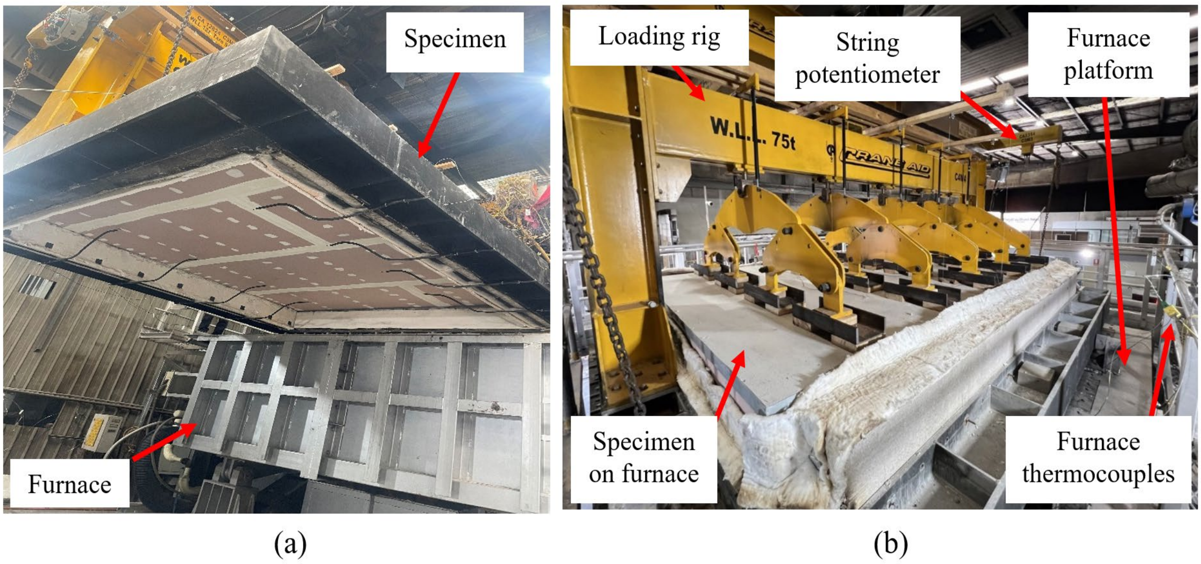

Figure 22. (a) Placement of specimens on the furnace (b) overall test set-up.

Notable Fire Test Results (Joist Floors):

Specimen FS3 (Two 16 mm plasterboard layers, fibre-cement flooring) – Sustained the design load for ~104 min until structural failure and achieved an FRL of 90/90/90 (i.e. met all criteria for at least 90 min). The floor's collapse was triggered by the joists' inability to carry the applied load after the plasterboard ceiling fell-off and the fibre-cement boards locally fractured under the applied load at about 104 min. Integrity and insulation were maintained up to that point (no flame-through).

Specimen FS4 (Three 16 mm plasterboard layers, fibre-cement flooring) – Withstood the fire for approximately 172 min before failure, corresponding to an FRL of 120/120/120. The additional ceiling layer delayed heat penetration significantly, allowing the joists to support the load for over 120 min. All three failure criteria were satisfied for at least 120 min (and nearly up to 173 min termination).

Specimen FS5 (Two 16 mm plasterboard layers, composite concrete slab flooring) – Reached structural failure at about 138 min and achieved an FRL of 120/120/120. The concrete-slab floor improved the thermal inertia of the system, contributing to a longer fire endurance despite having only two 16 mm gypsum boards. No integrity or insulation failure occurred prior to structural failure.

These results demonstrate the significant influence of the ceiling configuration and floor mass on fire performance. Adding a third layer of plasterboard increased the floor's fire resistance by roughly 66% (from ~90 min to ~170 min of structural adequacy, though standardised to a 120 min FRL). Likewise, the presence of a concrete slab (Specimen FS5) enhanced the FRL by about 30–32% compared to an equivalent lightweight floor (Specimen FS3) with the same two-layer ceiling. This finding is consistent with previous studies indicating that concrete or screed floors can improve the FRLs by around 20% or more relative to timber or fibre-cement floors. In contrast, the effect of cavity insulation was found to be minor – earlier short-span fire tests showed at most a 5% difference in FRL with or without insulation, so the full-scale joist floor tests were carried out without insulation.

All three joist floor specimens failed by structural adequacy criteria, with no early integrity or insulation failures. In fact, each floor maintained its integrity (no flame penetration) and insulation (safe upper floor surface temperatures) well past the 90-min mark. The governing failure mode in the two specimens (Specimens FS3 and FS4) was joist distortional buckling at high temperature: as the fire progressed, the steel joists' strength and stiffness degraded, leading to large deflections. In Specimen FS3, once the ceiling plasterboards had completely fallen-off (by about 105 min) and the joist temperatures rose above ~500 °C, the floor's mid-span deflection accelerated, and local collapse of the fibre-cement flooring occurred under the concentrated load pads (Figure 23). This marked the structural failure at 104–105 min (the point at which the floor could no longer sustain the applied load). In FS4, the thicker ceiling delayed the onset of joist overheating: the first plasterboard layer did not fall-off until about 84 min, and the final layer stayed in place until 120 min into the test.

This kept the joist temperatures lower for longer, allowing the floor to carry the load much further. The joists ultimately buckled at ~142 min once the protection was exhausted, but even at that time the unexposed floor surface had not exceeded the insulation limits. The concrete slab floor (Specimen FS5) showed the best overall behaviour: the heavy slab prevented any integrity failure (it stayed largely intact with only minor cracks), and the additional thermal mass helped keep the steel joists cooler, resulting in failure at around 138 min (also by joist buckling). In summary, the full-scale joist floor tests showed that a conventional LGS floor system with two layers of plasterboard ceiling can reliably achieve about 90 min fire resistance, which can be extended beyond 120 min by either adding an extra 16 mm plasterboard layer or using a concrete slab floor system. These test results were in consistent with the findings using short-span fire tests.

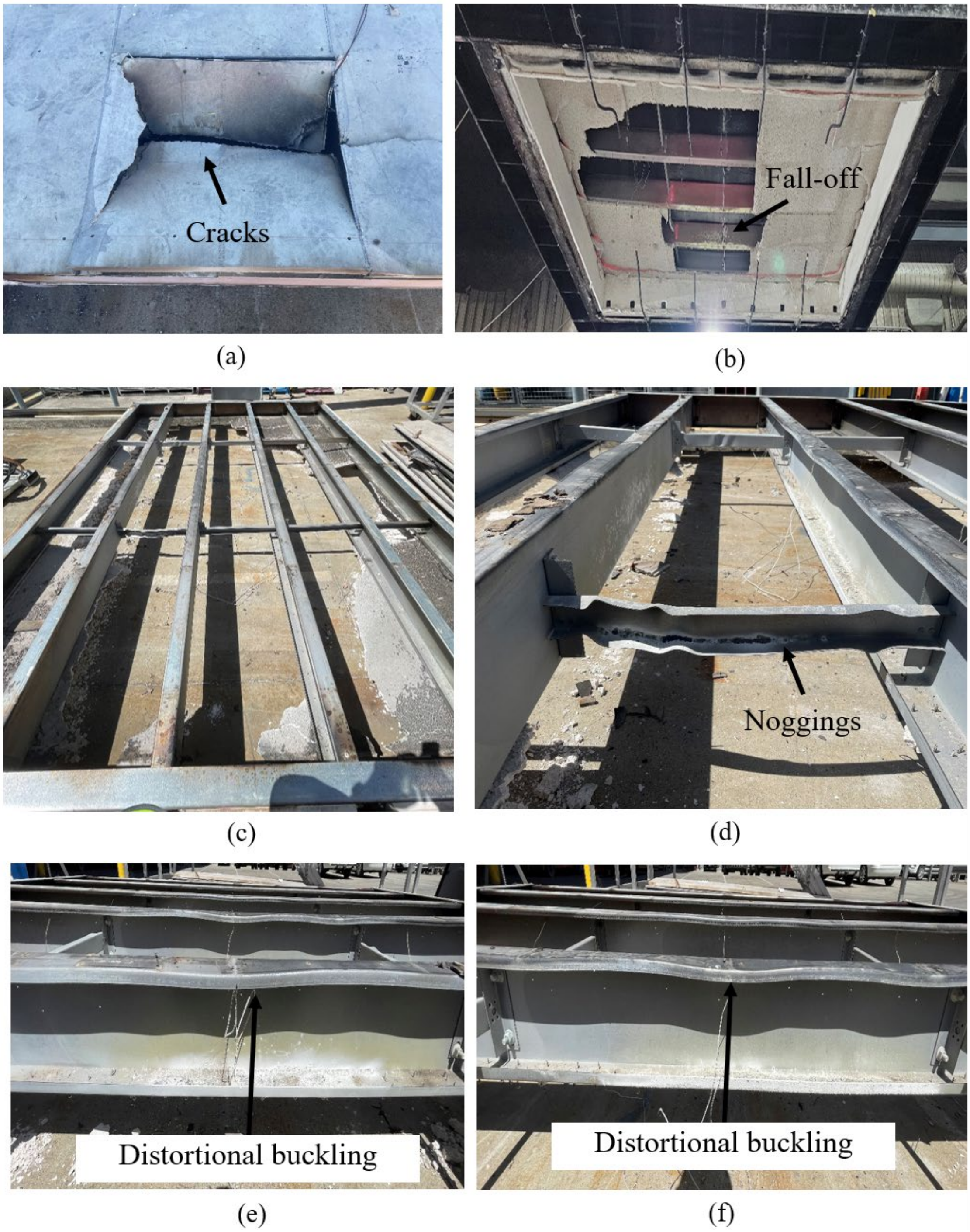

Figure 23. Post-test observations of Specimen FS3. (a) frame with steel deck (b) frame without steel deck (c) joist failure (d) nogging (e) plasterboard fall-off (f) steel deck

6.5 Truss Floor Systems – Fire Conditions

Two full-scale fire tests were similarly conducted on LGS floors constructed with trusses made of C-section minor axis trusses. The truss floor specimens measured approximately 4.3 m × 3.0 m in plan and consisted of six CFS trusses (200 mm depth) spaced at 600 mm, with fibre cement board flooring above and a plasterboard ceiling below. Each truss floor was built with blocking trusses as used in practice for floor trusses and 75 mm glass fibre insulation in the floor cavity, reflecting a typical insulated floor-ceiling assembly. The two fire tests mirrored the joist floor scenarios by using similar plasterboard ceiling layers but with cavity insulation:

Test Specimen FS1(Truss floor, two-layer ceiling): Truss floor with two layers of 16 mm fire-rated plasterboard ceiling and cavity insulation.

Test Specimen FS2 (Truss floor, three-layer ceiling): Truss floor with three layers of 16 mm fire-rated plasterboard ceiling and cavity insulation present.

Both truss floor specimens were loaded to about 2.8 kPa (40% of their ~7.0 kPa ambient temperature capacity) and exposed to the standard fire from below. Thermocouples recorded the temperature in various parts of the trusses and ceiling, and deflection of the trusses was recorded throughout. The behaviour observed in the truss floor systems closely matched that of the joist floors.

Notable Fire Test Results (Truss Floors):

Truss Specimen FS1 (two-layer ceiling + insulation) – Structural failure after 102 min, achieving an FRL of 90/90/90. This is essentially the same fire rating obtained for the two-layer channel joist floor. The truss began to deteriorate after about 90 min, once the plasterboard ceiling fell-off (face layer fall-off was noted around 74 min, base layer by 90 min) and the exposed steel truss bottom and top chords reached the critical temperatures (Figure 24).

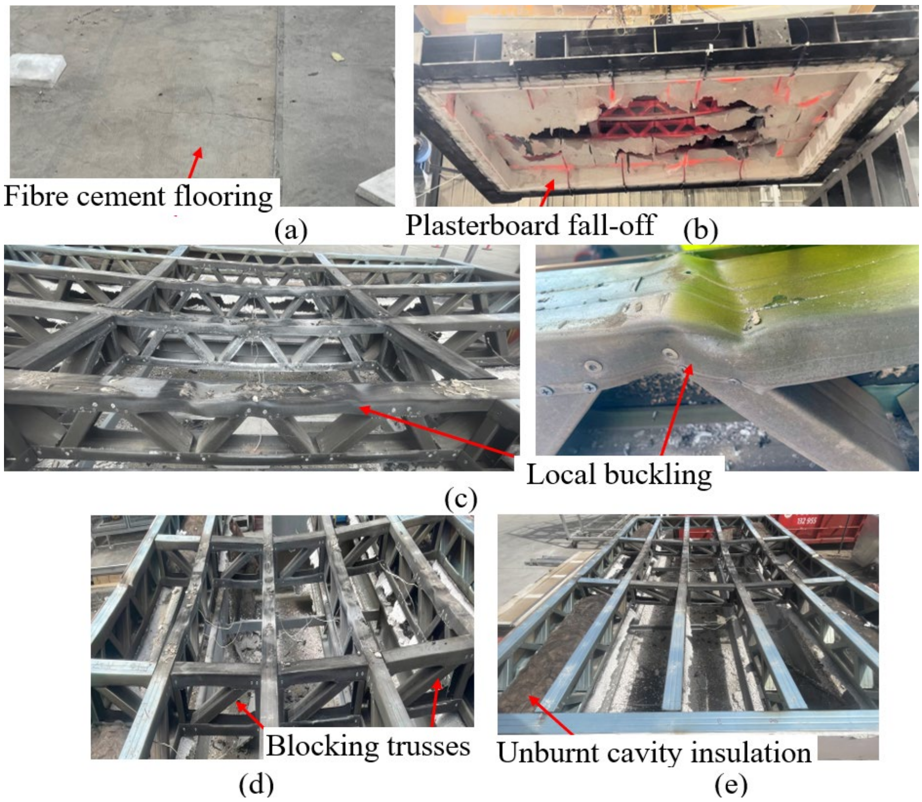

Figure 24. Post-test observations of Specimen FS1 (a) fibre cement board flooring intact with minor cracks (b) face and base layer fall-off (c) local buckling of main trusses (d) blocking trusses without any failure (e) post-test frame with unburnt cavity insulation

Truss Specimen FS2 (three-layer ceiling + insulation) – Withstood the fire for 142 min until failure, corresponding to an FRL of 120/120/120. The additional plasterboard layer significantly prolonged the protection of the truss; for instance, the first ceiling board did not fall-off until ~85 min and the assembly remained intact well into the second hour, keeping the truss relatively cool. The truss floor ultimately failed around 142 min as the steel top chords locally buckled, but by then it had exceeded the 120-min fire resistance benchmark.

In both truss floor tests, structural adequacy was the failure criterion (the steel trusses locally buckled when sufficiently weakened by heat). No integrity failure was observed – the fibre cement flooring stayed in place throughout the fire, showing only hairline cracks post-test. In fact, for the insulated truss floors, the underside plasterboard fell-off while the floorboards above remained largely intact, meaning the floor assembly failed by truss deformation rather than flooring collapse. The critical failure mechanism was the local buckling of the truss chords under load at high temperatures. The mid-span bridging members did not fail, and as expected, they provided some lateral restraint.

Crucially, the truss floor fire tests confirm that the fire resistance of an LGS floor system was found to be governed primarily by the passive fire protection (ceiling layers) and the load level, rather than the shape of the steel framing members. Both the two-layer and three-layer truss assemblies achieved FRLs identical to their channel joist counterparts (90 min and 120 min, respectively), supporting the conclusion that joist type has minimal impact on FRL when the ceiling and insulation configurations are the same. This observation is consistent with prior studies in the literature – for example, Sultan et al. (1998) found that the difference in FRL between floors with wood joists versus steel C-joists (of similar depth) was under 5% when both had equal fire protection layers. Likewise, the presence of conventional floor coverings (e.g. plywood versus fibre-cement) tends to have only a secondary effect on FRL compared to the effect of ceiling. In our tests, the insulated truss floor and uninsulated joist floor with the same two-layer ceiling both provided a 90 min FRL, underscoring that the number of plasterboard layers is the dominant factor in determining the fire rating.

Another important outcome of this research is the validation of short-span fire testing as a reliable predictor for full-scale floor fire performance. The full-scale fire results were compared with earlier 1.67 m span fire tests on smaller LGS floor specimens. In those short-span tests, a two-layer floor specimen achieved an FRL of 90/90/90, very close to the 90-min rating observed in the full-scale 4 m span fire tests. The failure modes and temperature profiles were also comparable, with only slightly faster plasterboard fall-off in the short-span specimen (attributed to more board joints per area). Overall, the short-span fire tests provided conservative but comparable results to the full-scale fire tests, typically underestimating the failure time by a small margin. This confirms that carefully designed short-span fire tests can be used as a cost-effective tool for evaluating LGS floor configurations before proceeding to expensive full-scale fire tests. The insights gained from both the ambient and fire tests in this study form the basis for improved design recommendations, ensuring that LGS floor systems in buildings can achieve the required fire resistance with appropriate detailing of the ceiling, insulation, and floor structure.

7 NUMERICAL STUDIES OF SHORT-SPAN AND FULL-SCALE LGS FLOOR SYSTEMS UNDER AMBIENT AND FIRE CONDITIONS

7.1 Introduction

This section provides the details of the numerical studies on the behaviour of short-span and full-scale LGS floor systems under ambient (room-temperature) and fire conditions, focusing on two common configurations: one using conventional lipped channel joists and another using trusses. In the following sections, details of the structural and heat transfer models developed and used are explained and the results are presented.

7.2 Short-span Lipped Channel Joist Floor Systems – Ambient Temperature

Recent experimental tests and advanced finite element (FE) simulations provide insight into the load-bearing capacity, failure modes, and the influence of key parameters for each floor system. Simplified single-joist models of LGS floors can be overly conservative when they ignore factors like the composite action of sheathing and the stiffness of connections. Therefore, high-fidelity FE models that explicitly include floor sheathing and fastener details have been developed to better predict the behaviour and capacity of floor systems. In this research, finite element models were developed and validated for short-span lipped channel floor joists under ambient conditions, using Abaqus/CAE. Three FE model configurations of the floor system were examined, differing in complexity:

<u>Two-joist sheathed model:</u> A detailed model with two parallel 1.67 m joists and a full 1200 mm × 2400 mm fibre cement board, replicating the test specimen's flooring system. This model explicitly included the sheathing's restraining effect via contact interactions (hard pressure-overclosure contact with friction μ≈0.2) between the joist top flanges and the fiber cement panel. Self-drilling screw connections were modeled as point-based fastener elements (connector stiffness 1.2 kN/mm) joining the joists and flooring. The plasterboard ceiling (attached to the joist's tension side in tests) was omitted in the FE model since it provided negligible structural capacity benefit.

<u>Single-joist sheathed model:</u> A simplified model using one joist with a 600 mm × 1200 mm fibre cement board (half the floor span), reducing model size while preserving composite action. This model retained the same joist-sheathing interaction definitions as above. The screw attachments were simulated either with the same fastener elements or with equivalent multi-point constraints, with both methods yielding nearly identical results. Because only one joist was present (and thus no joist-to-joist nogging members), the lateral bracing effect of noggings was approximated by tying the joist to reference nodes at its shear center near the loading pads, preventing any twist.

<u>Single-joist unsheathed model:</u> A bare joist model with no floor sheathing, relying on applied constraints to mimic sheathing effects. Lateral restraints (U1=0) were applied at the joist's bottom flange at the screw locations to represent the bracing provided by the plasterboard ceiling. This model eliminates all contact and connector interactions, greatly simplifying the analysis. Such an idealised joist-only model is computationally more stable and was intended to provide conservative results, consistent with prior studies using single-stud models for complex fire simulations.

All models shared common modelling assumptions and parameters. The joist was modeled with four-node thin shell elements (Abaqus type S4R) which are well-suited for slender CFS members. The fibre cement board, when included, was represented with eight-node solid elements (C3D8R), following the approach of Kyvelou et al. (2018). A mesh size of 5 mm was used for the steel joist, based on mesh sensitivity studies, while a coarser 20 mm mesh was sufficient for floor board/sheathing since its role was primarily to provide out-of-plane restraint. Material nonlinearities were incorporated: the steel joist's stress–strain behavior was defined by a two-stage elastic–plastic model capturing gradual yielding and strain hardening, calibrated to tensile coupon tests. The fibre cement board properties were taken from ambient temperature tests, with an elastic modulus of about 4.4 GPa and a modulus of rupture of 12.9 MPa. The joist end support conditions in the FE models closely mirrored the test setup where each end of the joist was tied via MPC constraints to a reference node (at the mid-span of the bottom flange) to simulate a warping-fixed connection to the track. Boundary conditions at these reference nodes were then set to achieve a pinned support at one end (restraining all translations and the torsional rotation) and a roller support at the other end (restraining lateral and vertical translation and torsion, while allowing longitudinal movement). This arrangement accurately reproduces the simply supported but warping-restrained joist ends in the test rig.

An eigenvalue buckling analysis was performed on the joist to identify its critical buckling mode shape. The short-span joist's governing buckling mode was distortional buckling, consistent with test observations. Initial geometric imperfections were then introduced in the nonlinear FE models based on this mode shape. Imperfection magnitudes followed the recommendations of AS/NZS 4600 (2018), for example L/1000 for member global buckling, and 0.3*t (where t is the plate thickness), scaled by the ratio of yield stress to elastic buckling stress for local and distortional buckling modes. These imperfection values were superimposed on the mesh using Abaqus's *IMPERFECTION command, ensuring a realistic initial geometry. Residual stresses in the CFS joist were not explicitly modeled, as prior studies have shown that cold-forming residual stresses have an insignificant effect on ultimate capacity due to concurrent cold-working increase in the yield strength in corner regions.

Nonlinear analyses were conducted under incremental static loading to simulate the joist's response until failure. Several solver schemes were explored (e.g. static Riks, implicit dynamic, explicit dynamic) and all produced very similar structural responses. To improve convergence in the detailed sheathed models with contact, a quasi-static implicit dynamic solver approach was adopted using Abaqus/Standard with very low loading rate. This allowed stable progress through load–deflection with minimal divergence, while adding negligible inertia effects. The simpler single-joist models with fewer contact interactions were able to be solved with the conventional static general solver. Small numerical damping (e.g. 5×10^−5) and automatic stabilisation (0.5%) were applied in those cases to control any local instabilities during post-buckling response.

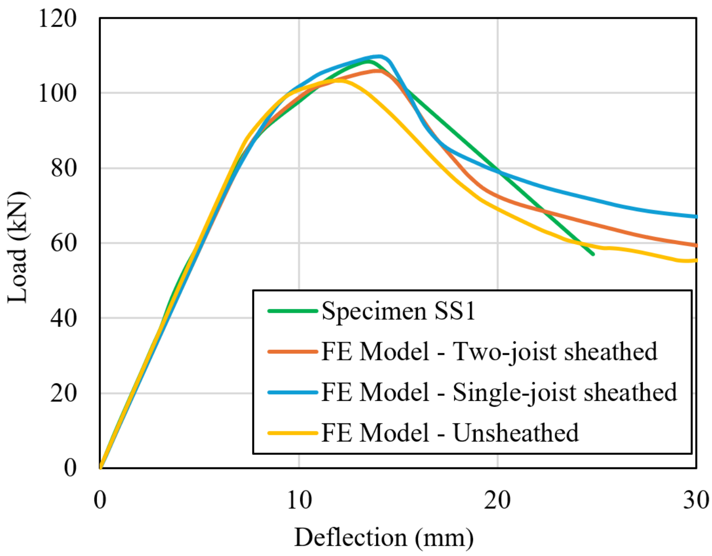

Figure 25. Comparison of load-deflection curves from Specimen SS1 and FE models

Figure 25 illustrates a good agreement between the FE simulations and the ambient temperature test results. The load versus deflection curves from both sheathed FE models closely match the experimental response of the joist, including initial stiffness and post-buckling behavior. The two-joist sheathed model predicted a peak load of ~106.5 kN (about 4% lower than the test failure load of 110.8 kN), while the single-joist sheathed model reached ~111.1 kN (within 0.3% of the test failure load). The unsheathed single-joist model was slightly more conservative, underestimating the failure load (~104.6 kN, ~6% below test failure load) due to the absence of any composite floor action. This small reduction indicates that the sheathing's contribution to strength was modest for the short span floor (as expected, given the limited 1200 mm panel width). Notably, all models captured the joist's distortional buckling failure mode observed in the physical test, confirming that the critical instability was correctly represented numerically. In summary, the sheathed FE models provided very accurate predictions of ambient performance, whereas the unsheathed model, while slightly under-predicting capacity, offered a conservative and much simpler simulation. Considering the computational effort, the full two-joist sheathed model required roughly three times the runtime of the single-joist model due to its more complex interactions. Thus, for ambient-condition analysis of floor joists, a single-joist sheathed model was found to be the most efficient choice. For advanced fire condition modelling (with elevated temperature and material degradation), this study recommends using the unsheathed single-joist model to avoid convergence difficulties, since it forgoes the complicated contact and composite interactions while still providing conservative strength estimates.

7.3 Short-span Truss Floor Systems – Ambient Temperature

Due to the complex buckling interactions observed, a detailed FE modelling study was undertaken to replicate and extend the truss test results. An advanced FE model of the LGS truss floor system was developed using Abaqus/CAE, explicitly including the full truss geometry, sheathing, and connection details. Initially, a high-fidelity model of a sheathed truss floor (including the fibre cement board on the top chord and screw connections) was created to simulate the experiment. This model employed four-noded shell elements (type S4R) to model the thin-walled steel sections of the truss chords and webs, which is the recommended approach for capturing local/global buckling in cold-formed steel members. The fibre cement board sheathing was modelled using solid elements (e.g. eight-node brick elements, C3D8R) tied to the top chord, following the method of Kyvelou et al. (2018). Connections (bolts and screws) and the effects of nylon spacers were also incorporated: bolts were simulated with connector elements or tied nodes, and spacer effects were modelled as discussed below. After verifying this detailed sheathed truss model, the study simplified the model to create a basic unsheathed truss model without the floorboard. In the unsheathed model, the load was applied directly to the top chord at the two loading points, as in the tests without sheathing. It was found that the initial unsheathed model was still unable to capture the early web member buckling precisely, so an improved unsheathed model was developed with special attention to replicating the nature of the connection. Specifically, the FE model introduced a small gap (≈5 mm) between the ends of each diagonal web member and the inner face of the chord, in cases where no spacer was used. This gap was based on the measurements from the physical tests – in truss specimens that had only a single bolt and no spacer, the web member did not snugly fit against the chord, effectively creating a gap that allowed the web to buckle more easily at the connection. By including this geometric imperfection in the FE model, the local buckling of the compression web member was accurately replicated in the simulation, reproducing the early web member failure observed in tests with minimal connection restraint. This modelling approach (introducing the measured initial imperfections at connections) proved essential for validating the behaviour of Specimens 1, 2, and 5 (Ranasinghe, 2025) – all of which had only one bolt per web joint (no extra screws) and showed early web member buckling. With these refinements, the FE models (sheathed, basic unsheathed, and improved unsheathed) achieved good agreement with the experimental load–deflection curves and failure modes of the truss floor system. For example, the model of the improved truss (Specimen 7) correctly predicted the elimination of early local buckling of web members and showed a top chord failure at a higher load, similar to the test. Overall, the validated FE modelling techniques allowed us to explore a wider range of parameters beyond those tested experimentally. Figure 26 shows the FE analysis (FEA) and experimental load versus mid-span deflection curves of Specimen 7.

Using the validated FE models, a comprehensive parametric study was conducted to examine how different design parameters affect the behaviour and capacity of the LGS truss floor system at ambient temperature. The parameters investigated include: thickness of the steel truss members, presence of nylon spacers, number of fasteners at each web-to-chord connection, the screw spacing of the floor sheathing, and the truss web configuration (number of panels for a given span). Following are the key results from the numerical parametric analyses, highlighting practical insights for design:

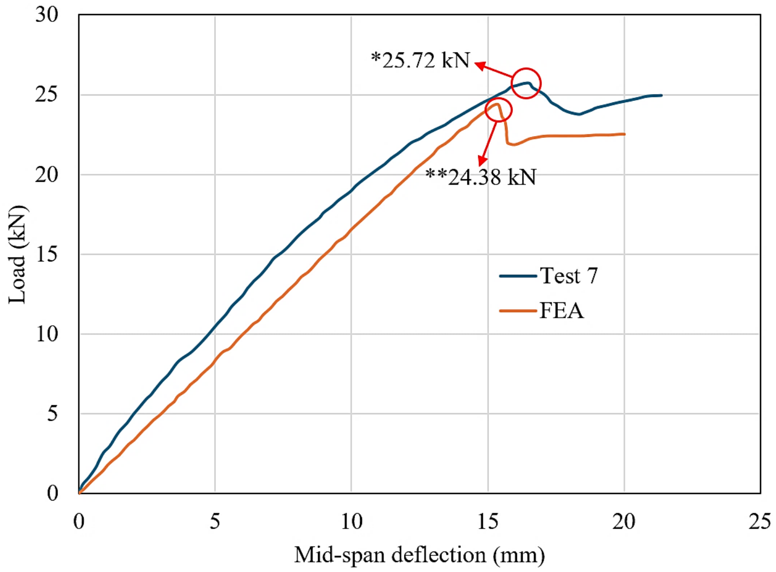

*test values and **FEA values

Figure 26. FEA and experimental load versus mid-span deflection curves of Specimen 7

Sheathing Screw Spacing: Reducing the screw spacing of the fibre cement board to the top chord significantly improves composite action and truss capacity. Reducing the spacing from a standard 200 mm to 50 mm (i.e. quadrupling the number of screws) increased the truss's capacity by about 18%. By contrast, moderate reductions to 150 mm or 100 mm spacing yielded less than 10% capacity increase. This trend aligns with findings on joist floors by Kyvelou et al. (2018), confirming that closely spaced sheathing screws can enhance strength and stiffness, although with diminishing returns beyond a certain density.

Connection Fastener Count: Adding more fasteners (Tek screws) at each web-to-chord connection substantially increases the capacity by delaying web member buckling. FE models showed that using two screws per connection (instead of only the primary bolt) raised the failure load by ~15%. However, even with two screws, some early web member buckling still occurred. However, it was delayed slightly (the load at web member buckling was ~4% higher than with one screw) but not fully eliminated. In contrast, using four screws per connection (two on each side of the chord) effectively prevented isolated early web member buckling and led to a much higher capacity. The model with four screws showed a 32% increase in capacity, and the failure mode shifted to simultaneous buckling of chord and web members (no distinct early web member failure).

Member Thickness: The thickness of the CFS sections was found to be the dominant factor governing the truss capacity. Increasing the chord and web member thickness (e.g. from 0.55 mm to 0.95 mm, as in some test comparisons) more than doubled the ultimate load capacity in the FE simulations. The parametric study confirmed that, for a given truss geometry, thicker steel sections yield significantly higher capacity, primarily by raising the buckling resistance of the top chord. For example, a change from 0.55 mm to 0.95 mm chord thickness (with spacers in place) increased the chord buckling load from roughly 6 kN to ~15 kN in one configuration. This indicates that selecting a higher gauge (thicker) steel for truss chords is an effective way to increase the floor capacity, albeit with some weight and cost penalty.

Truss Web Configuration: The number of web members (i.e. how many diagonal web members the truss has for a given span) had only a minor effect on the truss capacity, provided the chord member size remained the same. When more web members were used (smaller panel size), each web member carried a smaller force, which delayed local buckling of those web members under a given load. This means additional web panels can postpone the initial web member failure (improving the truss's serviceability and early failure), but they do not significantly raise the final chord-dominated failure load. The chord's buckling capacity is largely independent of how many web members support it; as long as at least one web member is present in each panel, the chord will reach a similar critical load. Thus, truss member thickness is more critical to truss capacity than the web layout. Different truss configurations may be chosen for constructability or to control deflections but simply adding web members without increasing the chord size will not greatly increase the truss capacity.

The numerical study of short-span LGS truss floors under ambient conditions provided valuable guidance for design and optimisation of these systems. The FE models, validated against experiments, highlighted the importance of connection detailing – specifically, the use of spacers and multiple screws – in preventing early web member buckling and achieving the full capacity of the truss. They also confirm that while adding sheathing can improve stiffness and contribute to strength (especially with small screw spacing), the governing factor for truss capacity is the strength of the steel members themselves (chord buckling capacity). For structural engineers, an implication is that to maximise an LGS truss floor's load capacity at ambient temperature, one should consider using slightly thicker chord sections or additional chord reinforcement and ensure web to chord connections are sufficiently robust (e.g. use of four screws or similar strategies) to eliminate weak links. On the other hand, using more web members than necessary (beyond what is required to control deflection and provide bracing) yields diminishing returns in capacity, since the chord will govern failure. The numerical modelling techniques developed – including the consideration of imperfections and composite action – formed the basis for future studies under fire conditions as well. Indeed, having verified the ambient temperature model, researchers can sequentially couple it with thermal analyses to predict the truss floor performance in standard fire, as discussed in subsequent chapters. The ambient-condition findings reported here are a critical baseline: they ensure that the FE model can capture all relevant early and final local buckling modes before introducing thermal effects. In conclusion, the short-span truss floor system can be numerically simulated with good accuracy, and the results emphasise key design strategies (enhancing member thickness and connection rigidity) to improve its ambient temperature load capacity while maintaining safety against early buckling failures. The insights gained from these ambient FE studies directly inform the fire performance assessment and design recommendations for LGS truss floor systems.

7.4 Heat Transfer Models of Short-span Lipped Channel Joist Floor Systems

Heat transfer models simulate the temperature–time development throughout the floor system during fire exposure. These thermal analyses eliminate reliance on measured test data by predicting the temperature profile in each component (plasterboard, insulation, steel members, flooring, air cavity, etc.) under standard fire conditions. The models account for all three heat transfer modes – conduction, convection, and radiation – which occur in a floor-ceiling assembly exposed to fire on the ceiling side. In contrast to LGS walls, where internal cavity convection is often negligible, floor systems have a horizontal cavity that can sustain convective heat flow; thus, cavity convection must be represented in the model. A typical one-sided fire exposure leads to a steep thermal gradient across the depth of the floor joist or truss, with the hot flange/chord on the fire-exposed side and a much cooler cold flange/chord on the unexposed side (Figure 27). Previous studies (e.g. (Abeysiriwardena & Mahendran, 2022; Ariyanayagam & Mahendran, 2019) have shown that using the measured temperature–time curves from fire tests and assuming a linear temperature gradient through the steel section is a reasonable approach. This linear distribution assumption was adopted in the FE models here and was validated by comparing predicted and measured temperatures at intermediate points (e.g. mid-depth of truss web members), which showed close agreement.

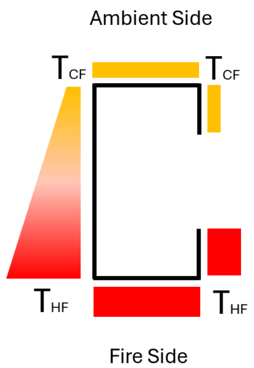

Figure 27. Temperature distribution across the joist exposed to fire conditions on one side

Project #24: Sub-project 2 – Fire resistance of light gauge steel (LGS) floor systems

For LGS floors constructed with CFS joists, a thermal FE model was developed to simulate heat transfer through a single joist bay exposed to the standard fire (ISO 834) from below. The model represented a floor bay of 1.2 m × 1.2 m (joist spacing 600 mm), including one steel joist, the attached plasterboard ceiling, any cavity insulation, and the top-floor fibre-cement board. Eight-node brick heat transfer elements were used for all components (Abaqus DC3D8), with a refined mesh (e.g. ~20 mm in-plane elements through plasterboard and ~10 mm for the steel joist) to capture steep thermal gradients. Appropriate thermal boundary conditions were applied: a convective heat transfer coefficient of h≈25 W/m²K on the fire-exposed (ceiling) surface and h≈10 W/m²K on the unexposed top surface, along with an emissivity of 0.9 for all radiating surfaces. Instead of using the idealised standard fire curve, the actual furnace temperature–time curve recorded in each test was applied as the fire-side air temperature, to more accurately reflect the exposure condition (Hisham, 2025).

Two significant modelling enhancements were introduced to better replicate real fire behaviour in the floor assembly:

Cavity Convection: Because the Abaqus software could not directly model convection within the floor cavity, an air volume was included in the cavity and treated as a solid element. An effective thermal conductivity for air was calculated (via an equivalent energy transfer approach equating convective and conductive heat flux) to simulate the convective heat exchange within the void. This allowed hot gases in the joist cavity to be represented, ensuring heat could transfer from the hot lower plasterboard up to the upper floor surface in a realistic way. In models with cavity insulation, the insulation material was explicitly included (75 mm glass-fibre batts) on the cold side of the plasterboard, using material properties and conductivity values from literature (Keerthan & Mahendran, 2012).

Plasterboard Degradation and Fall-off: Fire tests indicated that the gypsum plasterboard ceiling undergoes progressive degradation – joints cracking open and pieces of plasterboard falling off – which greatly accelerates heating of the cavity and joists. To capture this, the thermal properties of the plasterboard were not assumed constant. Temperature-dependent properties (conductivity, specific heat) were taken from high-temperature experiments on gypsum (Dodangoda et al., 2019) and modified beyond ~500 °C to account for ablation, moisture loss, and cracking at elevated temperatures. In the later stages of heating, the models implemented the removal of plasterboard elements at the times and locations where fall-off was observed in the corresponding fire tests. This piecewise elimination of ceiling material allowed the model to simulate the sudden exposure of the cavity and steel joist to direct furnace heating, which was critical for accurate temperature predictions. For example, in insulated floors the plasterboard retained heat longer and experienced more severe localised deterioration, so slightly higher thermal conductivity values were used to reflect the faster heat transfer once the board integrity was lost.

All material properties in the joist thermal model were defined as functions of temperature. For the steel joist, CFS design standard equations (AS/NZS 4600) were used to reduce thermal conductivity with temperature, and a constant steel density of 7850 kg/m³ was assumed. The fibre cement flooring properties at high temperature were based on laboratory thermal analysis of the material (specific heat, conductivity and density variation measured via STA/TGA) reported in Chapter 4.

Using the above enhancements, the heat transfer model was able to predict the temperature–time history in each part of the floor assembly with good accuracy. The computed temperatures of the steel joist (hot-flange and cold-flange) and of the sheathing layers showed reasonable agreement with the measured temperatures from short-span fire tests. For instance, the model closely reproduced the delay in heat rise in the cold flange and the plateau in gypsum temperature due to dehydration. For example, Figure 28. illustrates a good comparison of predicted versus measured temperature-time curves for one of the short-span fire tests, demonstrating that the FE model can capture the thermal response of the floor system. Such validated thermal models provide a crucial input for subsequent structural analysis, enabling failure time predictions without relying on extensive fire testing.

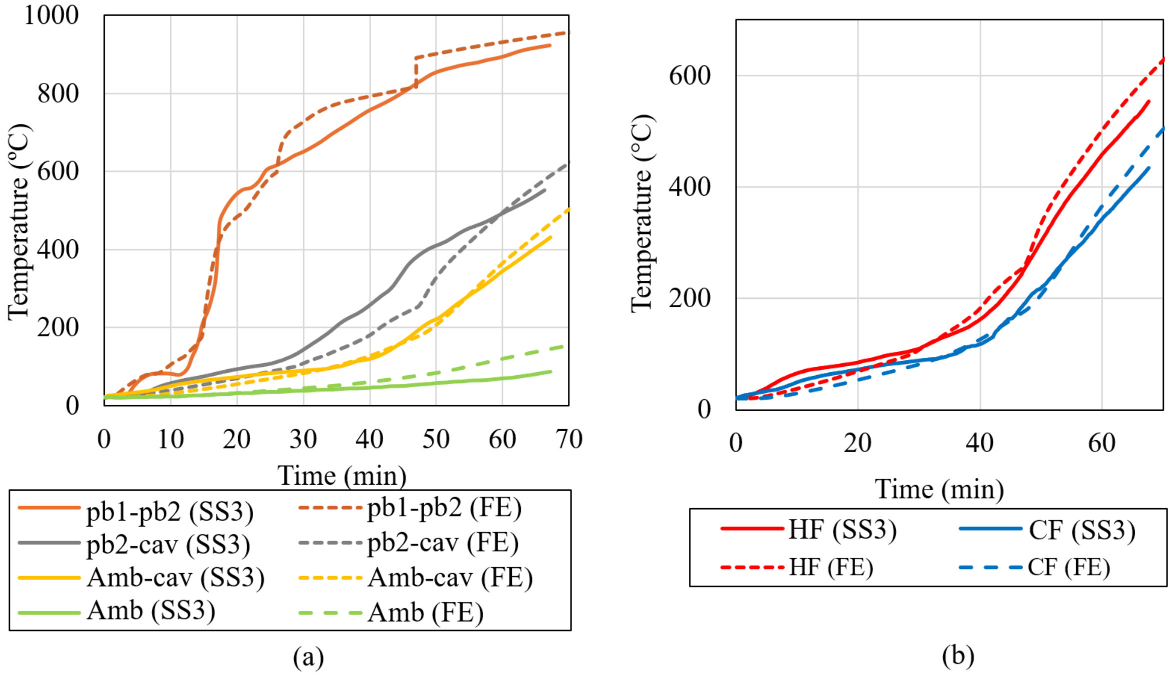

Figure 28. Example comparison of predicted and measured temperature–time curves for a short-span LGS floor joist assembly

7.5 Heat Transfer Models of Short-span Truss Floor Systems

The heat transfer modelling approach for floors with steel trusses followed a similar strategy, with adjustments for the truss geometry and materials. A thermal FE model was developed for each tested truss floor configuration (single short-span truss bay, with ceiling plasterboard and possible insulation, similar in extent to the joist model). Advanced techniques identical to the joist study were employed to incorporate the critical phenomena of cavity convection and plasterboard fall-off. In particular, air was included as a material in the open-web truss cavity to enable convective heat flow, and plasterboard elements were removed in the simulation at the times corresponding to joint openings or board fall-off observed during the truss floor fire tests. These measures allowed the truss heat transfer models to realistically simulate heating of the bottom chord (exposed to fire) and the top chord (protected by flooring) as well as the internal web members, which experience a thermal gradient along their length.

Boundary condition parameters (fire-side convection coefficient, emissivity, furnace temperature input) and material thermal properties for plasterboard, cavity insulation, steel, and floorboards were consistent with those used in the joist models, derived from the same standards and literature.

The truss thermal FE models were validated against three short-span fire tests, and they were found to simulate the temperature development accurately. The predicted temperature–time curves for key components (plasterboard, truss bottom chord, truss top chord, etc.) showed good agreement with the experimental data (Figure 29). For example, the model correctly captured the rapid heating of the uninsulated truss bottom chord and the slower, lagged heating of the top chord on the floor side. An idealised linear temperature gradient was assumed across the depth of each truss member (from the fire-exposed face to the protected face), and this assumption was confirmed to be valid – the mid-depth steel temperatures estimated by linear interpolation closely matched those measured in the tests. Overall, the heat transfer models for both joist and truss systems provided reliable temperature predictions to feed into structural analyses, enabling the sequentially coupled modelling approach described next.

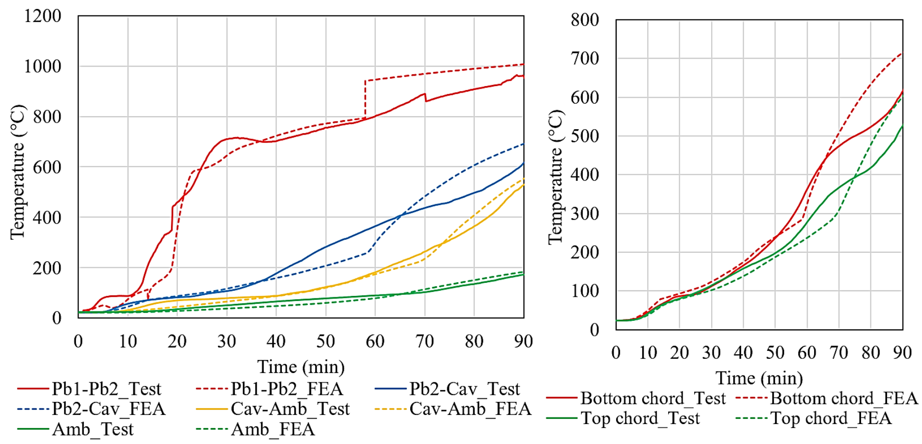

Figure 29. Example comparison of predicted and measured temperature–time curves for a short-span LGS truss floor assembly

7.6 Sequentially Coupled Model of Short-span Lipped Channel Joist Floor Systems

A sequentially coupled analysis was used to model the structural response of LGS floors under fire conditions, by first computing the temperature distribution in the assembly (either from fire test measurements or from the above heat transfer FE models) and then applying these temperatures to a structural FE model of the floor. This two-stage approach reflects the fact that thermal and structural responses occur on different time scales, and it allows complex temperature-dependent behaviour to be captured without fully coupling the thermal and mechanical calculations. In essence, the temperature-time curves obtained from the heat transfer simulation are input as thermal loads on the structural model, which then calculates time-dependent deformations and failure as the steel joist loses strength. The sequential method was implemented in transient-state FE analyses, wherein the structural model is subjected to a constant load while the temperature is gradually increased over time until failure occurs. This mirrors the conditions of a standard fire resistance test, where the load is applied at ambient temperature and kept constant as the furnace heats the specimen. An alternative is a steady-state approach, applying a snapshot temperature profile then ramping the load to failure, but prior studies have shown that both approaches give similar fire resistance times. The transient method was chosen here since it directly yields deflection versus time histories comparable to fire test observations.

For LGS floors using CFS joists, the structural FE model idealised the floor as a single joist span with appropriate boundary conditions, ignoring the sheathing in order to simplify the analysis. Past research on walls and floors has shown that including plasterboard in the structural model can lead to severe convergence difficulties with little benefit to failure time predictions. Therefore, an unsheathed single-joist model was adopted for the structural analysis of joist floors, consistent with the common practice in simulating LGS wall panels under fire conditions. This model consisted of a lipped channel joist simply supported at the ends (to replicate the test support conditions), with the fire-exposed flange (bottom flange) experiencing higher temperatures than the top flange as obtained from the thermal/heat transfer model or test data.

The mechanical properties of the steel joist were degraded as a function of temperature according to AS/NZS 4600 provisions. The temperature-dependent reduction of elastic modulus and yield strength for high-strength cold-formed steel (G550) was applied via the code's empirical formulae based on Kankanamge and Mahendran (2011). Thermal expansion of the steel was also included using the standard coefficients for CFS (thermal elongation increasing with temperature as per AS/NZS 4600). These material models ensure that the joist's stiffness and strength progressively decrease as the temperature rises, capturing the key effect of fire on load-bearing capacity.

FE Model Setup: The joist was modelled using four-node shell elements with reduced integration and a temperature degree of freedom (Abaqus S4RT elements). A mesh sensitivity study (5–25 mm element sizes) confirmed that a shell element size of about 20 mm yielded accurate results with acceptable computation time. Prior to the fire analysis, an eigenvalue buckling analysis was run to identify the likely buckling mode shapes, and the lowest buckling mode was introduced as an initial geometric imperfection in the joist (scaled as per the recommendations of AS/NZS 4600). This accounts for the effect of inevitable initial geometric imperfections on the joist's structural response.

The sequential thermal-structural analysis proceeded in two stages:

Load Application: A static preload was applied to the joist at ambient temperature. In the fire tests, the floor was loaded to about 40% of its ambient temperature capacity (0.4 load ratio). The FE model replicated this by gradually increasing the load on the joist (distributed or point load as per the test setup) until reaching the target load corresponding to a load ratio of 0.4 (e.g. 44.3 kN in one specimen). This load was then held constant for the remainder of the analysis.

Thermal Loading: The time-varying temperature distribution in the joist was applied incrementally. At each time step, the temperature of the joist's cross-section was updated according to the heating profile obtained from the heat transfer model or thermocouple readings (with the bottom flange/hot side following the higher curve and the top flange/cold side the lower curve, interpolating linearly through the web depth). In the FE model, these temperatures were applied uniformly along the length of the member, assuming each joist was heated similarly along the span. The analysis was run in small time increments, raising the steel joist temperature gradually and monitoring the deflection and internal forces. The simulation continued until failure, which was defined by the onset of a rapid increase in mid-span deflection (runaway deflection) accompanied by a drop in load-carrying capacity – essentially the point of structural collapse in fire.

During the heating process, the model captures the reduction in steel joist strength/stiffness and the increase in joist deflection over time. The output of interest from the structural FE analysis is the mid-span deflection–time history and the failure time (FRL).

Figure 30 shows a representative deflection versus time curve from the FE model alongside the corresponding fire test result, illustrating how closely the model reproduces the joist's behaviour until failure. The FE-predicted failure mode for all joists was distortional buckling as observed in the fire tests. This indicates that the model not only matched the time to failure but also the manner in which the joist failed (Figure 31).

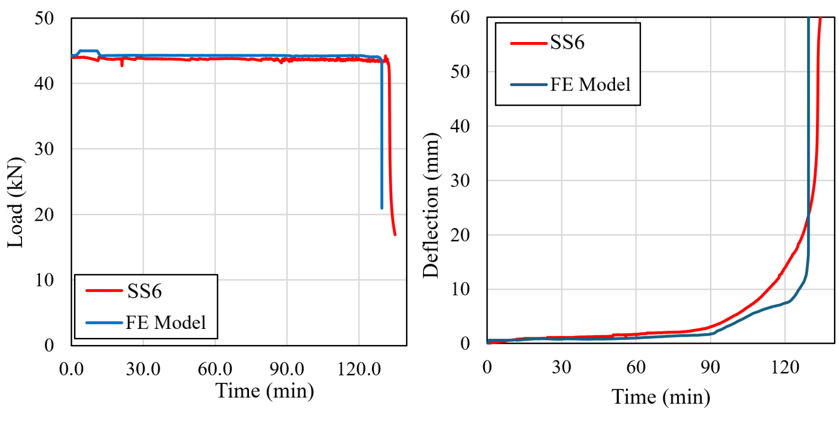

Figure 30. Measured versus FE-predicted mid-span deflection of a short-span LGS floor joist in fire

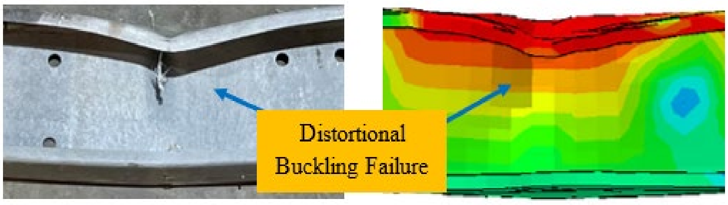

Figure 31. Comparison of failure modes from short-span joist FE model and test

Model Validation: The sequentially coupled joist model was validated against five short-span floor fire tests (Hisham, 2024). In all cases, the FE predictions closely matched the test results in terms of deflection and failure time. Using the average recorded temperatures in the joist (as opposed to a very conservative maximum temperature assumption) was important to accurately predict the time to failure. With average temperature input, the model's predicted failure times fell within a few minutes of the observed times. As summarised in Table 8, the FE-predicted FRLs were within about 1–4% of the experimental failure times for all simulations. For example, the test that failed at 83 min was predicted to fail at 80 min (a 3.8% difference), and a test that lasted 124 min was predicted at 125 min (0.8% difference). This level of accuracy is good for fire modelling and gave confidence that the joist FE model can reliably estimate fire resistance levels. Moreover, the buckling and failure deformations and modes from the FE analysis were in good agreement with those observed post-fire. Overall, the validated joist model can be used to predict the fire resistance (FRL) of similar LGS floor configurations, and to conduct parametric studies beyond the original tested cases.

Table 8. Comparison of FRLs from short-span joist FE models and tests

Specimen	Gypsum plasterboards	Load Ratio	Insulation	Test FRL (min)	FE FRL (min)	Difference (%)
SS3	Two 13 mm	0.4	No	67	66	1.5
SS4	Two 16 mm	0.4	No	83	80	3.8
SS5	Two 16 mm	0.4	Yes	90	87	3.4
SS6	Three 16 mm	0.4	No	132	128	3.1
SS7	Three 16 mm	0.4	Yes	124	125	0.8

7.7 Sequentially Coupled Models of Short-span Truss Floor Systems

For the LGS truss floor systems, a more detailed structural FE model was constructed to account for the composite action between steel truss and flooring. Unlike the joist model, here the floor sheathing (fibre-cement board) was explicitly included in the structural model of the truss floor due to the significant amount of composite action presented. Recent research by Peiris and Mahendran (2023) demonstrated that including the wall/floor sheathing with appropriate connections can significantly improve the accuracy of structural fire models. Furthermore, under ambient conditions it is known that composite interaction between the joists/trusses and the attached flooring increases the bending stiffness and capacity of the system (Karki et al., 2024). To capture this in the fire scenario, the structural model represented a simply-supported short-span truss with a fibre-cement board floor attached on top, similar to the tested specimens.

The CFS truss was modelled using shell elements (S4RT) for all chord and web members, with a mesh size of ~25 mm that was found to be suitable for capturing local buckling in the thin-walled sections. The floor slab was modelled with eight-node thermally coupled brick elements (to allow heat flow through the slab thickness) at an approximate 50 mm mesh. As with the joist model, an initial linear buckling analysis of the truss was performed to introduce geometric imperfections corresponding to the truss's likely buckling modes (global or local). All steel material properties were temperature-dependent (using the same AS/NZS 4600 reduction factors as for the joists), and the fiber-cement board's stiffness degradation with temperature was based on the experimental data reported earlier in the project. The connectors in the truss (rivets and bolts) and the screws attaching the board were modelled using mesh-independent fastener elements with rigid (tie) behaviour, effectively assuming they continue to hold until failure without slip. Contact interfaces were defined between the truss top surface and the floor slab to allow some slip: a friction coefficient of 0.2 was set to simulate the partial composite action (based on push tests by Kyvelou et al., 2018). The interfaces between truss web members and the chords were treated as frictionless, reflecting pinned connections at the gussets.

The sequential loading procedure for the truss floor FE model was analogous to the joist model. First, the service load was applied on the floor slab (distributed via two load pads to mimic the test setup) and increased to the target level used in the fire tests. The load represented ~40% of the ambient temperature capacity of the truss-floor system (about 10–11 kN in the short-span tests). This load was maintained constant on the model. Then, the temperature fields from the heat transfer analysis were mapped onto the truss and board elements as functions of time. As discussed earlier, a linear temperature gradient through the cross-section of each member was assumed, with the bottom chord reaching the highest temperatures and the top chord remaining cooler. Both average member temperatures (rather than peak/local hot spots) and average floorboard temperatures were used in the model, because using the average through-thickness temperature was found to give the best match to the test outcome. An initial comparison showed that using the maximum recorded temperatures led to a conservative underestimate of the failure time, whereas average temperatures yielded failure times within ~2 min of the test. The temperature of the fibre-cement board was applied on both its fire-exposed underside and its top surface equally, since the board was thin and thermally conductive enough to assume a near-uniform through-thickness temperature at any given time. Proper support boundary conditions were imposed by tying the truss end nodes (at the supports) to reference points that allowed rotation but prevented vertical displacement, emulating the pin support conditions in the test. The slab was laterally restrained at the supports (U_x=0) to represent continuity to adjacent bays, while free to expand in the longitudinal direction (U_y free).

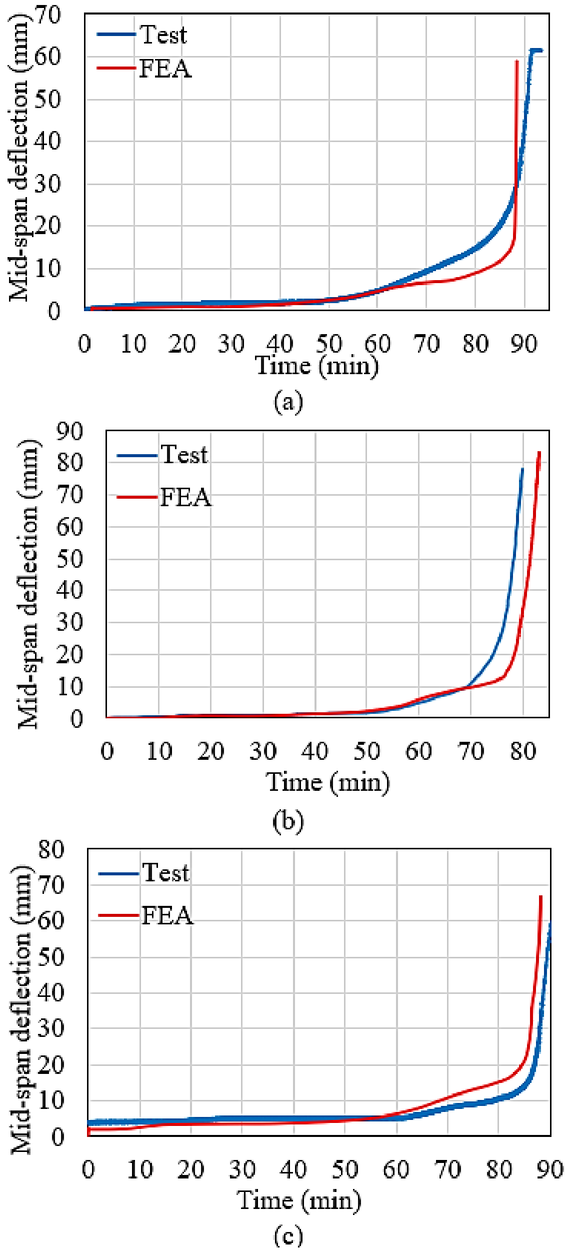

Figure 32. Comparison of mid-span deflection-time curves from tests and FEA of Specimen (a) F1 (b) F2 (c) F3 (Ranasinghe, 2025)

With the load and time-dependent temperatures in place, a nonlinear transient analysis was conducted to track the truss floor's deflection until failure. The model captured the gradual formation of runaway deflection in the truss – typically governed by weakening of the bottom chord in tension and eventual buckling of either a critical web member or the top chord as the stiffness degrades. The analysis was continued until a sharp increase in mid-span deflection showed imminent collapse (this criterion matched the definition of failure in the fire tests). The FE-predicted mid-span deflection versus time curves for the truss floors showed good agreement with the experimental curves from the fire tests (Figure 32), including the time at which deflection began to accelerate rapidly. The failure modes observed in the FE models (such as local buckling of the truss compression chord or fracture at a connection) closely resembled those seen in the post-fire examination of the test specimens. In all three truss tests, the numerical model's failure time predictions were within a few percent of the actual test results For example, the model predicted failure at 89 min for specimen F1 (versus 90 min in the test), 81 min for F2 (versus 82 min in the test), and 87 min for F3 (versus 85 min in the test). These correspond to differences of only 1.1%, 1.3%, and 3.3%, respectively – well within the experimental scatter. The deflection-time response was similarly well-captured, with the time of onset of significant deflection in the model being within <5 min of that in the tests for all specimens. Such close agreement validates the sequentially coupled truss floor model as an accurate tool for simulating the fire performance of LGS truss floor systems.

Both the joist and truss sequentially coupled models demonstrate that FE simulation can reliably reproduce the structural behaviour of LGS floors in fire. By integrating advanced heat transfer predictions (including plasterboard fall-off and cavity effects) with nonlinear structural analysis, the models achieved a high level of accuracy in predicting failure times and modes. The good agreement between model predictions and fire tests indicates that these FE models can be confidently used to evaluate the fire resistance for variations of floor geometry, loading, and protection details. This capability unlocks the potential for extensive parametric studies on LGS floor performance in fire, reducing the reliance on costly experimental testing by enabling the generation of FRL data through simulation. Such validated modelling techniques provide a powerful tool for developing fire-safe LGS floor designs and optimising systems for better fire resistance.

7.8 Full-scale Lipped Channel Joist Floor Systems – Ambient Temperature

Advanced FE models were developed in Abaqus to replicate the full-scale ambient temperature tests on lipped channel joist floors with fibre cement board flooring and plasterboard ceiling, and then streamlined to efficient single-joist representations for subsequent studies (Peiris & Mahendran, 2022; Vy et al., 2024). In the two-joist sheathed model, the joists were connected to the flooring via surface-to-surface contact with hard pressure-overclosure and a friction coefficient of 0.2 to simulate joist–fibre-cement board interaction; sheathing screw effects were represented by lateral restraints at screw locations (U1 = 0), consistent with prior LGS floor and wall models (Kyvelou et al., 2018). Multi-point constraint (MPC) beam-type equations tied nodes in the 135 mm × 1200 mm loading beam regions to centroidal reference nodes so the four-point loads could be applied realistically through the sheathing; equal-angle stiffeners and noggings near the load pads were reproduced by reference nodes located at the nogging centres, with adjacent joist shell nodes (10 mm strip) coupled to the references using MPC beam constraints (Peiris & Mahendran, 2023). The model used a dynamic implicit quasi-static solution strategy to handle contact and geometric/material nonlinearities efficiently (Abeysiriwardena & Mahendran, 2022).

Boundary conditions replicated the joist-to-track warping-fixed ends observed in the test rig using reference nodes at the bottom-flange shear centres at each end; end nodes were tied to these references with MPC constraints, and pinned/roller end support conditions were applied at the references by restraining appropriate translations and the rotation about the joist longitudinal axis, consistent with prior LGS practice (Peiris & Mahendran, 2023).

Material modelling for the joists adopted the two-stage elastic-plastic stress–strain model for CFS calibrated to tensile coupon data (Gardner & Yun, 2018), while fibre cement board properties (MOE ~ 4400 MPa; MOR ~ 12.9 MPa) were measured at ambient temperature and used directly in the FE model. Residual stresses were not included because their effect on distortional buckling capacity of CFS members is small, and the higher corner yield strength counters corner residual stress effects.

Initial geometric imperfections were introduced from an elastic buckling analysis and scaled to AS/NZS 4600 (2018) recommended values for global, local and distortional modes using Abaqus *IMPERFECTION, consistent with established LGS modelling practice (Gunalan & Mahendran, 2013b; Abeysiriwardena & Mahendran, 2022; Kyvelou et al., 2018).

To reduce the higher computational time for parametric or fire-sequential studies, the validated two-joist model was reduced to a single-joist sheathed model by using one joist beneath a 600 mm × 1200 mm sheathing patch with reference nodes placed near noggings/stiffeners at the shear centre and tied to the joist through MPC beam constraints. This simplification maintained stiffness transfer and torsion restraint without modelling the second joist; it matched the ambient test load–deflection within ~ 1–1.5% and the distortional-buckling failure mode while halving computational time. A further unsheathed single-joist variant often used to avoid convergence issues in sequential fire modelling provided conservative capacities but retained the same boundary conditions and loading at shear-centre references with small stabilisation (0.5%) and damping (0.00005) in the static general solver (Baleshan, 2012; Jatheeshan, 2015; Vy et al., 2024). Figure 33 shows the comparison of failure modes of a full-scale joist.

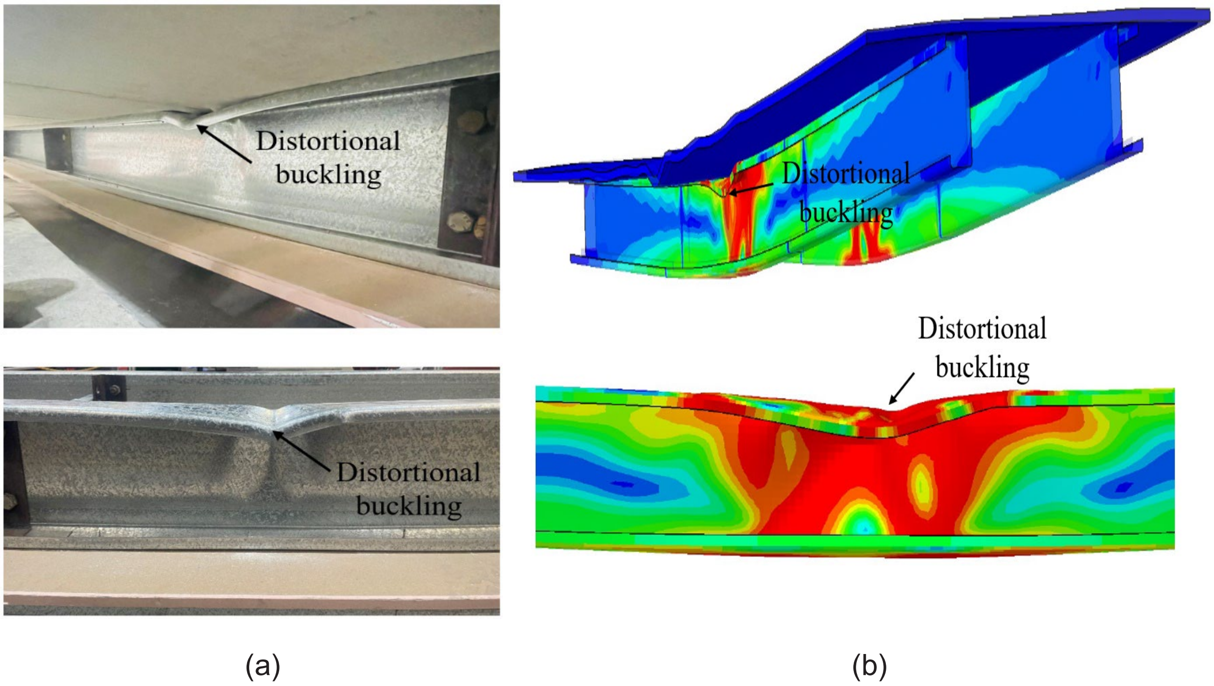

Figure 33. Comparison of failure modes of a full-scale joist (a) Test (b) FE model

The two-joist sheathed FE model reproduced the full-scale ambient temperature response of Specimen FS1, including local buckling near the loading beams and observed joist twisting, with failure load within ~ 3.5% of the test (46.0 versus 47.8 kN per joist) and close agreement in stiffness and post-peak behaviour (Hisham, 2024). Sheathed single-joist and two-joist models matched ambient temperature tests even more closely for short-span floors (e.g. ~ 0.3–4% difference), whereas the unsheathed single-joist model underpredicted the full-scale test failure load by about 6% due to the absence of composite action—which was expected to be modest in short spans with 1200 mm sheathing (composite action not dominant). Accordingly, for ambient capacity prediction the single-joist sheathed model is recommended; for large, fire-coupled modelling campaigns the unsheathed single-joist model offers a stable and conservative baseline.

7.9 Full-scale Truss Floor Systems – Ambient Temperature

Full-scale truss floor–ceiling systems were modelled in Abaqus and validated against ambient temperature tests prior to any sequential fire analyses, recognising that high-fidelity ambient calibration is essential for later thermo-mechanical analysis (Abeysiriwardena & Mahendran, 2022; Peiris & Mahendran, 2023). The models used explicit geometric representations of the CFS trusses and sheathing; sheathing was included because no cracking or permanent deformation was observed under ambient conditions, so elastic properties for fibre cement board (MOE ~ 4400 MPa) and gypsum plasterboard (MOE ~ 2649 MPa) were sufficient, while the steel truss material was taken as elastic-perfectly-plastic using G550 data measured by Rokilan & Mahendran (2020) (e.g. E ≈ 200–205 GPa; f_y ≈ 618–668 MPa depending on sheet thickness).

End conditions were modelled similar to what were used in the tests where main truss ends were connected to perimeter trusses that were supported on ideal pinned and roller supports. To mirror this, end nodes of the web members were linked to reference nodes placed at the actual rotation/movement points via MPC beam-type constraints; warping fixity about the truss longitudinal axis was imposed at both ends, with pinned and roller conditions reproduced by restraining the appropriate translational DOFs and the longitudinal rotation (Peiris & Mahendran, 2022). For unsheathed models, lateral restraints provided by sheathing were simulated at screw locations.

Geometric imperfections were introduced based on an initial elastic buckling analysis and using the coefficients obtained from AS/NZS 4600 (2018), which was followed by nonlinear analyses. Comparison with test results showed that the FE models were able to replicate the test behaviour with close agreement in load versus mid-span deflection, failure sequence and failure modes (Figure 34). For example, for one of the test specimens, the FE capacity (13.6 kN) matched the test capacity (13.5 kN), with both showing local buckling in the top-chord cross-section with straightened lips. Similar agreement was obtained for all other test specimens. Overall, the ambient temperature FE truss models provided reliable predictions for capacity, stiffness and failure mode, confirming their suitability for subsequent studies.

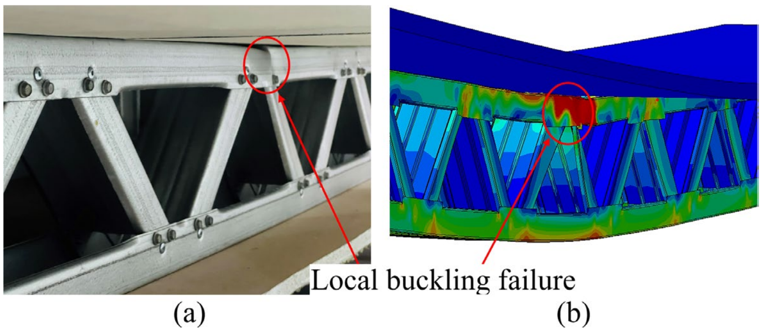

Figure 34. Comparison of failure modes of a full-scale truss (a) Test (b) FE model

7.10 Heat Transfer Models of Full-scale Lipped Channel Joist Floor Systems

Heat transfer in lipped-channel joist floors involves conduction through plasterboard and steel, radiation across gaps, and convection within the cavity. Three-dimensional FE models of a single joist (1.2×1.2 m area, 600 mm spacing) were developed in Abaqus using 8-node DC3D8 elements. The mesh used 10 mm×10 mm elements for the joist and 20 mm×4 mm through the plasterboard/fibre-cement layers, with a 50 mm×50 mm mesh for air filling the 200 mm cavity. Air was modeled as a solid with equivalent conductivity (k=h·L) to capture cavity convection effects. Boundary conditions included furnace-measured temperatures, surface emissivity of 0.9 and convective coefficients of 10 W/m²K (unexposed) and 25 W/m²K (exposed). Plasterboard fall-off was modelled by systematically removing the whole plasterboard layer at times observed in the tests (face layer at ~105 min, base layer at ~112 min). Thermal properties for gypsum plasterboard and fibre cement board were taken from literature (Hisham, 2024). As shown in Figure 35, comparison showed that the heat transfer FE model accurately reproduces the fire test temperature–time curves. Thus, the model is deemed reliable for FRL estimation of full-scale joist floors.

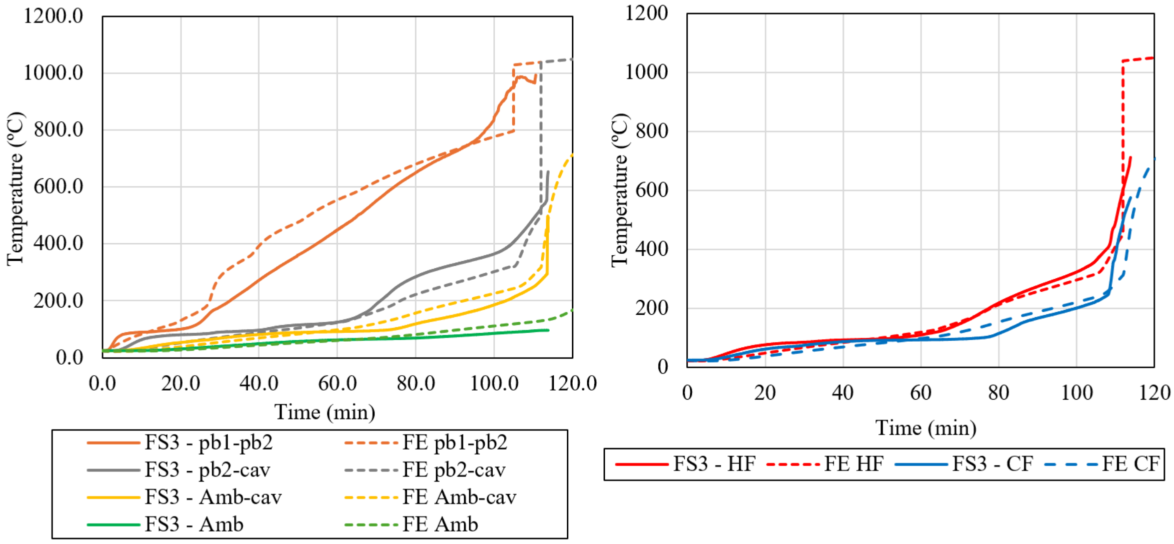

(a) (b)

Figure 35. Comparison of results from FE model and fire test for Specimen FS3 (a) sheathing temperatures (b) joist temperatures.

7.11 Heat Transfer Models of Full-scale Truss Floor Systems

Heat flow in truss systems is similar but includes conduction through web members and enhanced cavity convection due to a 200 mm cavity depth. Single-truss FE models (1.2×1.2 m, 600 mm spacing) were developed in Abaqus using 8-node DC3D8 elements. Plasterboard and fibre cement boards were meshed with 20 mm×4 mm elements and the truss elements with 10 mm×10 mm. The enclosed cavity (filled with air and 75 mm glass-fibre insulation on the fire side) was modelled with 50 mm×50 mm solid elements, capturing convection in lieu of explicit CFD. Interfaces between components used tie constraints. Plasterboard fall-off was simulated in phases: for a two-layer ceiling (FS1), the face layer was removed at 85 min and the base layer at 100 min based on test observations; for a three-layer ceiling (FS2), face, middle, and base layers were removed at 110 min, 131 min, and 141 min respectively. Model validation showed very good agreement between FE and experimental temperature profiles. For Specimen FS1, predicted and test curves of plasterboard and truss temperatures closely matched. For Specimen FS2 also, temperature–time curves for all layers and chords agreed reasonably well as seen in Figure 36. In both cases the heat-transfer model captured the timing of rapid temperature rises due to fall-off. These results confirm the truss FE model can reliably predict thermal response (and thus FRL) of truss floors (Ranasinghe, 2025).

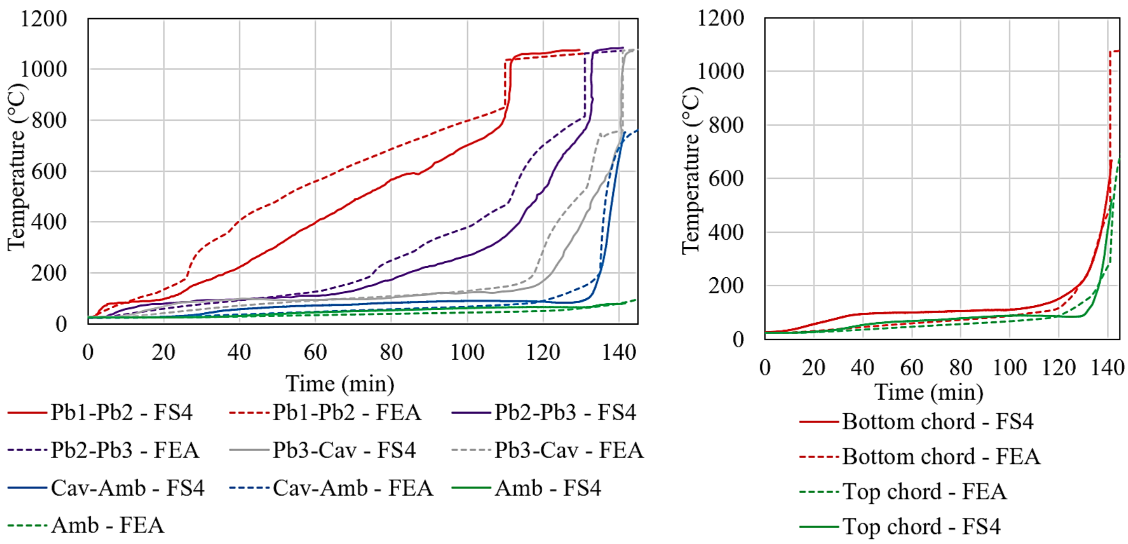

(a) (b)

Figure 36. Comparison of results from FE model and test for Specimen FS2 (a) sheathing temperatures (b) truss temperatures

7.12 Sequentially Coupled Models of Full-scale Lipped Channel Joist Floor Systems

Sequential coupling was performed by applying the thermal model's temperature profiles (either measured in tests or predicted by FE analyses) to a structural FE model of a single joist under fire loading. A transient-state approach was used where a constant load (based on the test load ratio of 0.4) was applied first, then temperatures were raised until failure. The structural model included lipped channel joist geometry (with/without sheathing modelled explicitly) and restraints matching the test setup. For Specimen FS3 (two-layer ceiling), the FE model replicated deflection–time behaviour and predicted a joist failure at 111 min which was comparable with test results (Figure 37). For Specimen FS4 (three-layer ceiling), the FE model showed close behaviour with predicted failure at 168 min (test failure 172 min). Using the FE-predicted temperature curves as input, the coupled analysis yielded failure times of 111 min (Specimen FS3) and 150 min (Specimen FS4), versus 111 min and 168 min when actual measured temperatures were used. The 2×16 mm plasterboard configuration (Specimen FS3) thus gave an FRL of 90/90/90 and the 3×16 mm case (Specimen FS4) 120/120/120 at the load ratio of 0.4. These predictions are conservative (the 150 min versus 168 min difference) but are acceptable. Previous work shows glass-fibre cavity insulation raises FRLs by ≈10%, but no insulation was used here. Overall, the sequentially coupled FE models accurately capture the structural fire performance of joist floors and predict accurate FRLs.

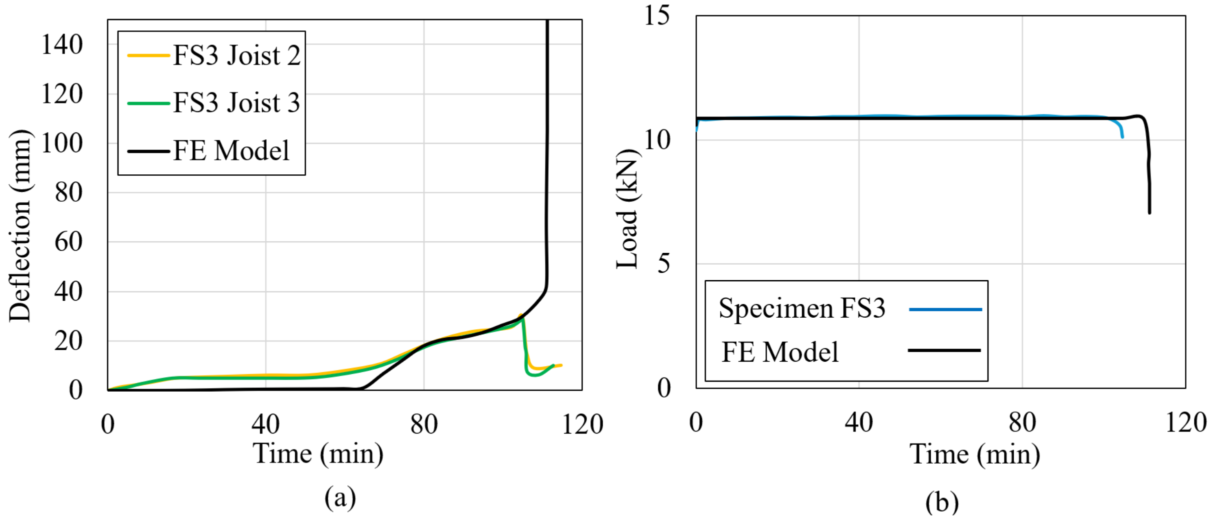

Figure 37. Comparison of results from structural FE model and test for a specimen (a) deflection versus time curve (b) load versus time curve

7.13 Sequentially Coupled Models of Full-scale Truss Floor Systems

The truss sequential models similarly used a transient procedure. In the first stage, recorded test temperatures of the critical top and bottom chords were imposed in the structural model with the applied load held constant. In the second stage, validated heat-transfer model temperatures were used to assess model reliability. As for joists, a load-first, heat-second scheme was followed. The FE analyses predicted failure times of ≈100 min for the two-layer ceiling and ≈141 min for the three-layer ceiling at the load ratio of 0.4. These results agree closely with the fire tests (≈105 min and 142 min, respectively), giving FRLs of 90/90/90 and 120/120/120 for the two- and three-layer configurations. FE models were also able to predict the deflection-time behaviour as seen in Figure 38. Again, cavity insulation had negligible effect on failure time (the use glass-fibre cavity insulation did not change the FRL). In summary, sequentially coupled truss models validated against the two full-scale fire tests (FS1/FS2) provide reliable FRL predictions for LGS truss-floor assemblies (Ranasinghe, 2025).

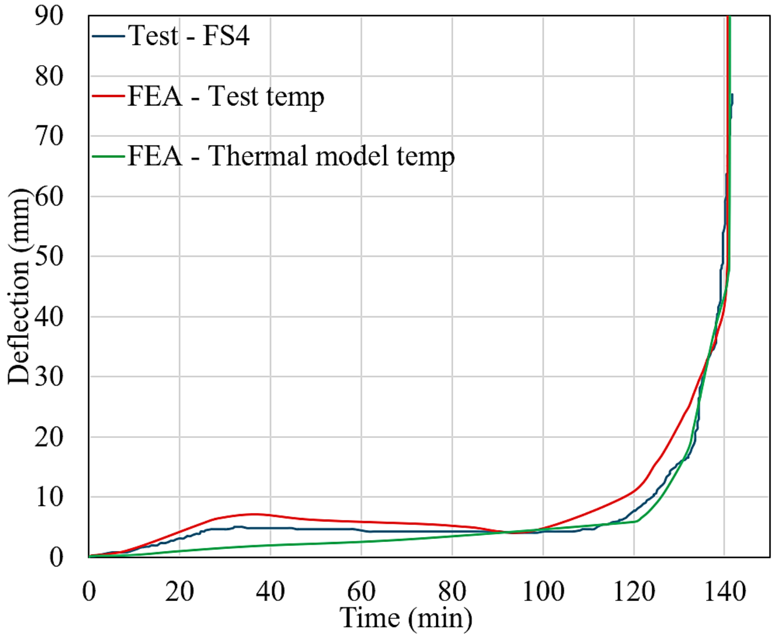

Figure 38. Comparison of deflection versus time curves of a truss specimen (a) test (b) FEA-test temperatures (c) FEA-thermal model temperatures

8 PLASTERBOARD FALL-OFF

8.1 Introduction

Gypsum plasterboards are the primary fire protection layer in lightweight floor systems, acting as a thermal barrier to structural members. However, plasterboard fall-off is critical to the performance of LGS floor systems in fire. Once the boards detach, joists are exposed to direct heating, leading to rapid strength loss and eventual floor failure. The duration for which plasterboards remain in place therefore directly influences the fire resistance level (FRL).

Given the enormous costs and time commitments associated with full-scale fire testing, it is not feasible to generate FRLs for every possible floor configuration using such tests. Therefore, the construction industry lacks a cost effective method to obtain the FRLs that can be used with confidence. This study therefore used the results from six full-scale standard fire tests conducted in this study and 50 previously conducted standard fire tests of lightweight floor assemblies to develop suitable plasterboard fall-off criteria in terms of time and temperature. New equations were proposed for predicting the plasterboard fall-off times using four different methods. These equations can be employed to predict the FRL, taking into account ceiling conditions and post-fall-off failure times.

The fire resistance of lightweight floor assemblies is significantly influenced by the fall-off of gypsum plasterboard; the longer the gypsum board remains in place, the greater the fire resistance. Once the gypsum board falls-off, the principal load-bearing component, the joist, is exposed to direct fire. At high temperatures, the mechanical properties of steel deteriorate, leading to a reduction in the load-bearing capacity of steel joists. Timber joists, when exposed to fire, gradually char and lose their strength. Therefore, increasing the duration for which the plasterboards stay in place can enhance the fire resistance of the floor assembly.

The plasterboard fall-off occurs more rapidly in a floor assembly with cavity insulation compared to one without cavity insulation. Typically, a floor assembly without cavity insulation fails within one to two min after the plasterboard falls-off due to direct exposure to high temperatures. However, this failure time increases when insulation is present in the cavity, as the insulation prevents heat from spreading throughout the cavity. Failure generally occurs in an assembly with cavity insulation after the insulation melts. However, the protection offered by insulation is significantly less compared to that provided by plasterboard. The time required for the insulation to melt depends on the density and type of insulation used. Denser insulations take longer to melt, but they can also cause plasterboard to fall-off more quickly because the insulation retains heat, leading to higher temperatures within the plasterboard. For example, a few minutes after direct exposure to fire, glass fibre insulation becomes ineffective as it melts and falls out of the joist cavities in droplets, leaving the floor and joists exposed. Rockwool insulation, on the other hand, melts and shrinks very slowly under typical fire conditions. Hence even after the plasterboard ceiling is compromised, rockwool insulation can continue to protect the floor and joists from the full effects of the fire. Similarly, a floor assembly with rockwool insulation has a shorter failure time after fall-off compared to one with cellulose fibre sprayed on the underside of the flooring. Cellulose fibre insulation sprayed on the underside of the flooring and the cold flange of the joist continues to protect the joists even after plasterboard fall-off. Since this insulation is applied to the underside of the flooring, its temperatures remain lower compared to other insulation materials placed above the plasterboards, delaying melting. Additionally, cellulose fibre insulation does not fall into the furnace after the base layer plasterboard detaches, unlike the other insulation types.

The average time to joist/floor failure following the fall-off of the base layer was analysed by examining the time elapsed after the first piece of plasterboard fall-off and the last piece of plasterboard fall-off before failure, based on 56 fire tests considered in this study (Table 9). For non-insulated assemblies, joist failure typically occurred approximately two min after the first piece of the base layer fall-off and less than one min after the final piece of the base layer fall-off. In assemblies with commonly used glass fibre cavity insulation, failure occurred around six min after the first piece and approximately three min after the last piece of the base layer fall-off. Assemblies with rockwool and cellulose fibre cavity insulation demonstrated a longer failure time because these materials took more time to melt, thus providing higher FRL compared to assemblies with glass fibre insulation.

Table 9. Average time to failure after base layer plasterboard fall-off in insulated versus non-insulated assemblies

Cavity insulation	Average time to failure after first piece fall-off (min)	Average time to failure after last piece fall-off (min)
Rockwool	16.5	9.4
Cellulose fibre	24.8	19.9
Glass fibre	6.8	2.8
No cavity insulation	2.1	0.9

8.2 Review of Related Studies

Numerous international studies have investigated the performance of plasterboard in fire. Sultan et al. (2005); Sultan et al. (1998) conducted extensive fire resistance testing in Canada on both timber and steel-framed floors. Their research identified that plasterboard fall-off could be identified using cavity temperature spikes, which coincided with board detachment. Later, Sultan and Roy-Poirier (2007) established temperature-based plasterboard fall-off criteria for face layer and base layer plasterboards for insulated and non-insulated assemblies.

In Europe, Konig and Walleij (2000) proposed that the critical ceiling fall-off occurs at 600 °C. Plasterboard failure times are proposed using simplified equations by many researchers. Researchers such as Just et al. (2010), (Kraudok, 2015), and Frangi et al. (2008) produced simple linear equations to calculate the fall-off time based on plasterboard thickness. While practical, these models were intentionally conservative, often predicting shorter fire resistance times than observed. As a result, they ensured safety, but sometimes led to overly cautious and expensive fire design outcomes.

More recently, researchers have turned toward integrating fall-off into finite element (FE) modelling. In Australia, Hisham (2025) demonstrated that FE heat transfer models calibrated with actual fall-off times produced joist temperature predictions that closely matched fire test results. This approach highlights the importance of reliable fall-off criteria not only for regulatory compliance but also for advancing cost-effective design and numerical simulation in the construction industry.

8.3 Gypsum Plasterboards in Lightweight Floor Systems

Gypsum plasterboard is manufactured from a gypsum core ($CaSO_4 \cdot 2H_2O$) encased in paper linings. Fire-rated boards are enhanced with additives such as glass fibres, vermiculite, and perlite. These components collectively improve high-temperature stability and delay structural exposure during fire.

The fire resistance of gypsum boards can be explained through three key mechanisms:

1. **Dehydration and calcination** – When heated above 100 °C, gypsum releases chemically bound water in two stages, at around 160 °C and 180 °C. This endothermic reaction absorbs heat, slowing temperature rise in the cavity (Steau & Mahendran, 2021a). Once water is fully released, the core becomes a brittle powder prone to disintegration.
2. **Fibre reinforcement** – Glass fibres embedded in fire-rated boards hold the gypsum together after dehydration (Figure 39). Instead of forming large cracks that trigger premature

detachment, fibres create fine crack networks, keeping the board attached until fibres themselves degrade around 700 °C (Thomas, 2002).

3. **Additives and shrinkage control** – Vermiculite expands under heating, offsetting gypsum shrinkage, while perlite reduces thermal conductivity and density. Together they slow crack propagation and heat penetration (Richardson, 2001).

The thickness and configuration of boards also matter. Thicker boards or multiple layers extend protection times, but the improvement is not proportional. A single 25 mm board can outperform two 12.5 mm boards because the joint and fixing behaviour also influences the performance in fire (Just et al., 2010). Thus, both material properties and assembly details combine to determine overall fire resistance.

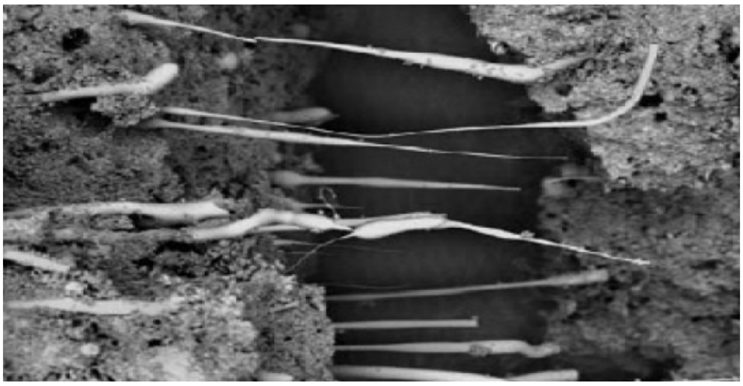

Figure 39. Microstructure of glass fibre-reinforced fire-rated plasterboard

8.4 Gypsum Plasterboard Fall-off in Floor systems Exposed to Fire

Plasterboard fall-off depends on multiple factors.

- **Board type and thickness:** Ordinary boards detach quickly compared to fire-rated boards. While thicker boards offer more protection, their increased weight also adds stress to fixings, leading to earlier detachment.
- **Layer configuration:** In multi-layer ceilings, the face layer offers the main resistance. Once it detaches, the base layer, already weakened by heat transfer, fails within minutes. Correct placement of thicker boards (on the fire side) is therefore critical (Just, 2010).
- **Fastening and spacing:** Wider joist spacing reduces the number of screws supporting each board. For example, increasing the screw spacing from 400 mm to 600 mm reduces fastener density by nearly 30%, which increases stress per screw and promotes earlier failure (Sultan, 2008).
- **Cavity insulation:** Insulation strongly influences plasterboard fall-off. While it delays heat transfer to joists, it accelerates plasterboard calcination by retaining heat. Glass fibre insulation fails quickly after heating, while rockwool and cellulose insulation continue to protect even after plasterboard detachment (Benichou et al., 2001).
- **Flooring material:** The type of flooring above the joists (e.g. plywood versus OSB) has limited impact on fall-off timing, although OSB tends to produce more smoke because of its resin content (Sultan et al., 2005).

Observations from fire tests confirm that plasterboard fall-off is not a sudden, single event but a staged process as shown in Figure 40. . Boards crack, joints open, and pieces detach over time, with face layers generally failing before base layers. Once this sequence starts, joists are increasingly exposed, and floor failure becomes inevitable.

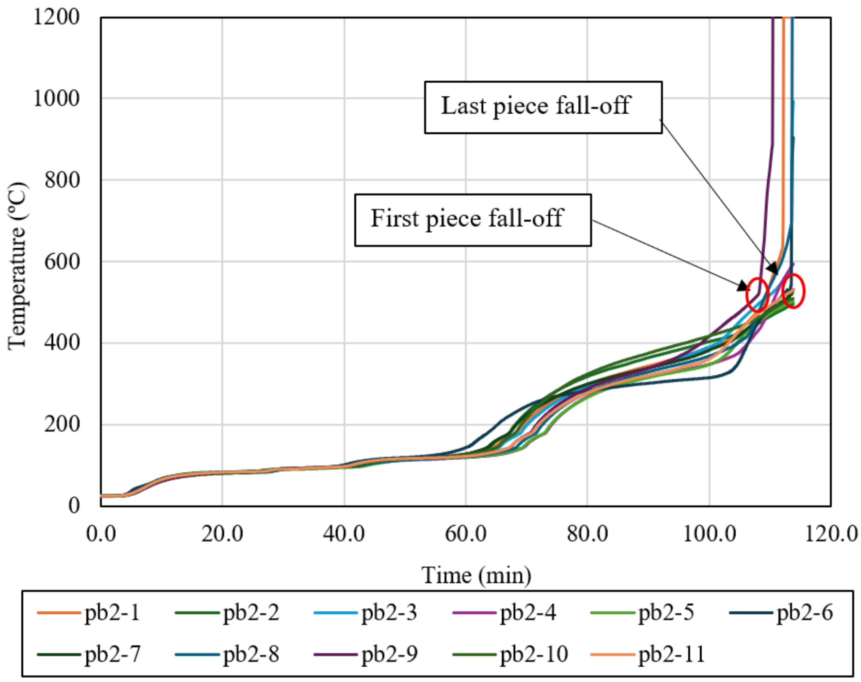

Figure 40. Plasterboard fall-off and joist exposure in a fire test

8.5 Fall-off Criterion for Gypsum Plasterboard

8.5.1 Gypsum plasterboard fall-off temperatures

Since previous studies on determining the plasterboard fall-off temperatures were conducted decades ago and plasterboards have undergone continual improvements since then, this study reassessed the accuracy of the fall-off temperatures reported in earlier research. Full-scale fire tests conducted as part of this study were used to evaluate the fall-off temperatures for each plasterboard layer, focusing on the temperatures recorded on the unexposed side of the plasterboard. In this study, joist spacing was maintained at 600 mm, and commonly used glass fibre was used as the cavity insulation material. The minimum fall-off temperatures observed for the first piece of face layer, middle layer and base layer plasterboards are summarised in Table 10. The fall-off temperatures determined in this study can be used in numerical modelling to remove plasterboard ceilings upon reaching the critical temperature, facilitating more accurate modelling of plasterboard fall-off in lightweight floor systems.

Table 10. Minimum plasterboard fall-off temperatures observed in fire tests

Assembly	Fall-off temperature (°C)		
	Face layer	Middle layer	Base layer
Insulated	630	615	640
Non-insulated	625	665	580

8.5.2 Gypsum plasterboard fall-off times

To derive reliable plasterboard fall-off equations, 56 fire test results, including those from this study as well as previous studies by Sultan et al. (2005); Sultan et al. (1998) and Ye et al. (2017) obtained for two layers of 13 or 16 mm and three 16 mm plasterboard configurations were analysed. Fall-off times were analysed separately for insulated and non-insulated floor assemblies, as fall-off occurs more quickly in cavity insulated floor assemblies. Equations were developed by considering the fall-off times of the first and last pieces of the base layer, which were obtained for insulated and non-insulated floor assemblies as shown in Figure 41 and Figure 42, respectively. Given the unpredictable nature of gypsum plasterboard behaviour, fall-off equations were also developed using the average fall-off times for the first piece of the base layer in all the tests, as well as a 5% fractile value as the worst-case scenario, following the approach of previous studies (Just, 2010; Kraudok, 2015). Similarly, the average and 5% fractile values were considered for the last piece fall-off, resulting in four equations each for insulated and non-insulated floor assemblies. The developed equations for insulated and non-insulated assemblies are shown next.

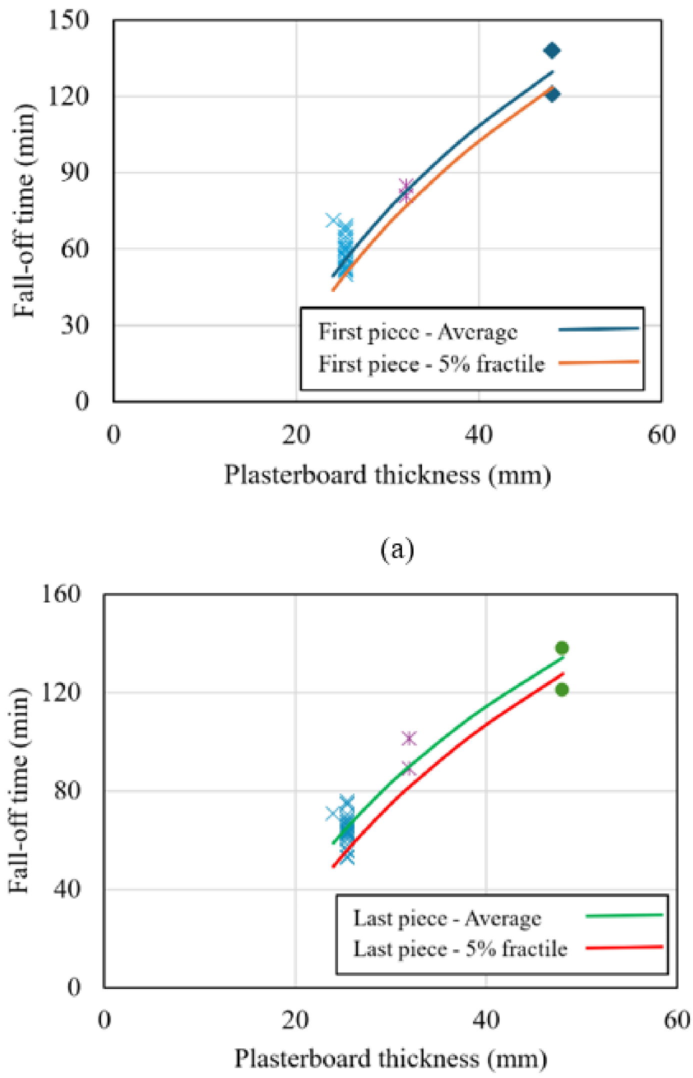

(b)

Figure 41. Developing the fall-off equations for the base layer plasterboard in cavity insulated floor assemblies (a) first piece fall-off (b) last piece fall-off

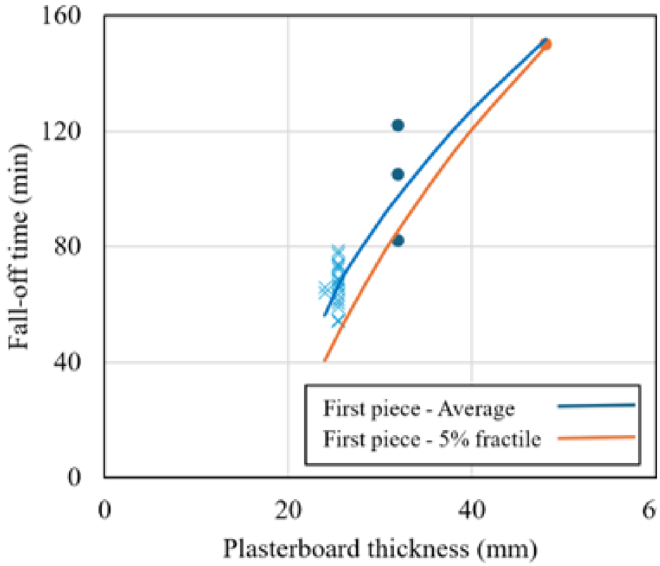

(a)

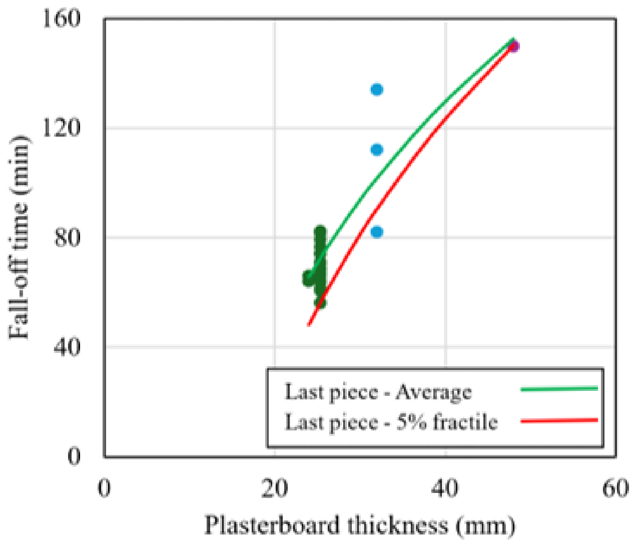

(b)

Figure 42. Developing the fall-off equations for the base layer plasterboard in non-insulated floor assemblies (a) first piece fall-off (b) last piece fall-off

Plasterboard fall-off times for cavity insulated floor assemblies

Average time for first piece fall-off (Method 1)	T_f = 115.7 ln(t) – 318.38
5% fractile time for first piece fall-off (Method 2)	T_f = 114.61 ln(t) - 320.35
Average time for last piece fall-off (Method 3)	T_f = 108.81 ln(t) - 287.06
5% fractile time for last piece fall-off (Method 4)	T_f = 112.83 ln(t) - 309.27

Plasterboard fall-off times for non-insulated floor assemblies

Average time for first piece fall-off (Method 1) $T_f = 133.8 \ln(t) – 366.11$

5% fractile time for first piece fall-off (Method 2) $T_f = 157.2 \ln(t) – 459.16$

Average time for last piece fall-off (Method 3) $T_f = 125.41 \ln(t) – 332.84$

5% fractile time for last piece fall-off (Method 4) $T_f = 147.4 \ln(t) – 421.3$

Table 11 presents the joist failure times/FRLs predicted based on the fall-off times provided by the equations discussed above, and the average time to joist failure after base layer plasterboard fall-off in Table 9, for each tested configuration. Among the four methods, the FRLs obtained using the fall-off times from Method 3 were the closest to the FRLs from the fire tests. The FRLs predicted by Method 2 were consistently conservative. The second most conservative approach was Method 4, which in most cases predicted FRLs closer to the fire test results, except for two configurations.

The recommended equations in this study has to be conservative enough to cover the potential use of materials with inferior performance, rather than for product development. These equations also should not be too conservative such that they are not cost effective. Therefore, Method 4-based equations are recommended for designers to predict the plasterboard fall-off times and the failure times/FRLs of lightweight floor configurations. Since Method 3-based equations provide the closest failure time predictions to the fire test results compared to other methods, they are recommended for researchers in their FE analyses and investigations of lightweight floor systems.

Table 11. Comparisons of predicted FRLs with fire test results.

Test Failure time (FRL)	Method 1	Method 2	Method 3	Method 4
60 (60/60/60)	65 (60/60/60)	59 (30/30/30)	69 (60/60/60)	61 (60/60/60)
111 (90/90/90)	99 (90/90/90)	88 (60/60/60)	103 (90/90/90)	90 (90/90/90)
138 (120/120/120)	99 (90/90/90)	88 (60/60/60)	103 (90/90/90)	90 (90/90/90)
103 (90/90/90)	88 (60/60/60)	83 (60/60/60)	93 (90/90/90)	85 (60/60/60)
150 (120/120/120)	153 (120/120/120)	151 (120/120/120)	153 (120/120/120)	150 (120/120/120)
141 (120/120/120)	135 (120/120/120)	129 (120/120/120)	136 (120/120/120)	130 (120/120/120)

The predicted fall-off times and FRLs using the recommended methods represent significant improvements over those suggested by previous researchers. These refined predictions provide more accurate and less conservative estimations of fall-off times and FRLs for floor assemblies, making them more suitable for practical design and modelling applications.

9 PARAMETRIC STUDIES

9.1 Introduction

Most building construction methods prioritise fire safety. To meet the fire safety requirements of building codes, structures must be designed with the required fire resistance levels (FRLs), which are determined by three key factors: structural adequacy, insulation, and integrity. These factors assess a building's ability to support its load, keep the temperature of the unexposed surface within safe limits, and prevent hot gases and flames from penetrating to the unexposed side. FRLs are usually determined through full-scale fire tests using the standard fire temperature-time curves outlined in AS/NZS 1530.4 (2014).

Conducting fire tests for every potential floor configuration used in the industry, as well as for new configurations that may be used, is not feasible due to the high costs and time demands of full-scale fire testing. Therefore, numerical models were developed to increase the knowledge of LGS floors. In Chapter 7, finite element software, Abaqus, was used to create suitable advanced heat transfer and structural FE models of LGS floor systems, which were verified against the fire test results. In this chapter, the verified models from the previous chapter were used to conduct a detailed parametric study to understand the behaviour of LGS floor systems in fire.

9.2 Factors Affecting the FRLs of Channel Joist/Truss Floor Systems

The behaviour and failure times of LGS floor systems in fire was studied using the results from past research, small- and full-scale fire tests and associated FE analyses, and numerical parametric studies conducted in this project. The following discussion is based these results.

9.2.1 Effect of cavity insulation

This study found that cavity insulation had only a limited effect on the FRL of floor systems. Previous research has reported varied outcomes: some studies identified small improvements in failure times, while others noted minimal differences compared to non-insulated systems. The effectiveness of insulation largely depends on the material type. Mineral wool (Rockwool) and cellulose fibre have been shown to provide better protection than glass fibre. In insulated assemblies, plasterboard often detaches earlier; however, the insulation layer can continue to shield the steel components for a short period. By contrast, non-insulated assemblies tend to fail immediately once the plasterboard falls-off. Denser insulation materials, such as mineral wool, offer greater benefits as they resist melting or detachment for longer, thereby extending the failure time. Overall, the difference in FRLs between light-gauge steel floor systems with and without cavity insulation was found to be minimal.

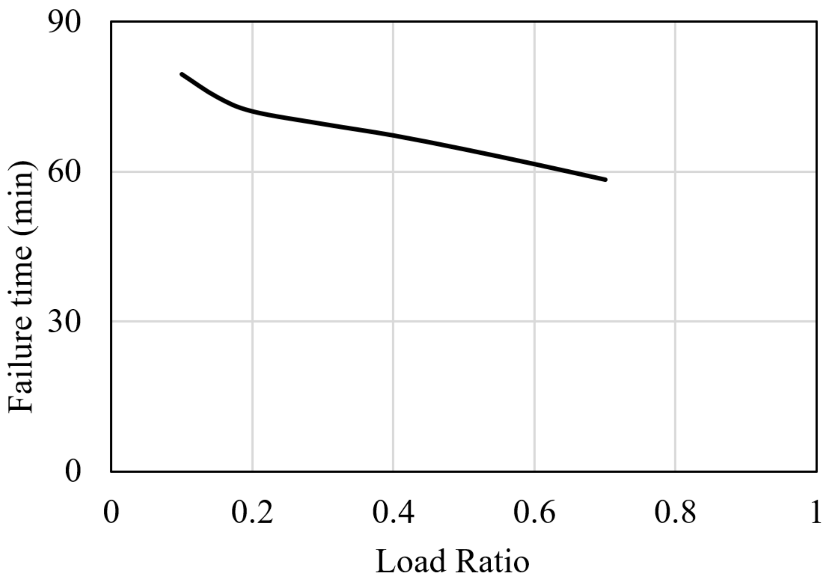

Figure 43. Failure time versus load ratio curve for two 13 mm plasterboard ceiling configuration

9.2.2 Effect of load ratio

Verified numerical models were used to investigate the effect of load ratios ranging from 0.1 to 0.7. An example is shown in Figure 43. This indicates that for floors with two layers of 13 mm plasterboard, the failure time decreases as the load ratio increases. This was the case with other configurations also. Overall, when the load ratio increases, the failure time of a LGS floor decreases.

9.2.3 Effect of joist/truss depth

A parametric study was conducted using different lipped channel joist and truss sections to analyse the effect of section depth on FRL. Examples of results are shown in Figure 44 and Figure 45. Overall, the effect of joist section depth can be considered insignificant. Nevertheless, it should be noted that if the failure times are close to a specific FRL bracket, this 5% difference could be critical in determining the appropriate FRL bracket. Hence, for configurations where failure times are near an FRL threshold, the FRLs for different section depths should be assessed separately.

9.2.4 Effect of span

Moe than 120 structural FE models were analysed to check the effect of span on the FRLs of LGS floor systems. The FRL comparison shows that for all FE models, the failure time remained almost the same, indicating that the effect of span on FRL is insignificant.

9.2.5 Effect of section thickness

Next, the effect of thickness on FRLs was evaluated. It was seen that the failure times are similar despite having structural members with different thicknesses. This shows that the effect of member thickness is negligible on the FRLs of LGS floor systems.

9.2.6 Effect of member spacing

In LGS floor systems, the channel joist/truss spacings are 300 mm, 450 mm, or 600 mm (maximum). This spacing is generally adjusted to support the design load applied to the flooring. When the spacing is reduced, the load carried by each individual channel joist/truss decreases, thereby reducing the load ratio (LR) and consequently increasing the failure time (FRL) of the floor system. Overall, when the member spacing is reduced, the failure time increases.

9.2.7 Effect of flooring type

Numerical analyses were conducted to identify the FRL when different floorings were used in LGS floor systems. Figure 46 shows the difference between plywood and fibre cement panel flooring with different load ratios for a configuration with three 16 mm plasterboard as an example. The difference in failure times between the considered models were very low. Therefore, it can be concluded that the effect of flooring type on the failure times/FRLs LGS floor ceiling configurations is negligible.

9.2.8 Effect of resilient channels

Resilient or furring channels are commonly used in floor systems to facilitate service penetrations within a floor cavity and avoid direct attachment of plasterboard to joists/trusses. The use of resilient channels, spaced similarly to the joists/trusses, increases the overall cavity depth and provides a slight increase in failure time, typically 1–2 min, as demonstrated by Sultan (2010). However, if the spacing of resilient channels is reduced while maintaining the same member spacing, the number of connections between the plasterboard and frame increases due to the additional screws. Since the load ratio remains unchanged, this reduces the stress borne by each screw connection, delaying plasterboard fall-off. This delay could delay the structural failure of joists and enhance the FRL.

9.2.9 Effect of noggings/blocking truss

Noggings are typically used to prevent the lateral deflection and twisting of joists in LGS floor systems. Twisting of joists primarily occurs in mono-symmetric sections such as channel joists. Blocking truss is typically recommended for truss spans exceeding 3.5 m. To further assess whether twisting would occur under ambient conditions when six joists were used without noggings, a six joist model was developed, similar to the full-scale fire test setup, with and without noggings.

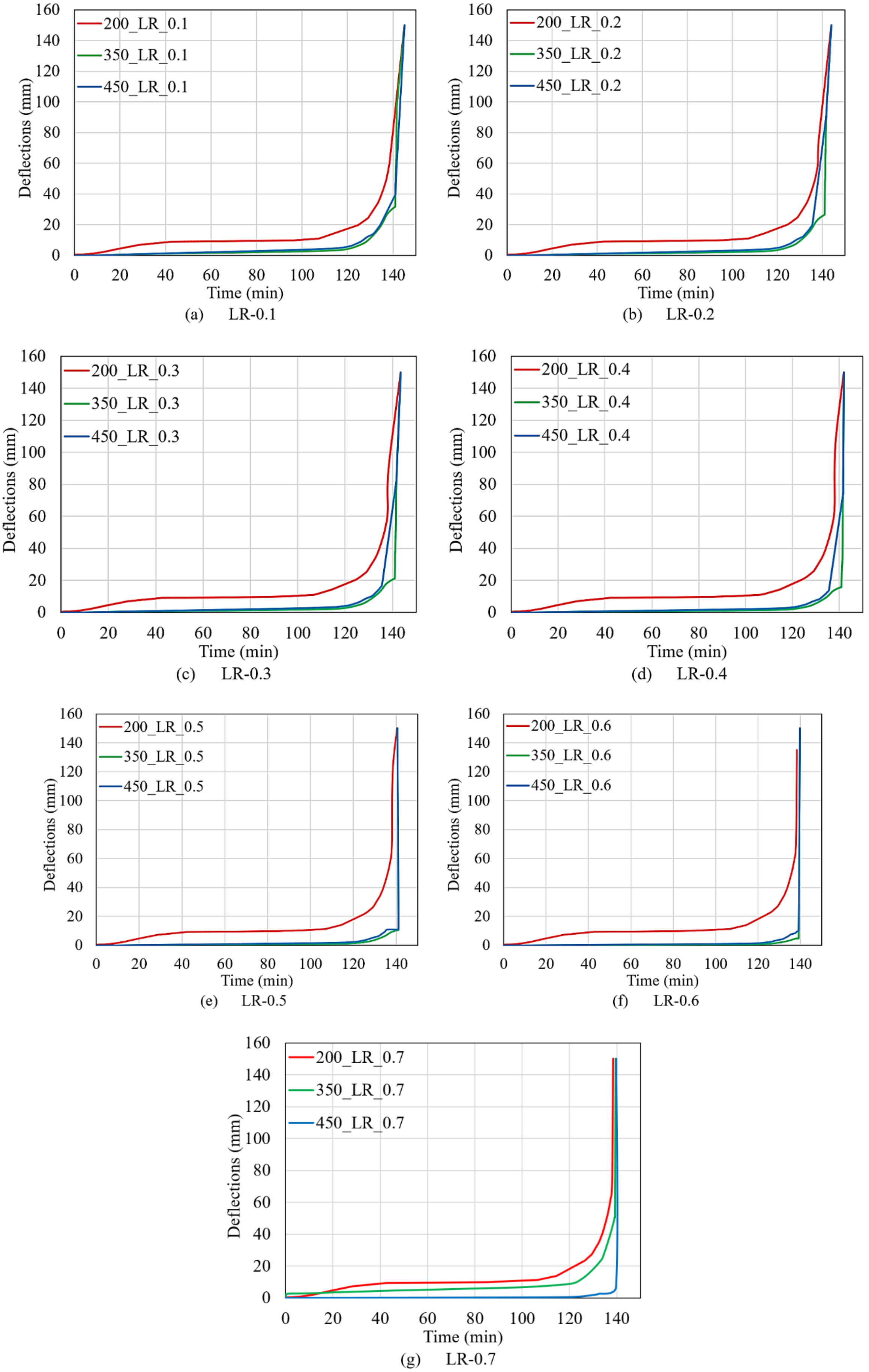

Figure 44. Deflection versus time plots of 200 mm, 350 mm and 450 mm truss depths for three 16 mm plasterboard ceiling configurations

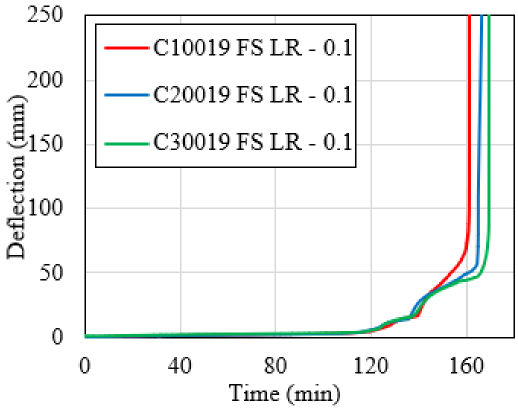

(a) LR – 0.1

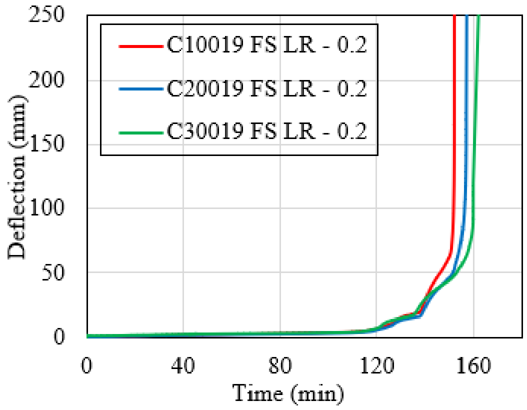

(b) LR – 0.2

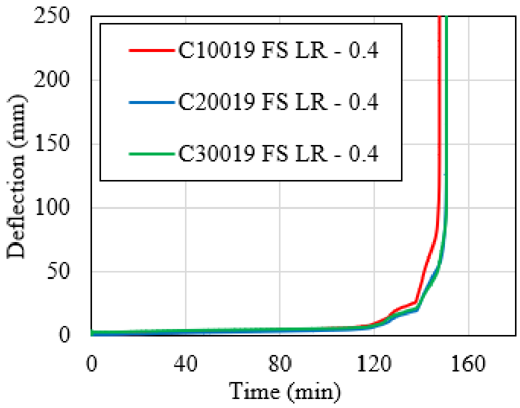

(c) LR – 0.4

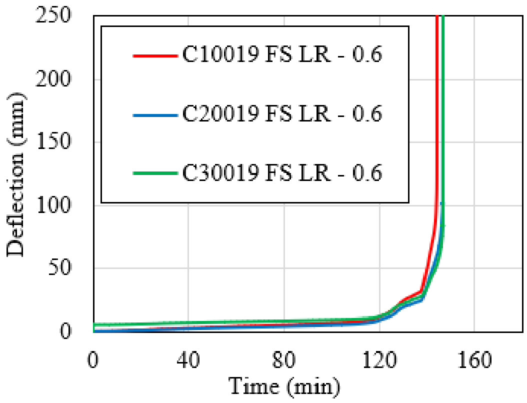

(d) LR – 0.6

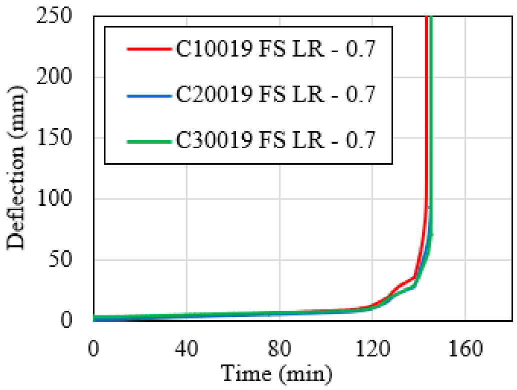

(e) LR – 0.7

Figure 45. Deflection versus time plots of 100 mm, 200 mm and 300 mm joist depths for three 16 mm plasterboard configurations

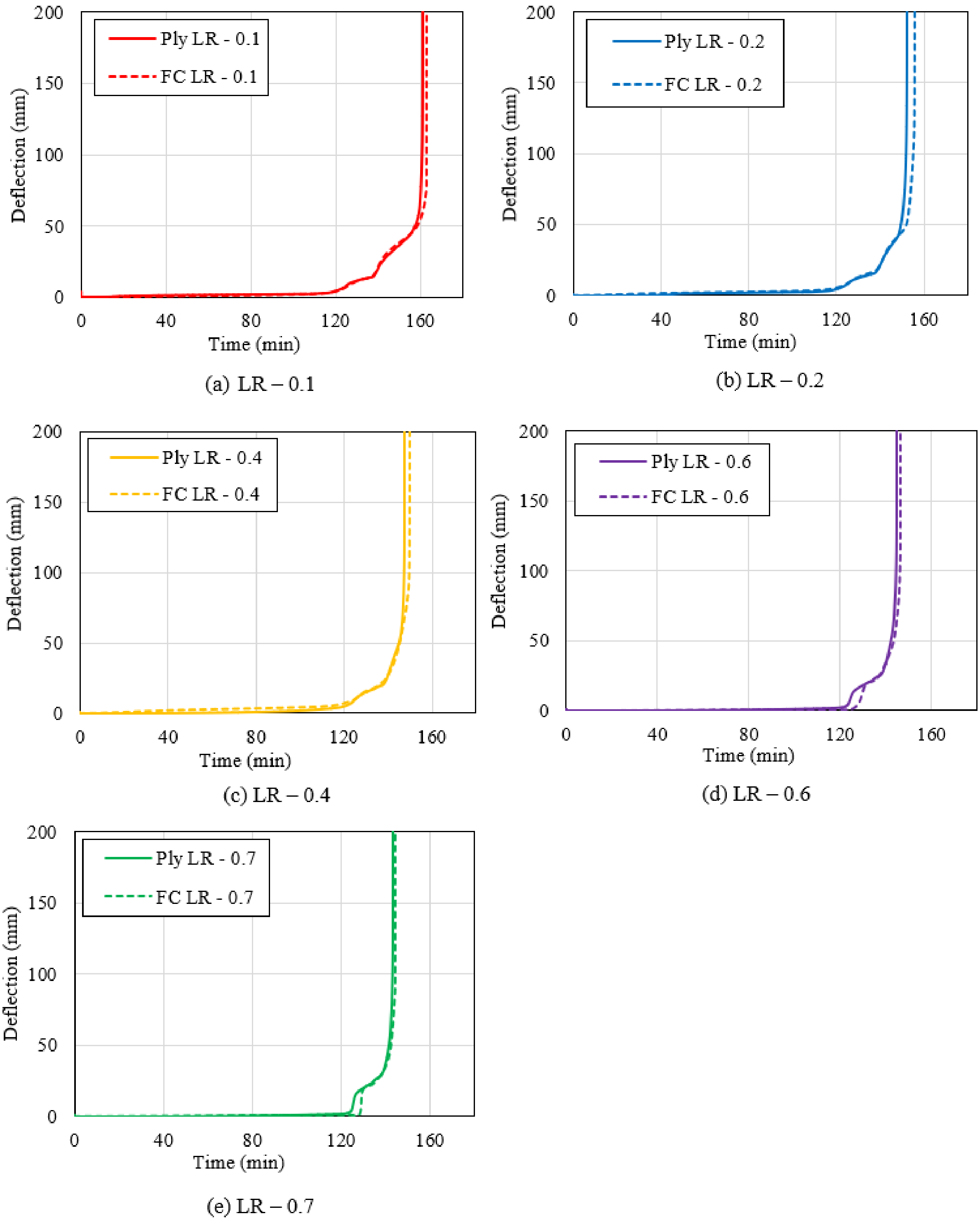

Figure 46. Comparison of deflection versus time plots for plywood and fibre cement panel flooring with three 16 mm plasterboard ceiling under varying load ratios

The introduction of noggings slightly increased the overall stiffness of the frame, but did not enhance the overall load-bearing capacity. Therefore, it is concluded that since the failure capacities were identical, the FRLs of floor configurations with and without noggings will also be the same for the same load ratio.

9.2.10 Effect of plasterboard thickness/layers

According to the FE analysis, the additional plasterboard layer increased the FRL by 35%. Similarly, increasing the board thickness from 26 mm to 32 mm, led to a 25% rise in FRL based on the FE analyses. Increasing the thickness from 32 mm to 48 mm at least increased the FRL by 39%. Thus, it is concluded that increasing the thickness of the gypsum plasterboards or adding an extra plasterboard layer significantly enhances the FRL of the LGS floor system.

9.3 FRLs of a Range of LGS Floors

Determining the FRLs of commonly used LGS joist and truss floor systems is essential for improving the fire safety and developing the lightweight construction industry. Extensive parametric studies were conducted in this project to determine the failure times and thus the FRLs of commonly used LGS joist and truss floor systems using the verified numerical models. The FRL tables generated in this study reveal that the FRL remains relatively consistent across different load ratios, except when the failure time approaches an FRL bracket. To facilitate ease of use for design engineers, a simplified table (Table 12) was produced by disregarding minor variations in failure times among joists with different depths and thicknesses for except for the two 13 mm plasterboard configuration.

Table 12. Summary of FRLs for LGS floor systems with different plasterboard ceiling configurations under varying load ratios.

Ceiling Configuration	Load Ratio	Insulation	Flooring	FRL (min)
13 mm + 13 mm	0.1-0.4	No	PW/PB/FC	60/60/60
13 mm + 13 mm	0.5-0.7	No	PW/PB/FC	30/30/30
13 mm + 13 mm	0.1-0.4	Yes	PW/PB/FC	60/60/60
13 mm + 13 mm	0.5-0.7	Yes	PW/PB/FC	30/30/30
13 mm + 16 mm	0.1-0.7	No	PW/PB/FC	60/60/60
13 mm + 16 mm	0.1-0.7	Yes	PW/PB/FC	60/60/60
16 mm + 16 mm	0.1-0.7	No	PW/PB/FC	90/90/90
16 mm + 16 mm	0.1-0.7	Yes	PW/PB/FC	90/90/90
16 mm + 16 mm	0.1-0.7	No	SC	120/120/120
16 mm + 16 mm	0.1-0.7	Yes	SC	120/120/120
13 mm + 13 mm + 13 mm	0.1-0.7	No	PW/PB/FC	90/90/90
13 mm + 13 mm + 13 mm	0.1-0.7	Yes	PW/PB/FC	90/90/90
13 mm + 13 mm + 13 mm	0.1-0.7	No	SC	120/120/120
13 mm + 13 mm + 13 mm	0.1-0.7	Yes	SC	120/120/120
16 mm + 16 mm+ 16 mm	0.1-0.7	No	PW/PB/FC	120/120/120
16 mm + 16 mm+ 16 mm	0.1-0.7	Yes	PW/PB/FC	120/120/120

PW - Plywood   PB - Particleboard   FC – Fibre cement   SC – Steel-Concrete Composite

9.4 Comparison with Equations Proposed in Chapter 8

Simplified equations to determine plasterboard fall-off times and failure times for floor systems were presented in Chapter 8, focusing just on plasterboard thickness and cavity-insulated assemblies. Since these equations consider only two variables, the parametric study results were used to assess the applicability of the simplified Method 4 based equations from Chapter 8 in predicting the FRL of LGS floor systems as shown in Table 13. This analysis shows that the plasterboard fall-off time equations developed in Chapter 8 are reliable and can be confidently used to conservatively predict the failure times and FRLs for design purposes.

Table 13. FRLs predicted by Method 4 developed in Chapter 8 for common plasterboard configurations.

Plasterboard configuration (mm)	Presence of cavity insulation	Failure time (min)	FRL (min/min/min)
13 + 13	No	60	60/60/60
13 + 13	Yes (glass fibre)	61	60/60/60
13 + 16	No	76	60/60/60
13 + 16	Yes (glass fibre)	73	60/60/60
16 + 16	No	90	90/90/90
16 + 16	Yes (glass fibre)	85	60/60/60
13 + 13 + 13	No	119	90/90/90
13 + 13 + 13	Yes (glass fibre)	107	90/90/90
16 + 16 + 16	No	150	120/120/120
16 + 16 + 16	Yes (glass fibre)	130	120/120/120

10 INVESTIGATION OF LGS WALLS WITH UNPROTECTED COMBUSTIBLE ELCTRICAL SOCKETS AND SERVICE PIPES

10.1 Introduction

This chapter provides the details of experimental studies conducted on small-scale LGS walls to understand the effects of using unprotected combustible electrical sockets and service pipes on their fire resistance.

10.2 Combustible Electrical Sockets

In Light gauge steel framed (LGS) wall systems, electrical sockets made of combustible materials (e.g. polycarbonate) are often installed on the plasterboard lining of the walls via suitable service openings. According to NCC, service openings for electrical sockets must be designed to be fire-rated in many cases, where electrical sockets are required to be protected by the use of fire-rated wall boxes. However, such protection could be inadvertently omitted and its potential impact on fire rated walls in terms of their fire resistance is unknown. In this study, the effects of unprotected combustible electrical sockets (non-compliant construction) on the behaviour of LGS walls exposed to standard fire conditions were investigated.

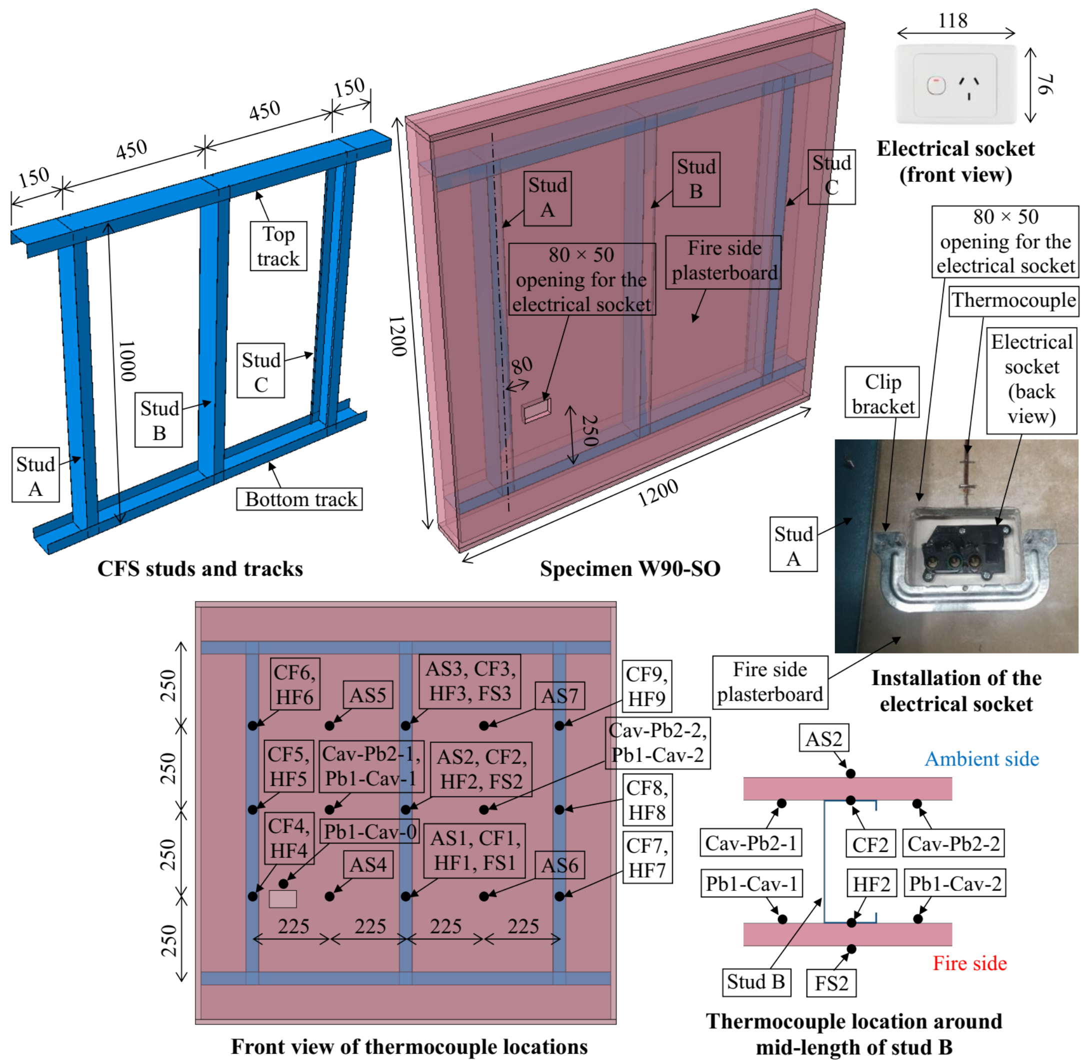

Figure 47. Small-scale wall test specimen with electrical socket and thermocouple locations

Two small-scale (1200 mm x 1200 mm) fire tests were conducted on cavity insulated (glas fibre insulation) and uninsulated LGS walls made of three G550 90 mm lipped channel studs at 450 mm spacing and one 16 mm fire-rated gypsum plasterboard lining on both sides, together with combustible electrical sockets installed on their fire side plasterboards (W90-SO and W90-SO-IN). An electrical socket made of polycarbonate was installed in a service opening using a clip bracket and screws. The service opening of dimensions of 80 mm × 50 mm (width × height) was located on the fire side plasterboard with the centre of the opening located 80 mm from the centre lines of the flanges of Stud A, and 250 mm from the web of the bottom track. Many K-type thermocouples were used to measure the thermal performance of the walls during the fire tests conducted on walls placed vertically in front of a 1.2m x 1.2m gas furnace. During the fire tests conducted for 120 min, the furnace was controlled such that the temperatures inside the furnace followed the nominal standard fire temperature-time curve. Figure 47 shows the above details for test wall specimen W90-SO.

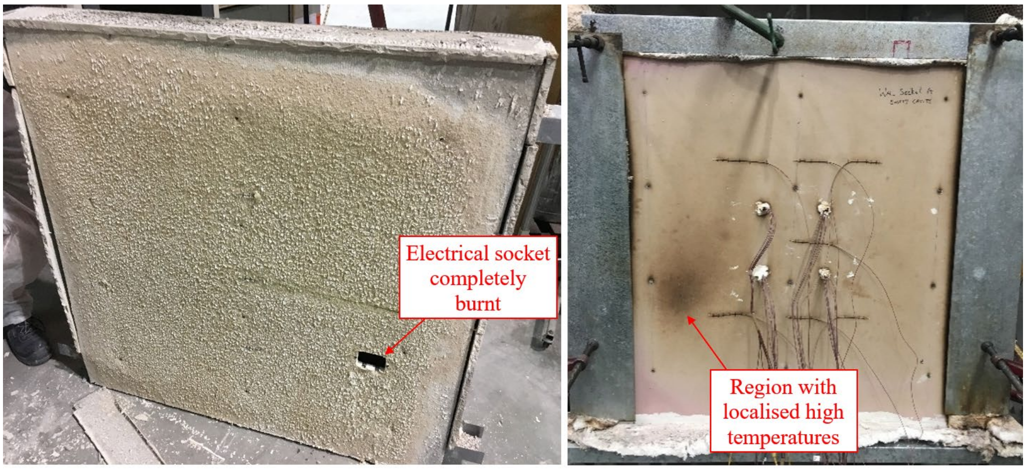

Fire side plasterboard **Ambient side plasterboard**

Figure 48. Small-scale wall test specimen with electrical socket after the fire test.

At the end of the tests, fire side plasterboards were significantly dehydrated, while the electrical sockets were totally burnt, which allowed hot gases to penetrate the wall cavities, however, no significant plasterboard fall-off was recorded. The paper layers on the outer surface of ambient side plasterboard were significantly discoloured, while the regions near the service openings experienced localised burning due to high temperatures as seen in Figure 48. This shows the effect of hot gases penetrating wall cavities through the service openings, causing localised high temperatures on the ambient side plasterboards.

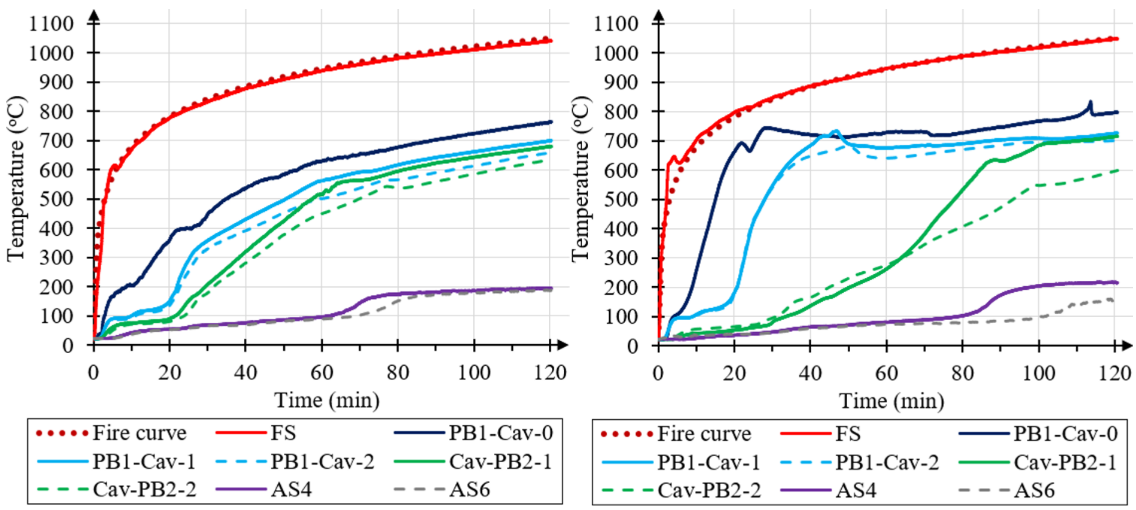

W90-SO **W90-SO-IN**

Figure 49. Temperature-time curves for plasterboard surfaces

As seen in Figure 49, for the two specimens, Pb1-Cav-0 temperatures measured near the location of the service openings were much higher than Pb1-Cav-1 and Pb2-Cav-2 temperatures, which were located at 250 mm above the electrical sockets. Besides, Pb1-Cav-1, Cav-Pb2-1 and AS4 temperatures were higher than Pb1-Cav-2, Cav-Pb2-2 and AS6 temperatures, respectively. This confirmed that the plasterboard temperatures were influenced by its distance from the service openings. The highest temperatures were only given by AS4 thermocouple near the opening. It was clear that combustible electrical sockets and service openings for installing them could lead to non-uniform temperature distributions on the plasterboard surfaces with the hottest regions located near the service openings. There was no integrity failure, but the maximum temperatures on the outer surface of plasterboards near the service openings reached 203 °C at about 70 min for both walls, ie. insulation failure. However, for the identical uninsulated wall specimen investigated Gnanachelvam et al. (2019), but without combustible electrical sockets, the insulation based FRL was about 100 min. In other words, combustible electrical sockets could lead to notable reduction to the insulation-based FRL, but the effects are localised around the service openings only.

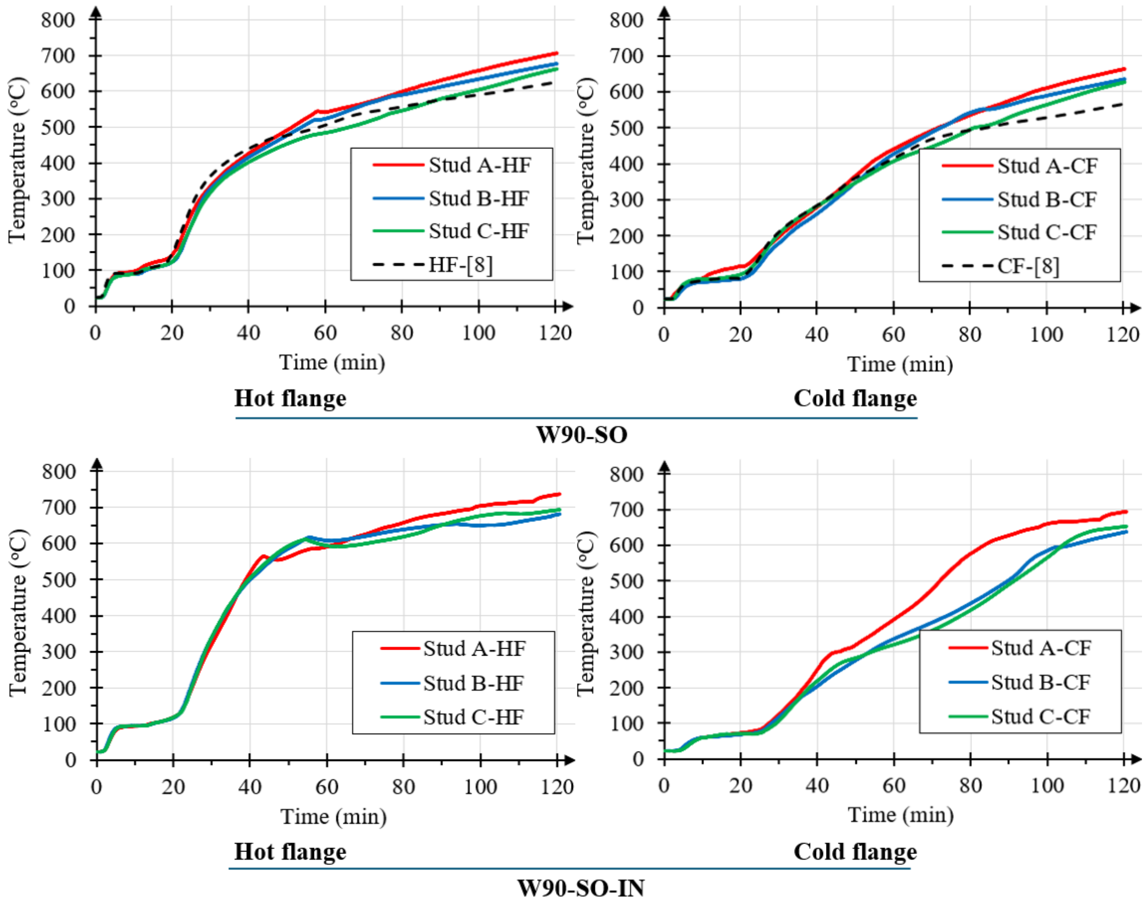

Figure 50. Temperature-time curves for stud hot flange and cold flange

The electric socket was located between Studs A and B in the two wall specimens. However, as shown in Figure 50, the hot and cold flange temperatures of Stud A were higher than those of Stud B because the electrical socket was located closer to Stud A than Stud B. This shows that the effects of a combustible electrical socket will be more significant for the studs located closer to it.

Figure 50 highlights that the maximum stud hot and cold flange temperatures measured on Stud C of Specimen W90-SO, which was located away from the combustible electrical socket and protected from the hot gases by Stud B, were similar to those of the studs in the same uninsulated LGS wall specimen without service openings and combustible electrical sockets in Gnanachelvam et al. (2019). Therefore, Stud C in Specimen W90-SO can be considered to be similar to the studs in uninsulated LGS walls without service openings and combustible electrical sockets. Compared with Stud C in Specimen W90-SO, Stud C in Specimen W90-SO-IN was also located away from the service opening and better protected from hot gases by both Stud B and cavity insulation. Hence, it is reasonable to consider that Stud C in Specimen W90-SO-IN is also similar to the studs in insulated

LGS walls without service openings and combustible electrical sockets. Overall, higher temperatures were only observed in Studs A and B located near the service opening. However, the maximum measured hot flange temperature of Stud A at mid-height during the 120 min of fire exposure was again only slightly higher than those measured on Stud C (<18%) in both walls.

The presence of combustible electrical sockets and service openings could reduce the structural adequacy based FRL of LGS walls, mainly due to the higher hot flange temperatures in the stud located closer to the electrical socket (Stud A). Hence the structural FRLs of the two types of LGS walls tested in this study were estimated for a common load ratio of 0.4 (defined as the ratio of applied compression load to the ambient temperature compression capacity of studs) based on a limiting hot flange temperature of 500 ℃, and they were 50 min (uninsulated) and 40 min (cavity insulated). The corresponding FRL for these LGS walls without any combustible electrical sockets using the hot flange temperatures of Stud C are 60 and 40 min, respectively. At higher load ratios, the differences in FRLs will be further reduced. Hence it is concluded that unprotected combustible electrical sockets is unlikely to significantly reduce the FRL of the walls in a fire and sudden collapses of LGS walls are unlikely in fire due to localised detrimental effects around the service opening.

In this study, electrical sockets used in the test specimen were made of a highly combustible material (polycarbonate), and hence they quickly disappeared during the fire tests. For LGS walls with electrical sockets made of other combustible materials, the same behaviour can be observed. Tests were conducted under standard fire conditions in this study. For realistic fire scenarios, which include ventilation effects, fire loads and localised fires, further research studies are recommended.

10.3 Combustible Service Pipes

In Light gauge steel framed (LGS) wall systems, service pipes made of combustible materials (e.g. polyvinyl chloride (PVC)) are often located through suitable service openings. In this study, the potential detrimental effects of such wall openings on the behaviour of LGS walls exposed to standard fire conditions were investigated.

Two small-scale (1200 mm x 1200 mm) fire tests were conducted on cavity insulated (glass fibre) and uninsulated LGS walls made of three G550 90 mm lipped channel studs at 450 mm spacing and two layers of 16 mm fire-rated gypsum plasterboard lining on both sides (W90-O and W90-O-IN). Both walls included a 100 mm diameter service opening on the plasterboards on both sides at a location closer to the middle stud as depicted in Figure 51 for Specimen W90-O. In fire, combustible pipes would burn quickly and lead to harmful smoke, and thus, they were not used as part of the test specimens in this study. Many K-type thermocouples were used to measure the thermal performance of the walls (Figure 52) during the fire tests conducted on walls placed vertically in front of a 1.2m x 1.2m gas furnace. During the fire tests conducted for 120 min, the furnace was controlled such that the temperatures inside the furnace followed the nominal standard fire temperature-time curve.

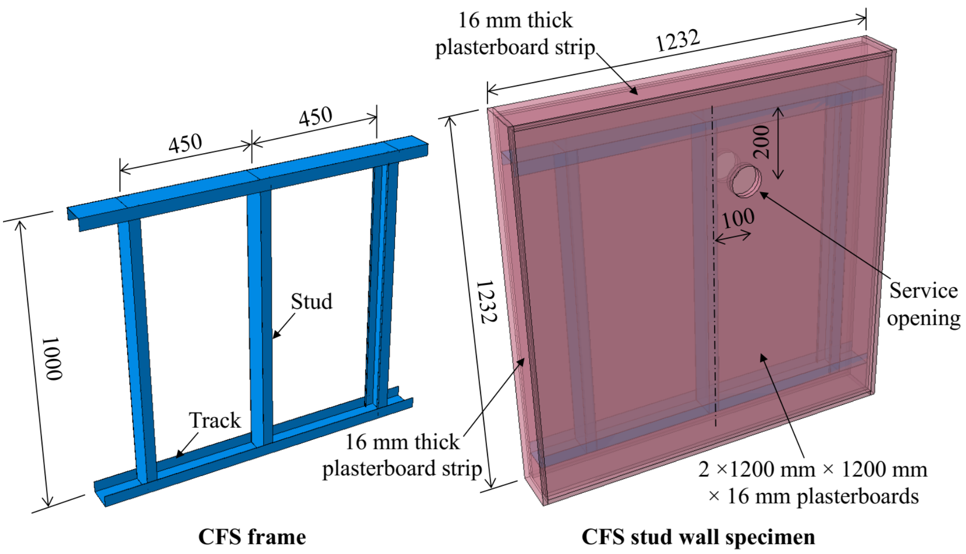

Figure 51. Small-scale wall test specimen with service opening

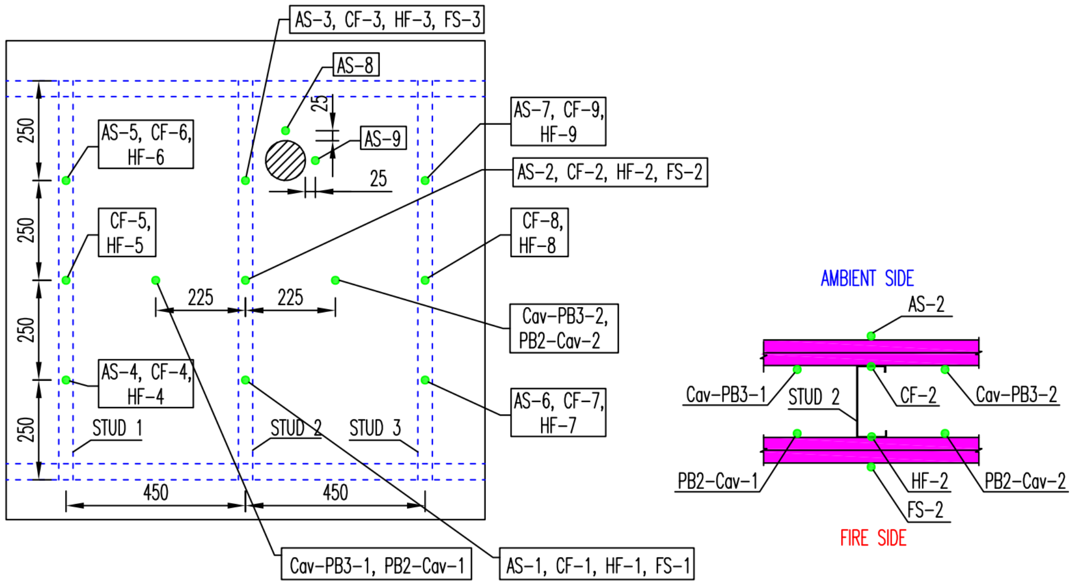

Front view of thermocouple locations in each specimen

Thermocouple locations arround mid-length of stud 2

Figure 52. Thermocouple locations

During the fire tests of both specimens, hot gases only burnt the paper layer of ambient side plasterboards in the region closer to the service opening. For other regions of the ambient side plasterboards, the paper layer was not burnt nor discoloured. Figure 53 and Figure 54 show that AS-8 and AS-9 temperatures measured closer to the service opening were higher than those at AS-1 to AS-7. Cavity side plasterboard surface temperatures measured at locations PB2-Cav-1, PB2-Cav-2, Cav-PB3-1 and Cav-PB3-2 also show large differences.

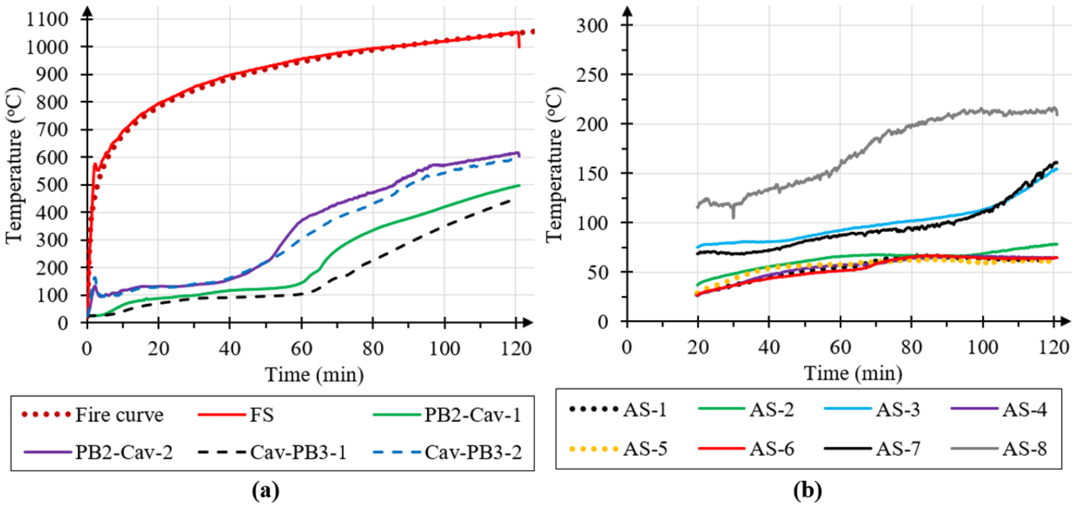

Figure 53. Plasterboard surface temperature-time curves for (a) fire and cavity sides (b) ambient side of Specimen W90-O

For Specimen W90-O-IN, the temperatures at Cav-PB3-2 rapidly increased after 70 min, which implied the melting of glass fibre insulation in the wall cavity with opening. This phenomenon was not recorded for the Cav-PB3-1 temperatures in the wall cavity without opening. In all the above-mentioned cases, the highest temperatures were measured at the locations near the service opening (AS-8 and AS-9; PB2-Cav-2 and Cav-PB3-2). Such temperature differences were not recorded in the fire test results of LGS walls without service openings reported in Dias et al. (2019). This indicates that the wall openings formed to locate combustible service pipes could lead to regions with localised high temperatures on plasterboard surfaces. However, such localised high temperatures were observed only in the regions closer to the service opening, while at other locations, the ambient side plasterboard temperatures were below 100 ℃ after 120 min of fire exposure for both test specimens.

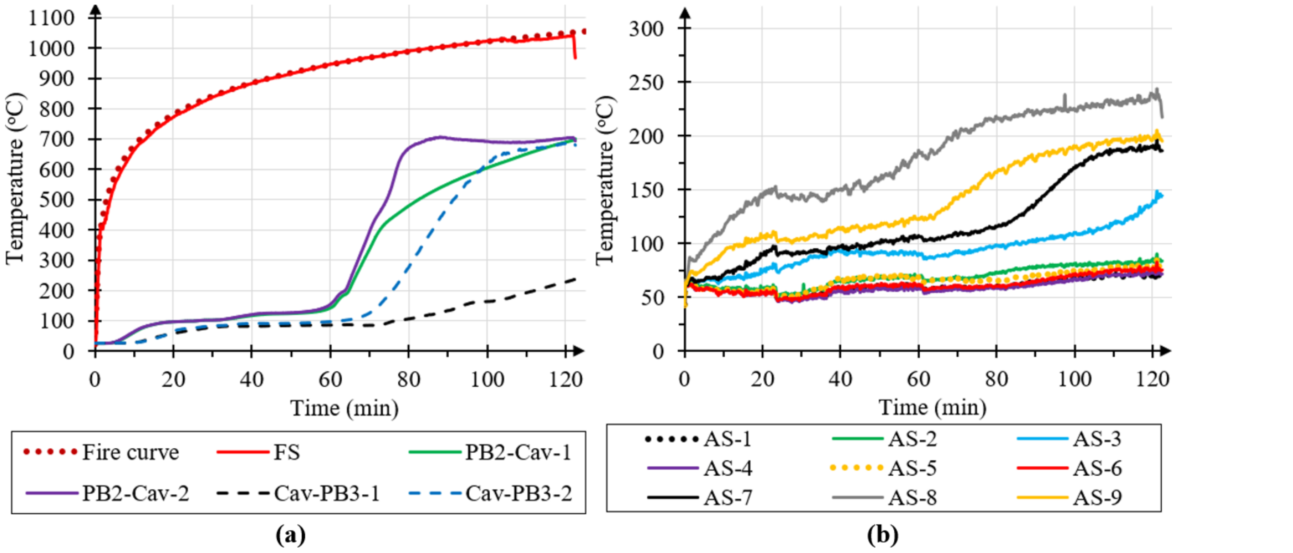

Figure 54. Plasterboard surface temperature-time curves for (a) fire and cavity sides (b) ambient side of Specimen W90-O-IN

Figure 55 and Figure 56 show the hot flange (HF) and cold flange (CF) temperatures of the three wall studs in Specimens W90-O and W90-O-IN. The hot and cold flange temperatures measured on Stud 1 located away from the service opening and thus protected by Stud 2 were the lowest. These temperatures were highly similar to those measured on the studs of the corresponding walls without service openings as shown in the same figures (Ref). This indicates that the effects of opening on the studs away from it are negligible. The highest hot and cold flange temperatures were measured around the top segment of Stud 2 (HF-3), which was closer to the service opening. The largest differences between the highest and lowest hot flange (HF) temperatures were about 400 °C for W90-O and 430 °C for W90-O-IN. Further the hot flange temperatures around the bottom segment of Stud 2 (HF-1) were only slightly higher than those measured on Stud 1 (HF-4 to HF-6), or the lowest values. Meanwhile, the hot flange temperatures measured at the top segment of Stud 2 (HF-3), which was closer to the service opening, were much higher than those measured at the top segment of Stud 3 (HF-9) although the opening was located between these studs. In conclusion, for both specimens, service openings caused large differences in the temperatures between studs and along the stud, with large increases in temperatures only in the stud segments near the opening.

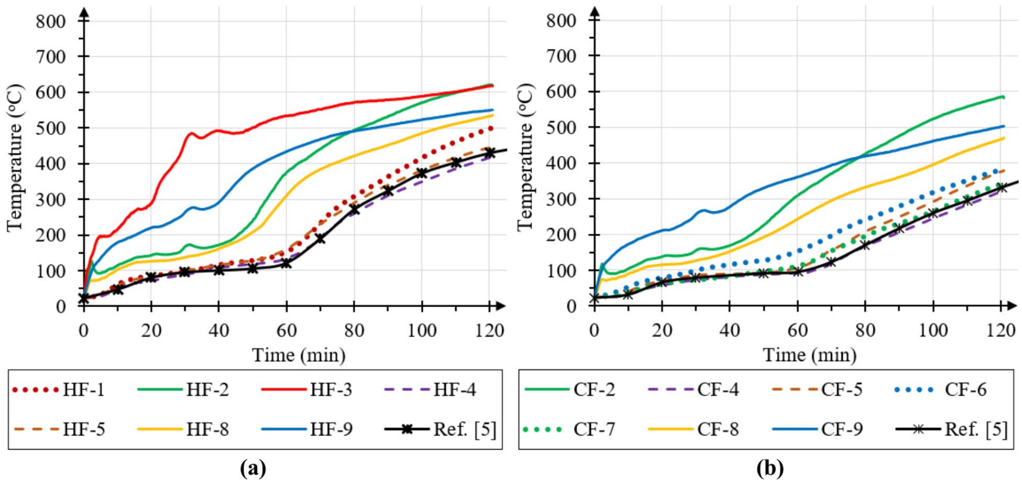

Figure 55. Temperature-time curves for (a) hot flange and (b) cold flange of Specimen W90-O.

Until about 60 min, the hot flange temperatures (HF-3) for the critical middle stud in cavity insulated Specimen W90-O-IN were much lower than those in Specimen W90-O. Especially, at 50 min, the HF-3 temperature for W90-O-IN was only about 200 °C while it was over 500 °C for W90-O. After 60 min, HF-3 temperature of W90-O-IN increased rapidly to over 700°C, while it increased to only about

600 °C for W90-O. This is because initially, glass fibre insulation in W90-O-IN protected the wall stud near the opening (Stud 2) from direct exposure of hot gases. With increasing furnace temperatures, the glass fibre insulation near the service opening and Stud 2 rapidly melted and disappeared at 60 min, but the glass fibre insulation placed between Studs 1 and 2 did not melt rapidly due to the protection of Stud 2 from hot gasses. Therefore, after about 60 min, both the top segments of Studs 2 of W90-O and W90-O-IN were directly exposed to hot gasses, however, there was more heat concentration on Stud 2 of W90-O-IN due to the presence of glass fibre between Studs 1 and 2, which prevented the heat transfer between wall cavities. This led to the more rapid rise in the temperatures of Stud 2 in W90-O-IN from about 60 min (Figure 56).

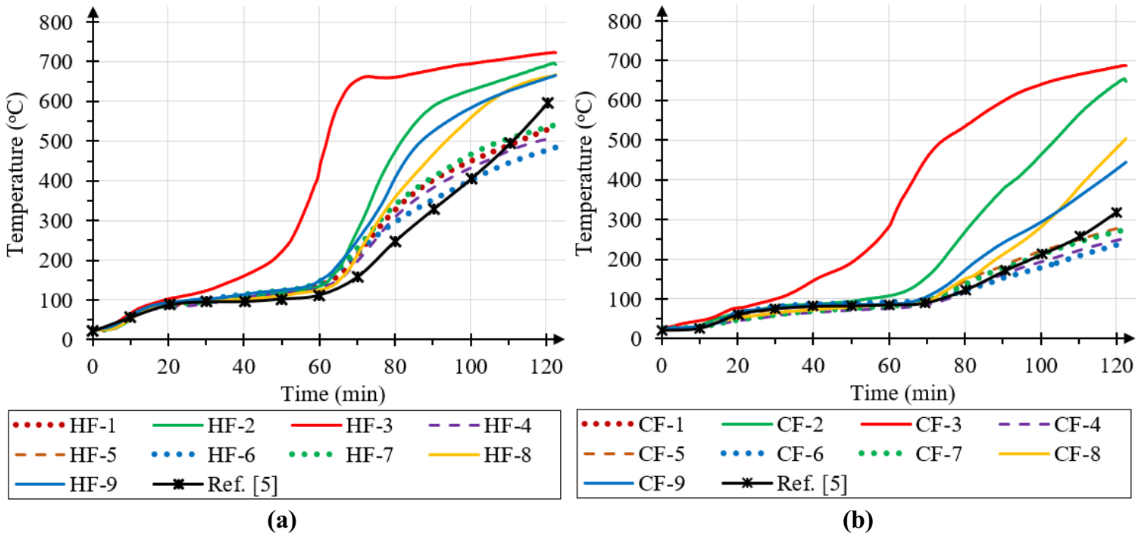

Figure 56. Temperature-time curves for (a) hot flange and (b) cold flange of Specimen W90-O-IN.

For the wall specimens in this study, the integrity criterion was not satisfied because the flame, smoke and heat can directly go through service openings to the unexposed side. The insulation criterion was reached at 80 min and 70 min for W90-O and W90-O-IN based on the measured ambient side plasterboard surface temperatures. The important structural adequacy criterion is discussed next. Until about 45 min, the hot flange (HF-2 and HF-9) and cold flange (CF-2 and CF-9) temperatures of the studs located near the service opening in W90-O were similar. For W90-O-IN, the differences between the hot flange (HF-2, HF-3 and HF-9) and cold flange (CF2, CF-3 and CF-9) temperatures were minor until about 55 min. This shows the unique behaviour of the stud segments near the service openings of both specimens. The highest stud hot flange temperatures in the critical middle studs of Specimens W90-O and W90-O-IN exceeded 500 °C after 40 min and 60 min, respectively. Since the critical hot flange temperature of studs in LGS walls in fire was about 500 °C for a load ratio of 0.4, structural adequacy based failure times are predicted as 40 min and 60 min for the full-scale LGS walls with the same configurations and service openings as W90-O and W90-O-IN. In comparison, the failure times of the uninsulated and insulated LGS walls without any service openings were reported as 123 min and 72 min (Dias et al. 2019), respectively. Hence structural adequacy based FRL of load-bearing LGS walls is reduced when service openings are introduced, but they can still have reasonable FRLs (higher than 30 min).

Overall, this study has shown that service openings caused large differences in the temperatures of wall studs and plasterboards, with localised high temperatures only in the wall studs located near the service opening. For the uninsulated and cavity insulated LGS walls with service openings investigated in this study, although the integrity and insulation criteria based FRLs were not satisfied or inadequate, their structural adequacy-based FRLs were estimated as 40 and 60 min, respectively, for a common load ratio of 0.4. Test results and the following analyses indicate that the effects of service openings are localised to the regions around the opening and that LGS walls could still have reasonable FRLs (>30 min) without any sudden collapse. However, it is recommended that combustible service pipes are not used in LGS walls, and when this is not possible, the service pipes should not be located near the wall studs while a cavity insulation with a higher melting temperature such as stone wool should be used.

11 INVESTIGATION OF LGS WALLS WITH NON-FIRE RATED FLOOR/ROOF TO WALL CLEAT CONNECTIONS

11.1 Introduction

This chapter provides the details of experimental and numerical studies conducted on LGS walls with non-fire rated floor/roof to wall cleat connections to understand the effects of such connections on their fire resistance.

In LGS building structures, CFS studs of LGS walls are connected to corresponding CFS joists or trusses of LGS floors/roofs. In many applications, LGS floors/roofs are designed with very low FRLs or without any fire rating, where the floor-to-wall connections can be directly exposed to fire. This implies that the load-bearing capacity and fire resistance of LGS walls can be reduced. This study investigates the potential detrimental effects of fire-exposed floor-to-wall connections on the fire resistance behaviour and FRL of LGS walls. A cavity insulated LGS wall was chosen as a case study with floor-to-wall cleat connections (Figure 57). A standard fire test was conducted on a small-scale (1.2 m × 1.2 m) cavity insulated LGS wall assembly with floor-to-wall cleat connections. A suitable thermal finite element (FE) model was then developed and validated using the fire test results. The thermal FE model was then modified to represent the full-scale standard fire tests of LGS walls and validated using test results, following which it was used to study the effects of steel cleat thickness and cleat-to-stud contact. Finally, the temperature predictions of the modified thermal FE model were incorporated in sequentially coupled structural FE models to assess the structural behaviour and the reduced FRLs of LGS walls caused by non-fire rated floor-to-wall cleat connections.

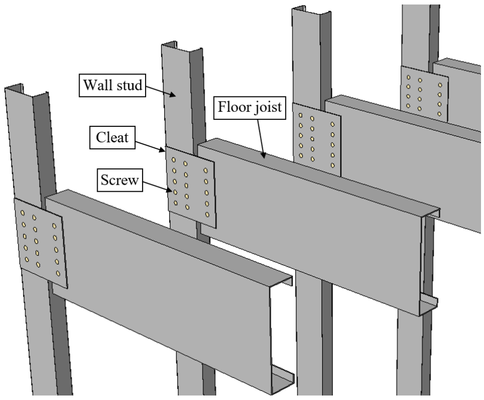

Figure 57. Typical floor-to-wall cleat connections.

11.2 Experimental Study

The specimen used in this study was designed based on those used for small-scale fire tests of non-load bearing LGS walls and Figure 58 shows its fabrication steps. The specimen was made of three 0.75 mm G550 90 mm lipped channel studs of 1000 mm length (A, B and C) fixed to two 1200 mm long unlipped channel tracks. At the mid-height of Stud A, a 150 mm × 230 mm × 1.9 mm G450 steel cleat (Cleat A) was attached to its web using two rows of four 6g screws, extending symmetrically on both sides (outer cleat edges at 70 mm from the stud flanges). Similarly, at mid-height of Stud C, a 150 mm × 160 mm × 1.9 mm G450 steel cleat (Cleat C) was fixed to its web using two rows of four 6g screws, extending 70 mm on one side only (Figure 58). Then, the stud flanges on the fire side were lined with two layers of 1200 mm × 1200 mm × 16 mm fire-rated gypsum plasterboards.

In the second step of fabricating the specimen, glass fibre insulation was utilised to fill the wall cavity. In the third step, stud flanges on the ambient side were lined with two layers of 1200 mm × 1200 mm × 16 mm fire rated gypsum plasterboards. Only Cleat A penetrated through the ambient side plasterboards. A 1000 mm long CFS channel member (same size as stud sections and located parallel to Stud A) was connected to Cleat A at mid-height of the stud on the ambient side using two screw connections as shown in Figure 58. This channel member attachment to the cleat was considered to represent a floor system made of joist sections as shown in Figure 57 or trusses. All the gaps between the cleats and plasterboards were filled with a fire-resistant sealant. Finally, the test specimen was fixed vertically in front of a 1200 mm × 1200 mm gas furnace and the test commenced when the furnace was automatically controlled to create the temperatures inside the furnace based on the standard fire curve. The test was stopped after 240 min.

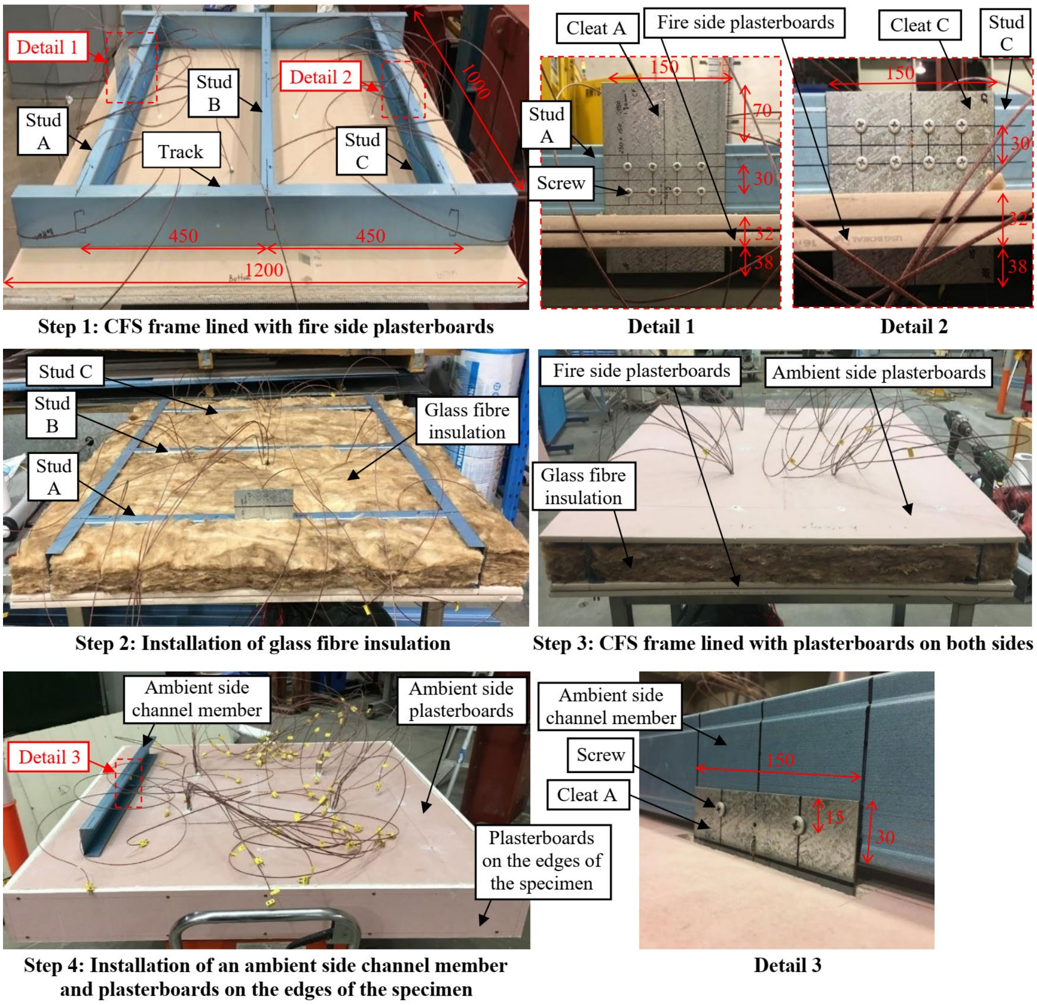

Figure 58. Fabrication of test specimen.

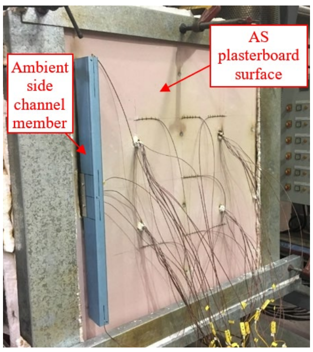

Figure 59. Outer surface of ambient side plasterboards after the test.

Figure 59 shows the wall specimen after the test while Figure 60 and Figure 61 present the average temperatures of various plasterboard surfaces and stud flanges measured in the fire test. Fire side plasterboards had totally fallen off at the end and the exposed regions of steel Cleats A and C were oxidised by fire. The glass fibre insulation had totally melted and disappeared after 180 min when cavity temperatures reached about 700 ℃. As seen in Figure 59, the outer surface of the ambient side plasterboards remained in good condition although their paper layers were partly discoloured.

Figure 60 shows that the temperatures of the additional CFS channel member attached to Cleat A on the ambient side were quite low, below 100 ℃ even after 240 min. In other words, this test has not shown any detrimental temperature rise in the channel member connected to Cleat A on the unexposed side. Further, it shows that the average ambient side plasterboard temperature to be 162.5 ℃, indicating that it has not reached the insulation temperature limit of 163 ℃. However, the maximum ambient side temperature recorded was 206 ℃ after 235 min, revealing that the insulation temperature limit of 203 ℃ was reached, ie. the insulation failure based FRL was 235 min.

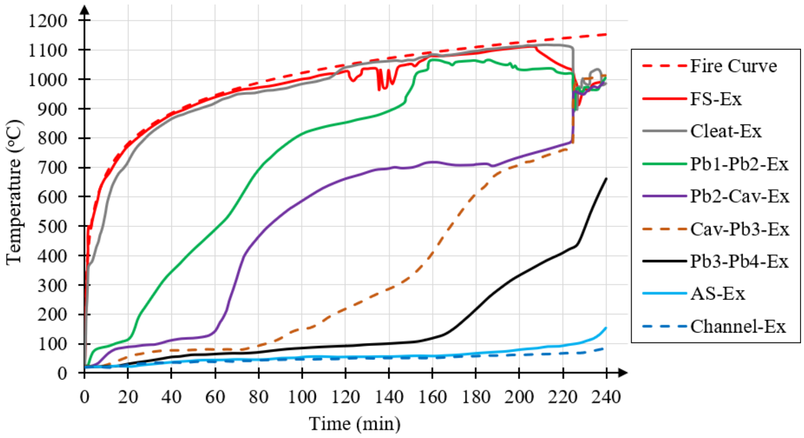

Figure 60. Average temperature-time curves of plasterboard, cleat and channel surfaces.

Figure 61 shows that until 120 min, hot flange temperatures measured at mid-height of Studs A and C, where the fire exposed steel cleats were attached, were significantly higher than those measured at 1/4 and 3/4 height (*L*/4 and 3*L*/4) of the same studs by up to about 170%, and those measured on Stud B without any steel cleats, by up to about 185%. After 120 min, hot flange temperatures at all the measured locations tended to converge. Until 180 min, cold flange temperatures measured at mid-height of Stud C were much higher than those measured at *L*/4 and 3*L*/4 of the same stud by up to about 180%, and those measured on Studs A and B by up to about 160%. After 180 min, cold flange temperatures at all the measured locations tended to converge. For Stud A, since the steel cleat attached to it was also fixed to a CFS lipped channel member on the ambient side, hot flange and cold flange temperatures at its mid-height were less than those measured at mid-height of Stud C by up to about 55 and 100℃, respectively. The measured temperature results therefore show that LGS wall studs with unprotected steel cleats experience localised high temperatures in their flanges, but they are reduced when steel cleats were also connected with CFS members on the ambient side.

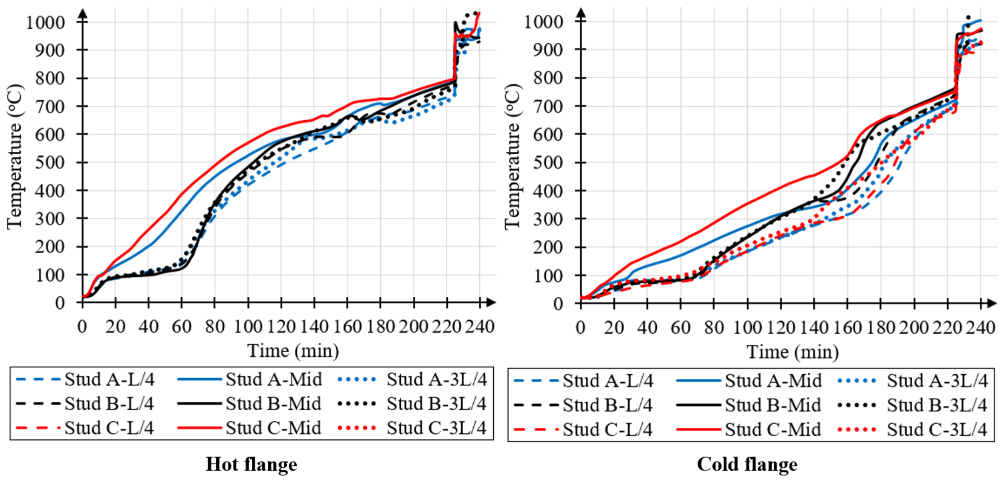

Figure 61. Average temperature-time curves of stud flanges.

11.3 Developing Verified Thermal Models and Parametric Study

A thermal FE model was developed to simulate the tested LGS wall specimen using Abaqus/CAE. The FE model (Figure 62) included accurate details of most components in the wall specimen. The DC3D8 element, a three-dimensional eight-node linear iso-parametric element for heat transfer, was used to simulate studs, plasterboards as well as glass fibre insulation blocks. The overall FE mesh size of every simulated component of the wall was 20 mm. Besides, for ambient and fire side plasterboards, the FE mesh size was 4 mm through their thickness.

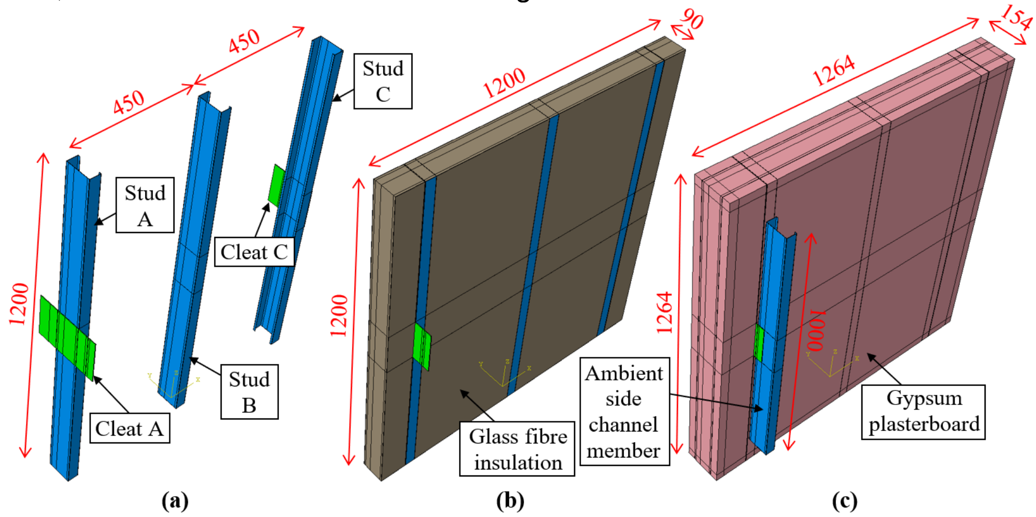

Figure 62. Thermal FE model of the wall specimen with (a) glass fibre insulation and gypsum plasterboards hidden, (b) gypsum plasterboards hidden, and (c) all details.

The important thermal properties, including the specific heat and thermal conductivity, of CFS studs, gypsum plasterboards and glass fibre insulation and their densities at elevated temperatures available in literature were used. Since there were no joints on the ambient & fire side plasterboards, the effect of plasterboard joints was not included in the thermal conductivity of gypsum plasterboard.

The contacts between gypsum plasterboards, glass fibre insulation, steel cleats and CFS studs were determined by the "find contact pair" procedure using 0.1 mm wide tolerance, and were set as tie contacts. The contacts between gypsum plasterboards and steel cleats were ignored since these contacts were eliminated by using a fire-resistant sealant in the test specimen. As the cleats were connected to the studs via two rows of four (6g) screws, only the effective cleat-to-stud contact region between the two screw rows was modelled as tie contact (other cleat-to-stud contact regions ignored.

The convective film coefficients of 10 and 25 W/m^{2}°C were defined for the outer surfaces of ambient side (AS) and fire side (FS) plasterboards, respectively, to define convection of these surfaces. The value of 0.9 was used for the emissivity of these surfaces to simulate the heat transfer radiation. The thermal boundary conditions of the ambient side channel member were set similar to those of the outer surface of ambient side plasterboards. The temperature on the outer surface of the fire side plasterboards (FS) was set to follow the standard fire curve. The temperatures on the fire exposed regions of steel cleats were defined based on the measured values during the fire test. The thermal FE model was based on transient state analysis of the heat transfer solver in Abaqus.

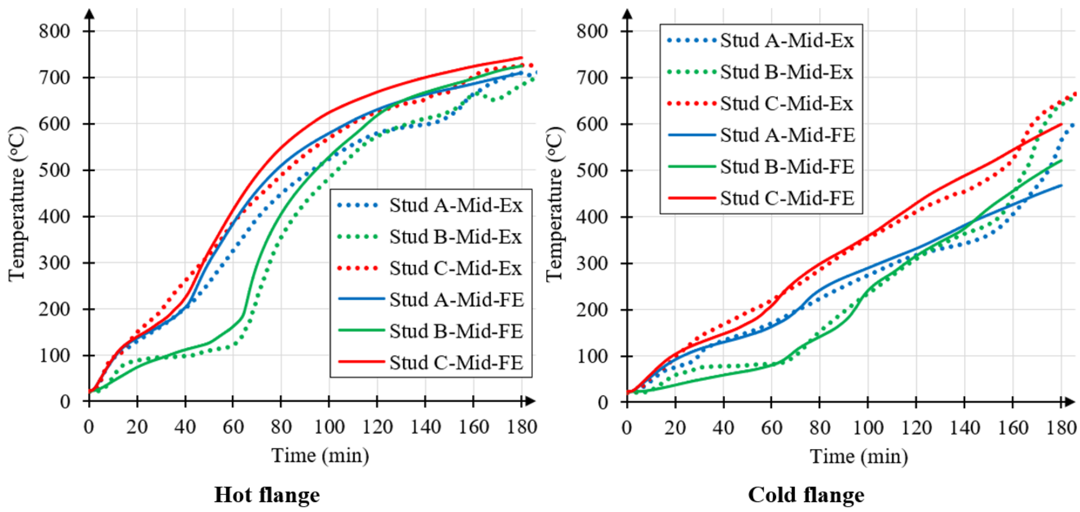

Figure 63. Temperatures of hot and cold flanges of studs at mid-height from thermal FE model and fire test.

Figure 63 shows that the predictions of the developed thermal FE model agree well with the fire test results in terms of temperature-time curves for hot and cold flanges at the mid-height and 3/4 (or 1/4) height of the studs. The model predictions agreed well with the fire test results until 180 min. After 180 min, such agreement was absent as fire side plasterboards had fallen-off. In conclusion, the developed thermal FE model was able to predict reasonably well the thermal behaviour of LGS walls with non-fire rated floor-to-wall cleat connections exposed to standard fire until 180 min.

The developed thermal models as described above were then modified by simulating the deteriorating effects of plasterboard joints present in the full-scale LGS walls. For this purpose, the elevated temperature thermal conductivity of gypsum plasterboard was modified as per Dodangoda's (2018) recommendation and then used to analyse the effects of non-fire rated floor to wall cleat connections on full-scale LGS walls. These analyses also showed the presence of localised high temperatures at the locations of steel cleats (mid-height) of Studs A and C of the LGS wall. Figure 64 highlights that hot and cold flange temperatures of Stud B and those at 1/4 or 3/4 height of Studs A and C were similar to those of the studs of LGS walls without any floor-to-wall cleat connections. In contrast, for about 120 min, hot flange temperatures at mid-height of Stud C were significantly higher than those of the studs in the walls without floor-to-wall connections by up to 150%. After 120 min, these hot flange temperatures tended to converge due to the deterioration of plasterboards at high temperatures. Until 120 min, hot and cold flange temperatures at the mid-height of Stud A were also considerably higher than those of the studs in the walls without floor-to-wall connections, however, slightly lower than those of Stud C as the heat was partly released to the ambient side channel member attached to it. This confirms that the additional heat transferred from fire to the studs via steel cleats led to the localised high temperatures at mid-height of Studs A & C.

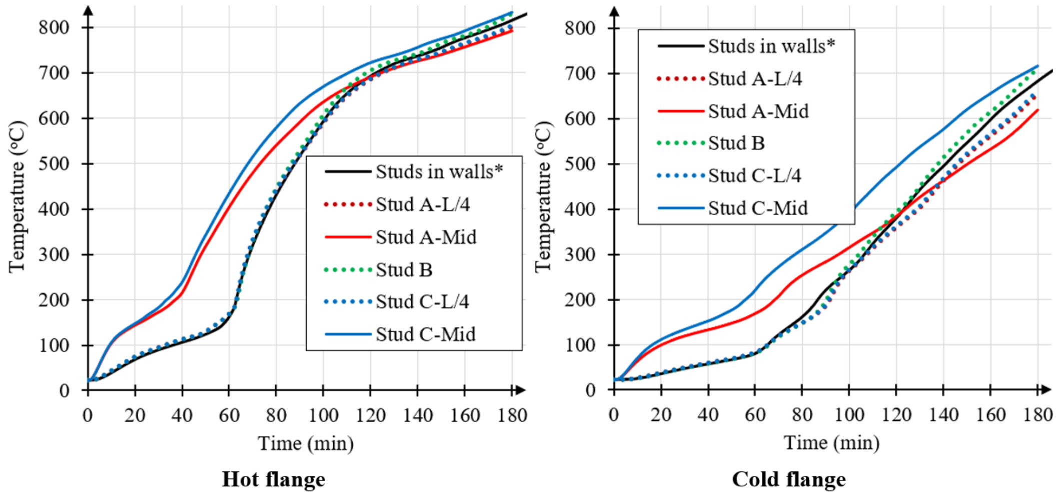

Figure 64. Temperatures of hot and cold flanges of studs in LGS walls with and without non-fire rated floor-to-wall cleat connections (Note: "walls" - walls without non-fire rated floor-to-wall connections exposed to fire on one side).*

The developed thermal model was also used to investigate the effect of cleat thickness. The results showed that when the cleat thickness was increased from 1.0 to 5.0 mm, there was a significant rise in the stud hot and cold flange temperatures at the cleat locations (Stud C mid-height). For example, at 60 min, the hot flange temperatures at cleat locations of LGS walls with cleat thicknesses of 1.0, 1.9 and 5.0 mm were about 470, 540 and 640 °C, respectively.

11.4 Developing Verified Sequentially Coupled Structural Models and Parametric Study

Sequentially coupled structural models were then developed through suitable modifications to that developed for LGS walls made of channel studs without non-fire rated floor-to-wall connections exposed to fire on one side. Such models without such connections have already been validated against full-scale fire test results by many previous research studies (e.g. Peiris and Mahendran, 2022). Hence the modified structural FE model was then used with the same techniques to investigate a 3000 mm high LGS wall with non-fire rated floor-to-wall cleat connections at the floor level. In this model, localised high temperatures obtained from the modified thermal model were applied at the top segment (150 mm) of the wall stud to simulate 150 mm cleats located at the top. To simulate the most critical case, the temperatures in that segment were based on those at the mid-height of Stud C with full cleat-to-stud contact. The temperatures applied for the remaining segment of the wall stud were based on those at the mid-height of Stud B from the same thermal model. These temperatures were mostly similar to those at 1/4 or 3/4 height of Stud C in the modified thermal FE model or studs in LGS walls without non-fire rated floor-to-wall connections.

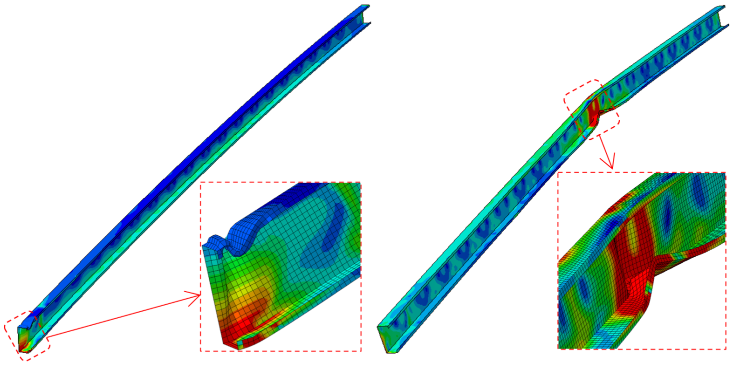

Figure 65. Failures of LGS wall studs with and without non-fire rated floor to wall cleat connections.

The results showed that due to the presence of localised high temperatures caused by non-fire rated floor-to-wall cleat connection at the top end, the stud failed within the top end segment with reduced thermal bowing effects as shown in Figure 65 in contrast to the local buckling stud failure at mid-height associated with thermal bowing effects for walls without such connections. Table 14 provides a comparison between the FRLs (failure times) of cavity insulated LGS walls with and without non-fire rated floor-to-wall cleat connections exposed to fire on one side. It shows that when non-fire rated floor-to-wall cleat connections were used, the FRL was reduced significantly at lower load ratios (<0.2), especially with 5 mm thick cleats. This is due to the thermal mass of thicker cleat plates causing them to remain at higher temperatures for longer periods. However, all the studied walls could still have reasonable FRLs (not less than 60 min) without any sudden collapse when the cleat size is 1.9 mm or less. In many cases, the FRLs of LGS walls with non-fire rated floor-to-wall connections using 1.0 mm or 1.9 mm thick cleats (wall stud thicknesses are usually in the range of 0.75 to 1.0 mm) were nearly equal to those of the same walls but without the mentioned connections.

Table 14. FRLs of the investigated LGS walls with and without non-fire rated floor-to-wall cleat connections.

LGS wall configuration	FRL (min) of LGS wall with varying load ratios						
	0.1	0.2	0.3	0.4	0.5	0.6	0.7
Without non-fire rated floor-to-wall cleat connections	163	106	97	83	72	66	62
With non-fire rated floor-to-wall cleat connections, cleat thickness = 1.0 mm	153	106	88	79	72	66	62
With non-fire rated floor-to-wall cleat connections, cleat thickness = 1.9 mm	141	103	76	67	64	60	57
With non-fire rated floor-to-wall cleat connections, cleat thickness = 5.0 mm	117	78	54	50	47	44	41

Overall, this study has shown that the use of non-fire rated floor-to-wall cleat connections leads to localised high temperatures on stud hot and cold flanges at the floor-to-wall connections, while the magnitude of such localised high temperatures was dependent on the thickness of the cleats. Hence these connections could considerably reduce the FRLs of cavity insulated LGS walls. However, the FRLs of LGS walls using 1.0 mm or 1.9 mm thick cleats were nearly the same as for walls without such connections. The FRLs of cavity insulated LGS walls with non-fire rated floor-to-wall cleat connections can still be reasonable (not less than 60 min). However, a reassessment of their FRLs is recommended and the need for protecting the floor-to-wall connections or primary load-bearing members is investigated such as the use of intumescent coating.

12 INVESTIGATION OF LGS WALLS WITH NON-FIRE RATED FLOOR/ ROOF TO WALL CONNECTION MADE OF STEEL BEARERS AND CLEATS

12.1 Introduction

This chapter provides the details of experimental and numerical studies conducted on LGS walls with non-fire rated floor/roof to wall connections made of steel bearers and cleats to understand the effects of such connections on their fire resistance.

In LGS building structures, CFS studs of LGS walls are connected to corresponding CFS joists or trusses of LGS floors/roofs. In many applications, LGS floors/roofs are designed with very low FRLs, or without any fire-rating, where the floor-to-wall connections can be directly exposed to fire. This implies that the load-bearing capacity and fire resistance of LGS walls can be reduced. This study investigates the potential detrimental effects of fire-exposed floor-to-wall connections made of steel bearers and angle cleats (Figure 66) on the fire resistance behaviour and FRL of LGS walls. A standard fire test was conducted on a small-scale (1.2 m × 1.2 m) cavity insulated LGS wall assembly with these connections. A suitable thermal finite element (FE) model was then developed and verified using the fire test results. The thermal FE model was then modified to represent the full-scale standard fire tests of LGS walls and verified, following which it was used to investigate the effects of the distance between steel cleats and studs and the thickness of steel cleat and bearer. Finally, the temperature predictions of the modified thermal FE model were incorporated in sequentially coupled structural FE models to assess the structural behaviour and the reduced FRLs of LGS walls caused by non-fire rated floor-to-wall bearer and cleat connections.

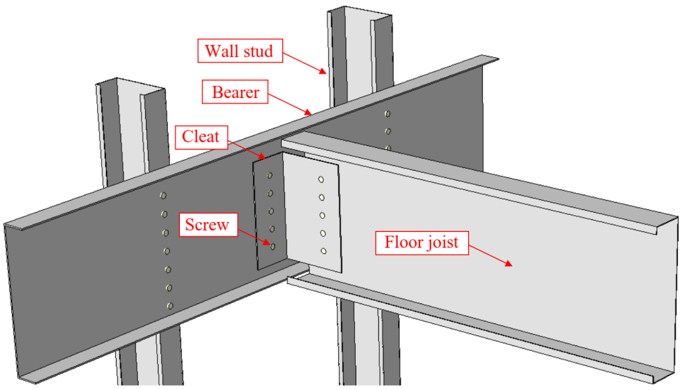

Figure 66. Typical floor-to-wall connections using steel bearers and cleats.

12.2 Experimental Study

Figure 67 shows the fabrication steps of the test specimen. It was made of three 0.75 mm G550 90 mm lipped channel studs of 1000 mm length (A, B and C) fixed to two 1200 mm long unlipped channel tracks. A G450 200 mm × 30 mm × 1.9 mm CFS unlipped channel was used as Bearer 1 of 935 mm length and its web element was fixed to the fire exposed side flanges of Studs A, B and C at mid-height using four 10g screws. Steel cleats A1, B1 and C1 made of 100 mm long G450 50 mm × 80 mm × 1.9 mm CFS angles were then connected to the web element of Bearer 1 by their short legs (50 mm long) and two 10g screws. Cleats A1 and C1 were located at the mid-height of Studs A and C with their long legs (80 mm long) aligned with the web elements of the studs. Cleat B1 was aligned with Cleats A1 and C1, but its long leg was located 150 mm away from the web element of Stud B (Figure 67). In the second step, the stud flanges and the web element of Bearer 1 on the fire exposed side were lined with two layers of 1200 mm × 1200 mm × 16 mm fire-rated gypsum plasterboards. In the third fabrication step, glass fibre insulation was used to fill the wall cavity. In the fourth step, a 600 mm long steel Bearer 2 made of a 200 mm × 30 mm × 1.9 mm unlipped channel was fixed to the unexposed flanges of Studs A and B at mid-height using four 10g screws. Steel cleats A2 and B2 made of 100 mm long 50 mm × 80 mm × 1.9 mm CFS angles were fixed to the web element of Bearer 2 by their short legs and two 10g screws. While the long leg of Cleat A2 was aligned with the web element of Stud A, that of Cleat B2 was located 150 mm away from the web element of Stud B and aligned with Cleat B1. Then, two layers of 16 mm fire-rated gypsum plasterboards were fixed to stud cold flanges using 6g screws, while two 16 mm gypsum plasterboards of 605 mm x 205 mm were placed on Bearer 2 to protect its web element. In the final step, two 1000 mm long channel studs were connected to Cleats A2 and B2 at their mid-length using two 6g screws. Finally, the test specimen was fixed vertically in front of a 1200 mm × 1200 mm gas furnace and the test was conducted based on the standard fire temperature-time curve.

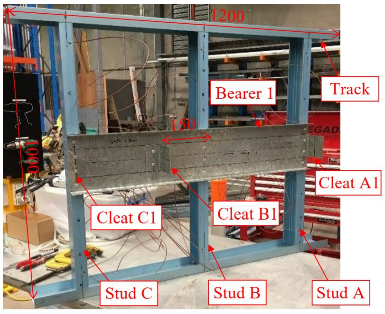

Step 1: CFS frame

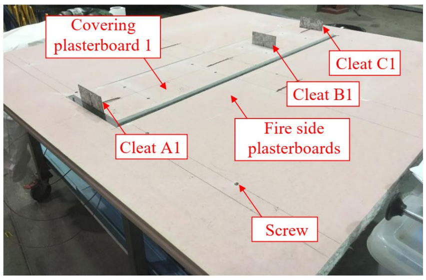

Step 2: CFS frame sheathed with fire side plasterboards

Step 3: Installation of glass wool insulation

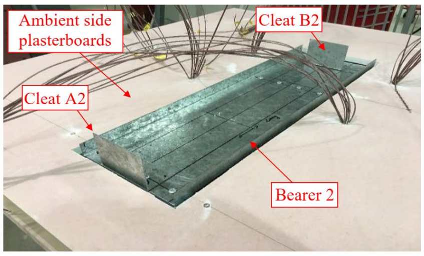

Step 4: Installation of ambient side plasterboards

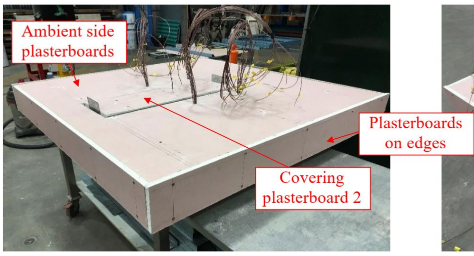

Step 5: Installation of plasterboards on edges

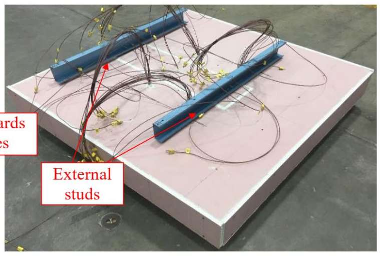

Step 6: Installation of external studs

Figure 67. Fabrication of test specimen.

Figure 68 shows the test specimen after the fire test: fire side plasterboards had mostly fallen off and Cleats A1, B1 and C1 and the flange elements of Bearer 1 were significantly oxidised. The ambient side (AS) plasterboards remained in place after the test as seen in Figure 68 with some discolouration of the outer surface. No changes can be seen for the external studs. The average and maximum temperatures measured on the outer surface of ambient side plasterboards did not exceed the limits, ie. 140 and 180 °C above the ambient temperature (23°C). Hence the insulation criterion was satisfied. The integrity criterion was satisfied until the end of the test, ie. 180 min.

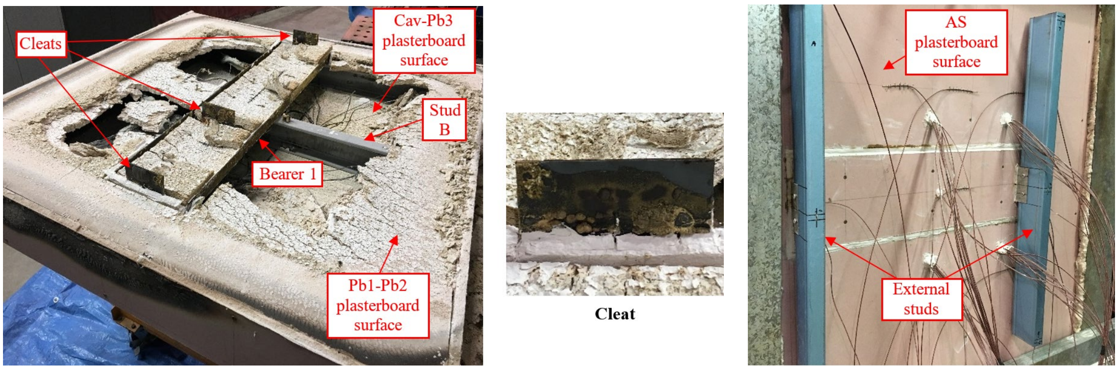

Figure 68. Test specimen after the test.

Figure 69 shows that the hot or cold flange temperatures measured at 1/4 and 3/4 height (*L*) of these studs are highly consistent. However, the temperatures of hot flanges at mid-height of Studs A and C, which were near the fire exposed Cleats A1 and C1, were significantly higher than those measured at *L*/4 and 3*L*/4 of these studs by up to 180%. This highlights the detrimental impacts of non-fire-rated floor-to-wall connections using steel bearers and cleats on the hot flange temperatures of LGS walls. The hot flange temperature measured at *L*/2 of Stud B, which was 150 mm away from the nearest fire exposed steel cleat (Cleat B1), was also higher than those measured at *L*/4 and 3*L*/4 of the same stud by up to 70%. However, it was considerably lower than those measured at *L*/2 of Studs A and C. This meant that locating the fire exposed steel cleats away from the studs can reduce the stud hot flange temperatures and mitigate the impacts of non-fire-rated floor-to-wall connections.

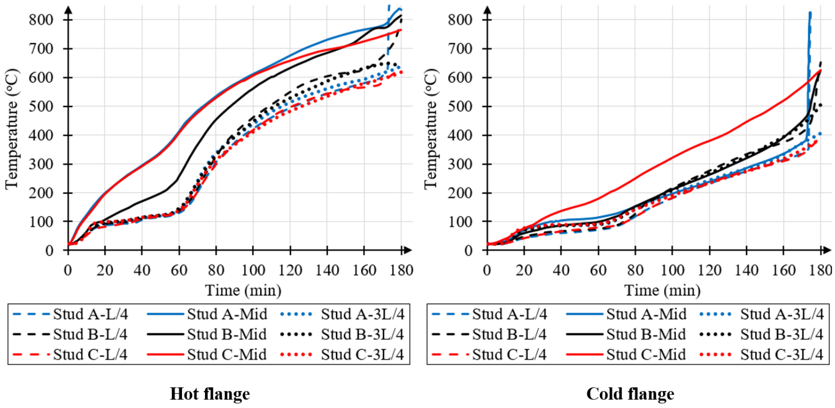

Figure 69. Temperature-time curves of stud flanges.

Since Stud C was not connected to Bearer 2, Cleats A2 and B2 and external studs on the ambient side, the cold flange temperatures of Stud C at mid-height were higher than those measured at *L*/4 and 3*L*/4 of Studs A, B and C. However, the cold flange temperatures of Studs A and B, which were connected to the ambient side external studs, were about the same as those measured at *L*/4 and 3*L*/4 of Studs A and B and were much lower than those of Stud C, which was not connected to the external studs on the ambient side. This implies that the effects of non-fire-rated floor-to-wall connections exposed to fire on the cold flange temperatures of LGS walls are mitigated when their studs are connected to external CFS members on the ambient side of the walls.

12.3 Developing Verified Thermal Models and Parametric Study

A thermal FE model was developed to simulate the tested LGS wall specimen using Abaqus/CAE. The FE model (Figure 70) included accurate details of most components in the wall specimen. The DC3D8 element, a three-dimensional eight-node linear iso-parametric element for heat transfer, was used to simulate studs, plasterboards as well as glass fibre insulation blocks. The overall FE mesh size of every simulated component of the wall was 20 mm. Besides, for ambient and fire side plasterboards, the FE mesh size was 4 mm through their thickness.

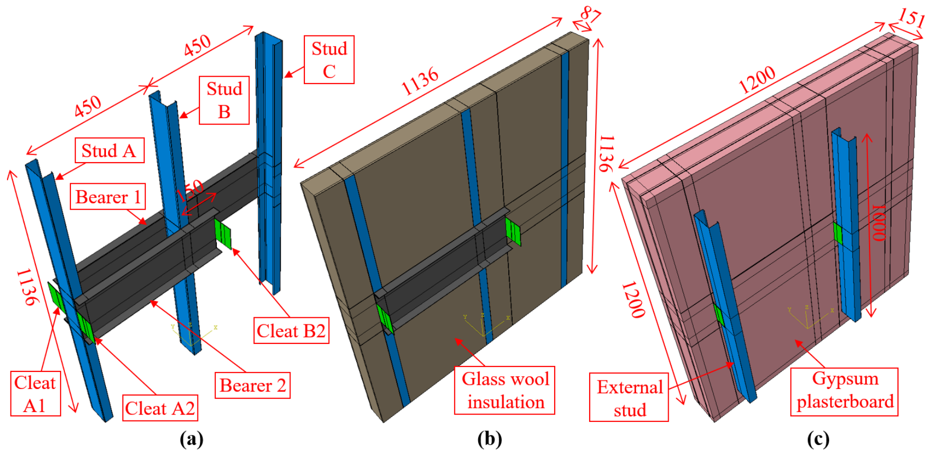

Figure 70. Thermal FE model of the wall specimen with (a) glass wool insulation and gypsum plasterboards hidden, (b) gypsum plasterboards hidden, and (c) all details.

The important thermal properties, including the specific heat and thermal conductivity, of CFS studs, gypsum plasterboards and glass fibre insulation and their densities at elevated temperatures available in literature were used. Since there were no joints on the ambient & fire side plasterboards, the effect of plasterboard joints was not included in the thermal conductivity of gypsum plasterboard.

The contacts between gypsum plasterboards, glass fibre insulation, steel cleats, bearers and CFS studs were determined by the "find contact pair" procedure using 0.1 mm wide tolerance, and were set as tie contacts. The contacts between gypsum plasterboards and cleats and those between gypsum plasterboards and the flange elements of bearers were ignored since these contacts were eliminated by using a fire-resistant sealant in the test specimen.

The convective film coefficients of 10 and 25 W/m^2°C were defined for the outer surfaces of ambient side and fire side plasterboards, respectively, to define convection of these surfaces. Their emissivity value was taken as 0.9 to simulate the heat transfer radiation. The convective film coefficients and emissivity of Cleats A1, B1 and C1 were assumed as similar to those of the outer surface of fire side plasterboards, while those of external studs and Cleats A2 and B2 were assumed as similar to those of the outer surface of ambient side plasterboards. The temperature on the outer surface of the fire side plasterboards (FS) was set to follow the standard fire curve. The temperatures on the fire exposed areas of cleats were defined based on the measured values during the fire test. The thermal FE model was based on transient state analysis of the heat transfer solver in Abaqus.

The predictions of the thermal FE model agreed reasonably well with the fire test results in terms of the temperature-time curves of plasterboard surfaces and hot and cold flanges at the mid-height of all studs as shown in Figure 71. They also confirmed that non-fire-rated floor-to-wall connections using steel bearers and cleats could significantly impact the temperatures of studs, as shown by test results. In the thermal FE analysis results, hot flange temperatures at the mid-height of Studs A and C were much higher than those at 1/4 or 3/4 height of these studs, while cold flange temperatures at the mid-height of Stud C, which was not connected to the external studs on the ambient side, were higher than the cold flange temperatures at other locations. Overall, the developed thermal FE model is considered capable of predicting the complicated thermal behaviour of the tested LGS wall with non-fire-rated floor-to-wall connections using steel bearers and cleats reasonably well.

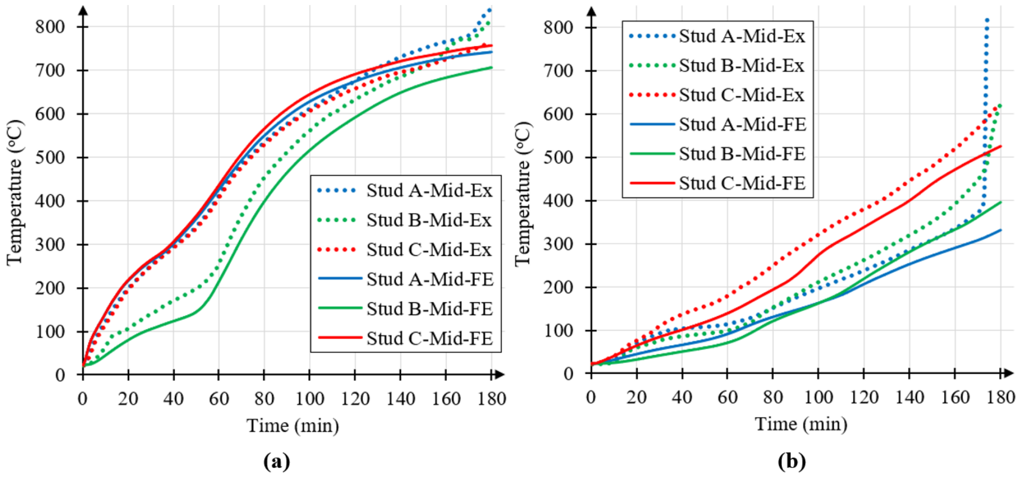

Figure 71. Temperature-time curves of studs at mid-height for (a) hot flanges and (b) cold flanges.

The investigated wall specimen is complicated. To better understand the effects of non-fire-rated floor-to-wall connections, the developed thermal FE model was modified to be more simplified and conservative. The results so far indicate that the connections between the wall studs and bearers, cleats and external studs on the ambient side could mitigate the higher temperatures in wall studs. Therefore, in the modified thermal FE models, such connections were excluded to consider the more severe scenarios, ie. Bearer 2, Cleats A2 and B2 and external studs were removed, and no plasterboard openings were set on ambient side plasterboards. To assess the effect of the distance between steel cleats and studs, two design cases were investigated, Case 1: fire exposed Cleats A1, B1 and C1 located near the web elements of studs and Case 2: Cleats AB1 and BC1 were located between Studs A and B, and Studs B and C, respectively. Details of the two modified thermal FE models are shown in Figure 72 and Figure 73. The developed thermal models as described above were then further modified by simulating the deteriorating effects of plasterboard joints present in the full-scale LGS walls. For this purpose, the elevated temperature thermal conductivity of gypsum plasterboard was modified as per Dodangoda's (2018) recommendations.

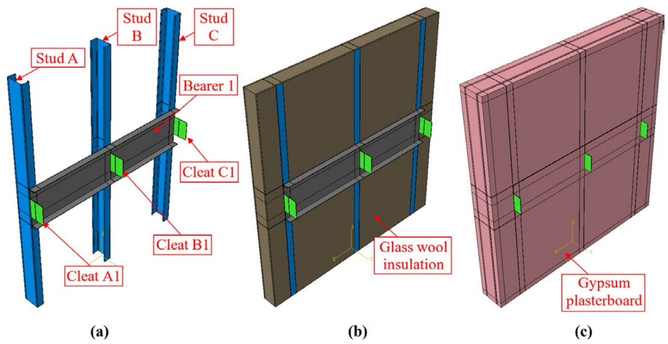

Figure 72. Modified thermal FE model 1 with (a) glass wool insulation and gypsum plasterboards hidden, (b) gypsum plasterboards hidden, and (c) all details.

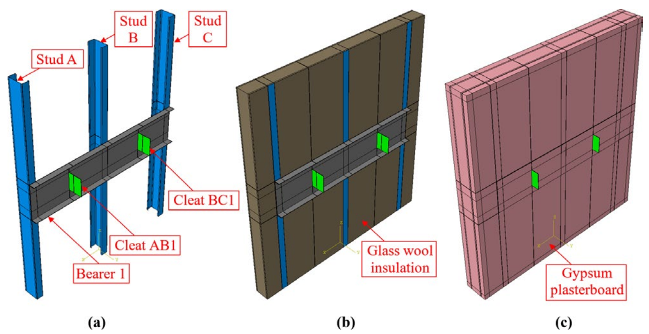

Figure 73. Modified thermal FE model 2 with (a) glass wool insulation and gypsum plasterboards hidden, (b) gypsum plasterboards hidden, and (c) all details.

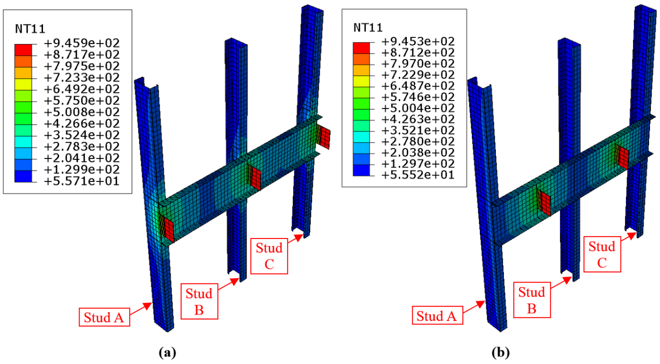

Figure 74. Temperature contours of steel studs, bearers and cleats at 60 min predicted by (a) modified FE model 1 and (b) modified FE model 2 (Note: NT11 is temperature in °C).

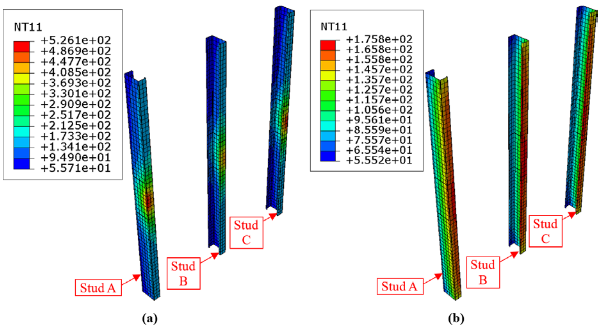

Figure 75. Temperature contours of steel studs at 60 min predicted by (a) modified FE model 1 and (b) modified FE model 2.

The modified thermal model results show that for the wall with steel cleats located near the web elements of studs (model 1), the hot flange temperatures at the mid-height of studs were highly similar to the maximum temperatures on the web element of the bearer (Figure 74). They were significantly higher than those at 1/4 (or 3/4) height of studs. The hot and cold flange temperatures measured at 1/4 (or 3/4) height of the studs of this wall were highly similar to those of studs in the same wall without non-fire-rated floor-to-wall connections in previous studies (Gunalan et al., 2013). In contrast, the hot and cold flange temperatures at varying locations of the investigated wall with cleats located in the middle between the studs (model 2) were very similar to those of studs in the same wall without non-fire-rated floor-to-wall connections. For the wall with steel cleats located between the studs in the middle (model 2), hot flange temperatures at the mid-height of studs were much lower than the maximum temperatures on the web element of the bearer. Figure 75 indicates that for the wall with steel cleats located near the web elements of studs, there were significant localised high temperatures on hot flanges at the mid-height of studs. However, for the wall with steel cleats located between the studs in the middle, such localised high temperatures were not present. The above observations show that fire exposed cleats could considerably impact the hot flange temperatures of LGS walls with non-fire-rated floor-to-wall connections if they are located near the studs, however, this impact could be minimal when they are located in the middle between the studs.

Effects of using steel bearers and cleats with varying thicknesses from 1.0 mm to 5.0 mm were investigated using the developed thermal FE model. When the cleats were located near the web elements of the studs, the hot flange (HF) temperatures at the stud mid-height were considerably increased with increasing thickness, while their cold flange (CF) temperatures were mostly unchanged. However, when the cleats were located in the middle between the studs, HF and CF temperatures were slightly reduced. To explain these observations, the increased thicknesses of steel bearers and cleats could enhance the heat concentration on components around the cleats. In the first case, as the cleats were located near the hot flanges of studs, the heat was quickly transferred to stud hot flanges. In the second case, the heat was transferred from the cleats to the studs via the bearer. As the cleats were located far from the studs, this heat transfer was delayed.

12.4 Developing Verified Sequentially Coupled Structural Models and Parametric Study

Sequentially coupled structural models were then developed using Abaqus/CAE through suitable modifications to that developed for LGS walls made of channel studs without non-fire rated floor-to-wall connections exposed to fire on one side. Such models without such connections have already been validated against full-scale fire test results (e.g. Gunalan and Mahendran, 2013, Peiris and Mahendran, 2022). Hence the modified structural FE model was developed using the same techniques reported in these papers to investigate a 3000 mm high LGS wall with non-fire rated floor-to-wall bearer and cleat connections at the floor level (Figure 76). In this model, localised high temperatures on stud flanges obtained from the modified thermal model at mid-height (as a conservative measure) were applied at the top segment (equal to the bearer height of 200 mm) of the wall stud to simulate the bearer and cleat connection located at the top. The temperatures applied to the remaining segment of the stud in the modified structural FE model were based on those at 1/4 or 3/4 height of studs from the modified thermal FE models, or those of studs in LGS walls without floor-to-wall connections reported in previous studies mentioned above.

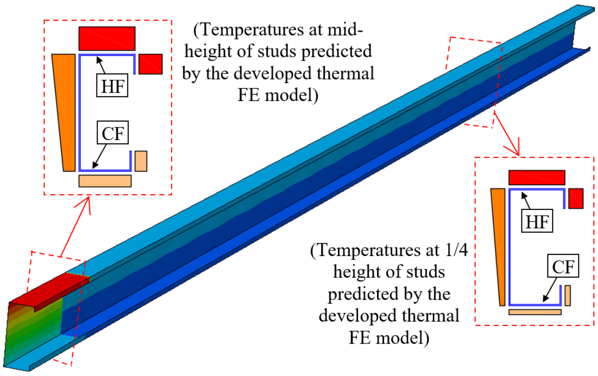

Figure 76. Simulation of temperatures in the modified structural FE model.

Thermal models of LGS walls with non-fire-rated floor-to-wall connections using steel cleats, located between the studs in the middle (ie. away from the studs), and steel bearers showed that there were no localised high temperatures on stud flanges and were highly similar to those of the walls without floor-to-wall connections. When the thicknesses of steel bearers and cleats were increased, the stud flange temperatures at the floor-to-wall connections were slightly reduced. Hence, the structural behaviour and FRL of these walls with steel cleats located between the studs in the middle are highly similar to those of LGS walls without non-fire-rated floor-to-wall connections exposed to fire.

However, localised high temperatures on stud flanges increase when the distance between the steel cleats and studs is reduced and thus the behaviour and failure time can deteriorate. As shown in Figure 77 and Table 15, in fire conditions, the failures of LGS walls with non-fire-rated floor-to-wall connections using steel cleats, located near the studs, and steel bearers could happen at either the mid-height of studs or their top end segments. While the thermal bowing effect, caused by the difference between stud hot and cold flange temperatures contributed to the failures at the mid-height of studs, the failures at the top end segments were due to localised high temperatures caused by non-fire-rated floor-to-wall connections.

Table 15 shows that the failure times (FRLs) were slightly reduced when the thicknesses of steel bearers and cleats (t_{be} and t_{cl}) were increased in the case of cleats located near the studs. Importantly, the use of non-fire-rated floor-to-wall connections led to some reductions in the failure times of LGS walls exposed to fire on one side, but they were insignificant. As seen in Table 15, the maximum reduction was only 17%, while in many cases, the maximum reduction was minimal. All the investigated walls in this study could still have reasonable FRLs (not less than about 60 min).

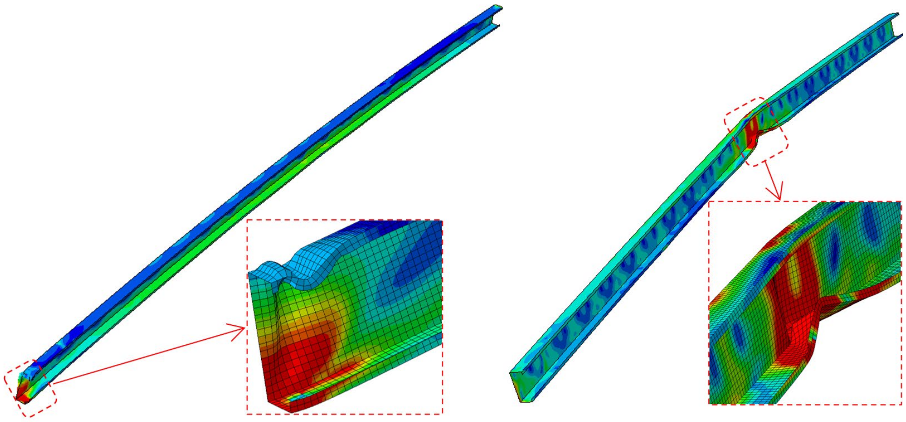

Figure 77. Failures of the investigated walls at (a) stud end segment and (b) mid-height.

Table 15. Failures times of LGS walls with non-fire rated floor-to-wall connections made of bearers and cleats.

Wall configuration	Failure times (min) at varying load ratios						
	0.1	0.2	0.3	0.4	0.5	0.6	0.7
Walls without floor-to-wall connections	163*	106*	97*	83*	72*	66*	62*
Walls with t_{be} = t_{cl} = 1.0 mm	158*	105*	97*	83*	71*	66*	62*
Walls with t_{be} = t_{cl} = 1.9 mm	152**	105**	91 **	80**	72*	65*	62.*
Walls with t_{be} = t_{cl} = 5.0 mm	139*	104**	86**	73**	70**	65**	61**

Note: * Studs failed at mid-height, ** Studs failed at the end segment.

This study has shown that LGS wall systems with non-fire rated floor-to-wall bearer and cleat connections as used in this study have the robustness to prevent immediate collapse in the event of exposure to standard fire on one side. However, a reassessment of their FRLs is recommended and the need for protecting the floor-to-wall connections is investigated such as the use of intumescent coating.

13 PROJECT FINDINGS AND OUTCOMES

This chapter provides a summary of important findings and outcomes from this project under specific headings such as material properties, experimental and numerical studies and parametric study.

13.1 Thermal and Mechanical Properties of Materials

Plywood flooring, being combustible, poses a risk to occupants and a safety hazard during fire tests. Thermal properties of four fibre cement boards were tested to find a suitable alternative. James Hardie Secura board exhibited higher specific heat, lower thermal conductivity, and lower mass loss values compared to the other boards, making it the best-performing fibre cement board among the four boards tested in this study.

13.2 Fire Tests of Short-span LGS Floor Systems

Comparison with previous full-scale fire tests showed that the short-span fire test setup proposed in this study can be effectively used to investigate the fire behaviour of both existing and new LGS floor configurations and obtain conservative FRLs.

The FRLs of commonly used LGS channel joist and truss floor systems with ceilings made of two 13 mm, two 16 mm or three 16 mm fire-rated gypsum plasterboards, with and without cavity insulation at a load ratio of 0.4, were determined as 60/60/60, 90/90/90 and 120/120/120, respectively.

The use of cavity insulation initially led to faster plasterboard fall-off due to increased heat retention within the fire-side components. However, it effectively protected the joists from high temperatures, maintained lower cavity air temperatures, and had a minimal effect on the FRL of LGS floors. This study used glass fibre insulation, which melts at about 700 ℃. The use of other insulation materials with higher melting temperatures is likely to provide additional benefits, including higher FRLs.

Increasing the plasterboard thickness or adding an extra layer significantly enhances the FRL. Increasing the total plasterboard thickness by 6 mm can provide a gain of 16 min in failure time (24% increase). Introducing another 16 mm plasterboard layer increases the failure time by at least 37%.

Plasterboard fall-off often starts near a joint. Hence, plasterboard joints in the ceiling are potential vulnerabilities, and improving their performance would lead to higher FRLs for the floor systems.

Fire-rated joint sealants are preferred to prevent premature melting, burning, or the emission of toxic smoke, which could result in insulation failure of the floor system. Although ambient-side flooring temperatures may remain below 200°C, certain sealants may still prove unsuitable.

All the ambient temperature and fire tests revealed distortional buckling of the lipped channel joists. The cold flange temperatures at failure were almost the same in all the fire tests with a load ratio of 0.4. The primary failure mode was local buckling of the top chord in all short-span fire tests with different truss types and the corresponding ambient temperature tests.

For a given ceiling configuration, a comparable rate of heat transfer occurred until face layer plasterboard fall-off despite the differences in the primary structural member (channel joist or truss). Overall, temperature–time profiles were found to be independent of the type of primary structural member. The thermal behaviour was primarily governed by the ceiling configuration and the presence or absence of cavity insulation, which significantly influenced the rate of heat transfer. The presence of cavity insulation did not influence the failure times in short-span fire tests significantly unlike the cavity insulated load bearing LGS walls in fire.

13.3 Numerical Modelling of Short-span LGS Floor Systems under Ambient and Fire Conditions

An advanced two-joist sheathed short-span structural joist model, designed to replicate the test setup, showed good alignment with the ambient temperature test behaviour. However, due to its complexity, this model required substantial computational time. The single-joist sheathed model provided good agreement with the ambient temperature short-span test results, while the simplified unsheathed model yielded reasonably conservative outcomes. The single-joist sheathed model required approximately one-third of the computational time compared to the two-joist sheathed model. Thus, the single-joist sheathed FE model is recommended for accurately predicting the structural behaviour and failure load of LGS floors under ambient conditions.

To minimise convergence errors and reduce analysis time, unsheathed single-joist model was recommended for simulating the structural behaviour and FRLs of short-span LGS joist floors exposed to fire. The developed FE models for the five short-span fire tests successfully captured the behaviour and joist failure times (FRLs) observed in the fire tests. Predicted FRLs, failure modes, and deflection patterns closely matched the fire test results, confirming their reliability in predicting the FRLs. For LGS truss floors, single truss sheathed FE model was used as the composite action between fibre cement board flooring and truss top chord was found to be substantial.

Accounting for cavity convection within the LGS floor is essential to develop a verified heat transfer FE model. Air within the cavity was modelled as a solid material with an equivalent thermal conductivity to indirectly account for convection.

Accurate modelling of joint openings and plasterboard fall-off was identified as critical for developing reliable heat transfer FE models capable of replicating the thermal response observed in short-span fire tests. Joint and plasterboard pieces were systematically removed based on the observed times of joint openings during fire testing, allowing the resulting heat penetration and temperature rise to be realistically captured. Thermal models with this novel method for plasterboard fall-off and by simulating cavity convection demonstrated good agreement with experimental temperature-time data of both channel joist/truss members and sheathing.

The combined use of sequentially coupled thermal and structural FE models developed and verified in this study enabled detailed parametric studies to establish the FRL data for various LGS floor systems, eliminating the need for expensive full-scale fire tests.

13.4 Ambient Temperature and Fire Tests of Full-scale LGS Floor Systems

For a configuration with two 16 mm fire-rated plasterboards on the ceiling and fibre cement panel flooring without cavity insulation at a load ratio of 0.4, the FRL achieved was 90/90/90 from the full-scale fire tests. When three 16 mm plasterboards were used instead of two boards, the FRL achieved was 120/120/120. For a configuration with two 16 mm fire-rated plasterboards on the ceiling and composite flooring consisting of a corrugated steel deck and concrete flooring, the FRL achieved was also 120/120/120 at a load ratio of 0.4. Identical FRLs were obtained from the fire tests of truss floor systems, for which cavity insulation was used. The temperatures within the cavity, joists, and the ambient surface of the flooring increased due to ablation, calcination, and plasterboard fall-off. Delaying any of these phenomena can lower the joist/truss temperatures, resulting in higher FRLs.

Comparisons with previous full-scale fire tests of vertically placed floor panels in Australia showed a similarity in the temperature-time profiles initially, but they diverged afterwards since the vertical panels did not experience rapid plasterboard fall-off and the subsequent sudden rise in temperatures. Therefore, the FRLs estimated from such tests are considered unsafe to use.

The study provided plasterboard fall-off temperatures and times for the five full-scale fire tests conducted. These fall-off times or temperatures can be used as inputs to develop accurate FE models and establish a plasterboard fall-off criterion.

Short-span tests showed similar FRLs and conservative failure times in comparison with full-scale fire tests with the same ceiling and insulation configurations. The comparison of curvature–time behaviour showed that the curvatures of the short-span and full-scale systems were comparable until the face and base layer fall-off and base layer calcination occurred. While both test methods exhibited similar behaviour in terms of channel joist/truss failure modes and temperature profiles over time, the use of more plasterboard joints within a small area in short-span tests led to higher temperatures within the cavity, resulting in reduced failure times. Considering that full-scale fire tests are costly and time-consuming, short-span tests offer a practical alternative for verifying the FRLs of existing floor systems and conducting initial assessments of new floor systems.

Adding a third 16 mm plasterboard layer to the ceiling of an LGS floor configuration without insulation increased the FRL by about 60% while the use of a composite floor made of a corrugated steel sheet deck and concrete provided a 32% increase in failure time compared to fibre cement panel flooring. Previous research indicated this increment to be about 20%. Therefore, conservatively, this increment provided by lightweight concrete deck can be taken as 20%.

Blockings or noggings are commonly installed in floor joist/truss systems with spans exceeding 3500 mm to enhance stability and load distribution. However, test results showed that the inclusion of blocking trusses did not significantly influence the overall structural behaviour, failure mode, or ultimate load capacity of LGS truss floor systems. This suggests that blocking trusses may not be essential for truss floors and the lateral restraints provided by sheathing is sufficient.

Full-scale floor truss fire tests showed that cavity insulation accelerates plasterboard degradation by retaining heat in the fire-exposed ceiling layers, leading to earlier face and base layer fall-off. However, the insulation also provides thermal protection to the trusses until it is fully compromised, thus allowing the FRLs to remain unchanged, ie. cavity insulation has negligible impact on the FRL of LGS floors with two or three plasterboard layers, despite some minor differences in failure times.

Critical temperatures recorded for the trusses and channel joists were found to be similar, regardless of the ceiling configuration or the presence of cavity insulation. Furthermore, the bottom chord and top chord temperatures remained comparable until base layer calcination commenced, after which the bottom chord temperatures increased rapidly because of base layer fall-off.

Failure time variations among floor assemblies incorporating different framing systems such as solid wood joists (235 mm deep), wood I-joists (241 mm), steel channel joists (203 mm), and steel trusses (200 mm) were found to be less than 5%, indicating that frame type has minimal influence on FRLs.

13.5 Numerical Modelling of Full-scale LGS Floors under Ambient and Fire Conditions

The advanced two-joist/truss sheathed FE model and the single-joist/truss sheathed model both accurately predicted the ambient temperature behaviour of LGS floors. However, the single-joist/truss sheathed model required less than half the computational time compared to the two-joist model, making it a more efficient choice for structural fire modelling. The plasterboard ceiling is attached to the tension side of the LGS floor joist/truss, providing minimal capacity enhancement. Hence the predicted capacities with and without the plasterboard ceiling were almost identical.

In contrast to the short-span unsheathed structural FE models, the unsheathed model developed for full-scale tests underpredicted the failure load by more than 10% in joist floors. This discrepancy arose because the full-scale unsheathed model did not account for the composite action provided by fibre cement flooring. The sheathing length attached to the joist was only 1200 mm in the short-span tests, compared to 4200 mm sheathing in the full-scale tests. The reduced sheathing length in the short-span tests resulted in minimal composite action, allowing its effects to be neglected.

While LGS wall systems with 90 mm cavities experience minimal convection, cavity convection becomes significant in LGS floor systems with cavities exceeding 200 mm.

Plasterboard fall-off governs the failure time of LGS floors in fire. Accurately modelling plasterboard fall-off is essential for reliable heat transfer models. In this study, plasterboard pieces were systematically removed from the model at test-observed times, effectively capturing the heat increase caused by fall-off. Modelling air within the cavity as a solid material with an equivalent thermal conductivity (k = hL) effectively captured the convection. The developed heat transfer model with plasterboard fall-off and convection accurately predicted the temperature-time profiles of both the channel joists/trusses and the sheathing during the fire tests.

For an accurate representation of the fire test conditions, the advanced single-joist sheathed FE model was expanded to simulate the behaviour of LGS floors in fire. These models successfully captured the structural behaviour of LGS floors exposed to fire.

Advanced structural and heat transfer FE models were also developed to predict the failure times and FRLs of the tested full-scale truss floor systems. The advanced structural FE models, which incorporated flooring and considered configurations both with and without blocking trusses, were validated using the results of ambient temperature tests.

Capacity predictions of LGS truss floors under both ambient and fire conditions were conducted using AS/NZS 4600. The ambient temperature capacity predictions were consistently conservative and were able to identify the critical failure mode in the straightened lip of the top chord. The conservatism observed in the predicted failure loads under ambient conditions suggests the potential for developing safer and more efficient design methods. Truss temperatures obtained from the validated heat transfer models were used to estimate the truss capacities at the failure times from the fire tests. The predicted load ratios showed close agreement with the experimental load ratios, demonstrating the feasibility of using validated heat transfer FE models to predict truss temperatures and, subsequently, determine the relevant load ratios using DSM equations.

13.6 Gypsum Plasterboard Fall-off Behaviour in Fire

Gypsum plasterboard fall-off is a key factor governing the failure of lightweight frame floor systems when exposed to fire. For an assembly without insulation, on average, the floor fails two min after the first piece of base layer plasterboard fall-off and less than one min after the last piece fall-off. Although plasterboard fall-off occurs more quickly in an assembly with glass fibre insulation, the failure occurs around seven min and three min after the first and last piece fall-off, respectively. The use of rockwool and cellulose fibre insulation instead of glass fibre insulation can result in higher FRLs, as they melt and shrink much more slowly when exposed to fire.

New minimum fall-off temperatures were proposed for fire rated gypsum plasterboards based on the conducted full-scale fire tests. Eight equations were developed for predicting the plasterboard fall-off times for insulated and non-insulated assemblies using four methods: average first piece fall-off (Method 1), 5% fractile of first piece fall-off (Method 2), average last piece fall-off (Method 3), and 5% fractile of last piece fall-off (Method 4). Method 2 predicted the most conservative fall-off times, while Method 3 provided the closest estimates to the fire test results obtained in this study. Method 4 was recommended for designers to obtain the fall-off times and subsequently predict the FRL of floor configurations. Method 3 was considered more suitable for researchers investigating the behaviour of both new and existing lightweight frame floor configurations.

13.7 Parametric Studies and FRLs of LGS Floors

As the load ratio (applied load in fire/ambient temperature capacity) increases in a LGS floor system, the joist/truss failure time reduces. However, such reductions in failure time/FRLs are small compared to LGS wall systems.

Reducing the joist depth from 300 mm to 100 mm increased joist temperatures, leading to a failure time difference of about 5%. While this difference is negligible, it becomes significant when the failure time is close to a FRL bracket, and can move to the next FRL bracket (e.g. 30/30/30 to 60/60/60).

The temperature-time profiles of joists/trusses with different spans were similar and primarily depended on plasterboard thickness and fall-off characteristics. Therefore, for the same load ratio, the same FRLs were obtained for floor systems with varying spans.

Using an additional plasterboard layer increased the FRL by 35%. Similarly, increasing the board thickness by 6 mm, led to a 25% rise in FRL based on the FE models. Both results confirm the significant effect of thickness and number of layers of plasterboard.

When the thickness of the channel joist/truss was changed with the rest of the configurations being the same, the heat transfer profile did not vary significantly. Therefore, the FRLs for a specific load ratio remained the same.

When the joist/truss spacing is reduced, the load carried by each individual joist decreases, thereby reducing the load ratio and consequently increasing the failure time and FRL.

Substituting plywood for fibre cement panels raised the cavity and joist/truss temperatures; however, the maximum difference in failure times across all load ratios and floor configurations studied was negligible.

Using resilient channels spaced similarly to joists increases the cavity depth, giving an additional, negligible failure time of 1-2 min. Conversely, if resilient channel spacings are reduced while maintaining the same joist spacing, the failure time will increase.

Introduction of noggings for joists slightly increased the overall stiffness of the frame, but did not enhance the overall capacity. Therefore, the FRLs of floor configurations with and without noggings will also be the same for a specified load ratio.

FRLs in this study were determined for simply supported floors. These same FRLs can be applied to continuous floors/beams, as the sagging moment in the middle will be lower. Furthermore, at support locations, where hogging moments occur, temperatures will be lower because the plasterboard will not fall off near the supports.

13.8 Comparison of FRLs with Plasterboard Manufacturers' Data

Table 16 compares the FRLs determined from this research with plasterboard manufacturers' data, and highlights the significant advancements made by this research by providing new FRL data for many varying key parameters such as load ratio, cavity insulation, joist/truss type and depth. It also highlights several cases in which enhanced FRLs are provided.

Table 16. Comparison of FRLs with plasterboard manufacturer's data

Type	Siniat Fireshield	FRLs from this study
FRLs with load ratio	No	Yes
FRLs with joist/truss type	No	Yes
FRLs with joist/truss depth	No	Yes
FRLs with flooring type	No	Yes
FRLs with cavity insulation	No	Yes
Two layers of 16 mm	60/60/60 (450 mm maximum spacing)*	90/90/90 (600 mm maximum spacing)
Three layers of 16 mm	120/120/120 (450 mm maximum spacing)*	120/120/120 (600 mm maximum spacing)

**- The board manufacturer recommended FRLs could be achieved with larger joist/truss spacing as shown in this study. Same finding was also confirmed for two and three layers of 13 mm gypsum plasterboard.*

13.9 Experimental and Numerical Studies of LGS Walls with Non-fire Rated Floor/Roof to Wall Connections and Unprotected Combustible Electric Sockets and Service Pipes

Combustible electrical sockets and service openings allowed hot gasses to penetrate the wall cavities, but mostly led to localised higher temperatures on plasterboard and stud surfaces near the service openings. The reductions in insulation and structural adequacy based FRLs of these LGS walls were small due to localised detrimental effects around the service opening.

Service pipe openings caused large differences in the temperatures of wall studs and plasterboards, with localised high temperatures only in the regions near the service pipe opening. Although the integrity and insulation criteria based FRLs were not satisfied or inadequate, their structural adequacy-based FRLs were estimated as reasonable.

When non-fire rated floor/roof-to-wall cleat connections were used with LGS walls, it led to localised high temperatures on stud hot and cold flanges near the floor-to-wall connections depending on the cleat thickness. However, the FRLs of LGS walls with connections using 1.0-1.9 mm thick cleats were nearly the same as for walls without such connections. The FRLs of cavity insulated LGS walls with non-fire rated floor-to-wall cleat connections can still be reasonable.

When non-fire rated floor/roof-to-wall connections using steel bearers and cleats were used with LGS walls, it led to considerable localised high temperatures on the flanges of top stud segment when cleats were located near the studs. However, their effects on the FRLs of the walls were insignificant with the reduction to the FRL being less than 17% and were negligible in many cases.

In general, non-fire rated floor/roof to wall connections and unprotected combustible electric sockets and service pipes were shown to have minimal impact on the FRLs of load-bearing LGS walls, demonstrating the robustness of LGS construction. However, reassessment of their FRLs and the need for protecting them are recommended.

13.10 Final Remarks

Overall, the findings from this research involving three detailed studies not only enable fire safety designers to optimise LGS floor-ceiling designs but also contribute to the National Construction Code (NCC), particularly Part 1, Section C. The comprehensive findings and recommendations of FRLs provided by this research can now be effectively employed to ensure compliance and enhance structural safety across various building classes employing LGS floor-ceiling systems. They will be utilised by our industry partners, BlueScope Steel and NASH, together with previously available FRL data for LGS walls from QUT research, in preparing and publishing the proposed Fire Design Handbook for use by fire design engineers of LGS buildings. Engineers can use the NASH Fire Design Handbook without relying on plasterboard manuals and expert opinions. The project outcomes will lead to significant benefits to our industry partners and the steel building industry in constructing cost-efficient and fire-safe mid-rise residential and commercial buildings.

Since this research project showed that three layers of 16 mm plasterboard are needed to provide 120/120/120 FRL with conventional floor systems, studies were also conducted using the short-span test method and numerical approaches developed in this project to develop new floor configurations with enhanced FRLs. These studies have successfully developed three ceiling configurations: (1) two layers of 16 mm gypsum plasterboard connected via 16 mm furring channels with Rockwool cavity insulation (2) one layer of 16 mm gypsum plasterboard with 25 mm Rockwool insulation used externally (3) 37 mm lightweight AAC (Autoclaved Aerated Concrete) panel with minimum FRLs of 120/120/120. Cost evaluation and full-scale fire testing are needed to verify these findings.

During the last three years, two PhD students and one post-doctoral research associate have worked together with many undergraduate thesis students to achieve the key objectives of this project. In the third year, a third PhD student also contributed towards the development of new floor configurations with enhanced FRLs. This research project has thus trained many young researchers in the field of light steel design and construction, enabling them to develop experimental, numerical, research and design skills needed to work as competent fire research and/or design engineers.

14 RESEARCH OUTPUTS

Following are the significant outputs from this research project. Importantly, the proposed Fire Design Handbook to be published by National Association of Steel Framed Housing (NASH) will utilise such enhanced knowledge, understanding and valuable research data given in these research outputs.

14.1 PhD Theses

Mohamed Hisham, Fatheen (2025) Fire Resistance of LGS Floor Systems Made of Lipped Channel Joists. PhD thesis, Queensland University of Technology. https://eprints.qut.edu.au/259163/

Ranasinghe,Gihan (2025) Behaviour and Design of LGS Truss Floor Ceiling Systems under Ambient and Fire Conditions. PhD thesis, Queensland University of Technology.

14.2 Journal Publications

Ten Q1 journal papers have been published, while five more papers are under review.

Hisham F., Vy S.T., Mahendran M., Ariyanayagam, A., Ngo, T. (2024), Fire tests of short-span LGS floor systems made of lipped channel joists, Thin-Walled Structures, Vol.204, 112257. https://doi.org/10.1016/j.tws.2024.112257

Hisham F., Vy S.T., Mahendran M., Ariyanayagam, A. (2025), Numerical modelling of LGS floors under fire conditions, Structures, Vol.71, 108014. https://doi.org/10.1016/j.istruc.2024.108014

Hisham F., Mahendran M., Ariyanayagam A., Vy, S.T. (2025), Fire tests of full-scale LGS floor systems, Fire Safety Journal. Vol.156, 104463. https://doi.org/10.1016/j.firesaf.2025.104463

Hisham F, Mahendran M, Vy S.T., Ariyanayagam, A. (2025), Numerical modelling of light gauge steel framed floors under standard fire condition, Journal of Constructional Steel Research. Vol.233, 109626. https://doi.org/10.1016/j.jcsr.2025.109626

Hisham F., Mahendran M. (2025), Investigation of plasterboard fall-off in lightweight floor systems under fire conditions, Fire Safety Journal, Under Review

Ranasinghe G., Vy S.T., Mahendran M., and Ariyanayagam A. (2025), Experimental study of LGS truss floor-ceiling systems made of top hat sections, Thin-Walled Structures, Vol.212, 113193. https://doi.org/10.1016/j.tws.2025.113193

Ranasinghe G., Mahendran M., Vy S.T. and Ariyanayagam A. (2025), Numerical modelling of LGS truss floor-ceiling systems made of top hat sections, Journal of Constructional Steel Research, Vol.234, 109654. https://doi.org/10.1016/j.jcsr.2025.109654

Ranasinghe G., Mahendran M., Ariyanayagam A. and Vy S.T., Experimental and numerical studies of LGS truss floor-ceiling systems under standard fire conditions, Thin-Walled Structures, Vol.217, 113883. https://doi.org/10.1016/j.tws.2025.113883

Ranasinghe G., Mahendran M., Ariyanayagam A. and Vy S.T., Behaviour of LGS truss floor-ceiling systems under standard fire conditions, Journal of Constructional Steel Research, Vol.235, 109860. https://doi.org/10.1016/j.jcsr.2025.109860

Ranasinghe G., Mahendran M., and Ariyanayagam A. (2025), Finite element modelling of full-scale cold-formed steel truss floor-ceiling systems under ambient and fire conditions, Structures, Under Review.

Vy, S.T., Steau, E. and Mahendran, M. (2025), Fire Tests of CFS Stud Walls with Openings for Combustible Service Pipes, Fire Safety Journal, 152, 104341.

Project #24: Sub-project 2 – Fire resistance of light gauge steel (LGS) floor systems

Vy, S.T., Steau, E. and Mahendran, M. (2025), Effects of combustible electrical sockets on the fire resistance of LGS walls, Journal of Building Engineering, Vol.111, 113272.

Vy, S.T., Steau, E. and Mahendran, M. (2025), Fire resistance behaviour of LGS walls with non-fire-rated floor-to-wall connections using steel bearers and cleats, Engineering Structures, Under Review

Vy, S.T., Steau, E. and Mahendran, M. (2025), Fire resistance behaviour of LGS walls with non-fire rated floor-to-wall cleat connections, Thin-Walled Structures, Under Review

Sivapalan, S., Mahendran, M. and Ariyanayagam, A. (2025) Improving the fire resistance of light steel floor–ceiling systems through enhanced materials and construction methods, Thin-Walled Structures, Under Review.

14.3 Workshop Presentations, Webinars and Conference Presentations

Two presentations at the *National Association of Steel Framed Housing (NASH) Engineering Workshop in Newcastle* in October 2024, attended by about 100 industry professionals including structural engineers, architects, designers, builders, detailers, and manufacturers of structural steel products.

1. Fire Resistance and Design of LGS Floors by Mahen Mahendran
2. Fire Resistance and Design of LGS Walls by Mahen Mahendran

Presentation at the NASH Queensland Chapter Meeting, November 2024 by Mahen Mahendran

Presentations at the NASH Standards Meetings during 2022-2024 by Mahen Mahendran

NASH Webinars 2025

Webinar on Fire Resistance of LGS Floor Systems Made of Lipped Channel Joists by Fatheen Hisham in April 2025, attended by about 40 industry professionals.

Webinar on Behaviour and Design of LGS Truss Floor Ceiling Systems under Ambient and Fire Conditions will be presented by Gihan Ranasinghe in October 2025

International Conference Paper:

Ranasinghe, G., Mahendran, M, Ariyanayagam, A, Vy, S.T. (2025) Investigation of full-scale LGS truss floor-ceiling systems under ambient and fire conditions, Proc. of the 12th International Conference on Advances in Steel Structures (ICASS 2025) and the 4th International Symposium on Industrialized Construction Technology (ISICT 2025), December 9–12, 2025, Singapore.

15 RECOMMENDATIONS AND FUTURE RESEARCH PLANS

Based on the findings of this study, the following recommendations and directions for future research are proposed.

- Existing design manuals provided by plasterboard manufacturers overlook the effects of load ratio and fail to address other parameters, such as joist spacing, cavity insulation, joist depth, etc. on the FRL. This study has examined these factors and provided accurate FRL data for 1134 joist and truss floor configurations with varying section types, depths, flooring and five different plasterboard configurations, ensuring their applicability for confident use by fire design engineers. It is recommended that such valuable data are included in the proposed Fire Design Handbook to be published by National Association of Steel Framed Housing (NASH).
- The heat transfer analysis in this study was conducted using Abaqus software. However, since Abaqus does not support convection, air was modelled as a solid material to incorporate convection effects. Future studies could explore alternative approaches, such as fire dynamic simulations, to model convection more accurately and simulate plasterboard fall-off by removing plasterboards when a critical temperature threshold is reached.
- Despite significant advancements in heat transfer and structural models, the current analyses rely on sequentially coupled thermo-mechanical simulations. Future research should focus on developing fully coupled models to account for the interdependency between thermal and structural responses in LGS floors.
- It is recommended that the visual observations of fire side sheathing boards are incorporated in numerical modelling to model plasterboard fall-off, instead of the current practice of adjusting the thermal conductivity values.
- The current Eurocode design equations for calculating the plasterboard fall-off time are overly conservative. This study has proposed significantly improved equations and recommends using them along with the provided average failure time values to calculate the FRL of LGS floor systems with two or three layers of gypsum plasterboard.
- Current design methods for LGS floors under standard fire conditions in AS/NZS 4600 provide suitable equations primarily for floor joists subject to local buckling. Further investigation is required to develop design equations for floor joists prone to distortional buckling or local-distortional interaction buckling and floor truss members subject to local buckling in fire.
- It is recommended that short-span fire test is used as an effective alternative to expensive full-scale fire tests for obtaining conservative FRLs and studying the fire behaviour of existing and new floor configurations.
- Short-span and full-scale fire tests of LGS joist and truss floors were conducted at a load ratio of 0.4. Future studies are recommended for different load ratios to confirm the findings of this study. Additionally, the FRLs and fire behaviour were analysed for conventional floor systems. It is suggested that future research investigates the FRLs of innovative ceiling and flooring systems to identify potential improvements in fire resistance.
- In this study, two primary truss types made of top hat and C-section minor axis sections were tested and analysed under ambient and fire conditions. However, future studies can be conducted on other truss types such as C-section major axis trusses, particularly under ambient conditions, as the truss type does not significantly affect fire behaviour.
- The minimum temperatures for plasterboard fall-off were derived from six full-scale fire tests recently conducted in Australia. To obtain more accurate results, additional recent fire test data should be incorporated into the current analysis.

Project #24: Sub-project 2 – Fire resistance of light gauge steel (LGS) floor systems

- This study focused on the mechanical properties of conventional sheathing materials such as gypsum plasterboard and fibre cement board. Future research is recommended to determine the mechanical properties of novel ceiling and flooring materials such as Sureboard, composite floor panels, and geopolymer concrete panels.
- Top hat trusses were investigated using short-span tests to study the complex behaviour of lip cut web members under ambient conditions. Full-scale top hat trusses, which contain more web members, could be investigated under both ambient and fire conditions.
- The floor trusses in this study were analysed using conventional methods, where the web-to-chord connections were assumed as pinned. A more robust design approach that considers the stiffness of connections between trusses and sheathing and trusses is useful.
- No connection failures were observed during the tests, and thus connection failure was not considered in the analysis. It is recommended that advanced models are developed by explicitly modelling the connections to study potential connection failure scenarios.
- The use of a composite floor made of a corrugated steel sheet deck and concrete provided a 32% increase in failure time compared to fibre cement panel flooring. It is recommended that further experimental and numerical studies are undertaken to investigate the composite behaviour of this type of floor system in fire.
- It is recommended that the new floor configurations consisting of reduced number of gypsum plasterboard layers and new AAC panels are investigated further using full-scale fire testing and cost evaluations.

REFERENCES

Abeysiriwardena, T., & Mahendran, M. (2022). Numerical modelling and fire testing of gypsum plasterboard sheathed cold-formed steel walls. *Thin-Walled Structures*, *180*(109792), 19. https://doi.org/https://doi.org/10.1016/j.tws.2022.109792

American Iron and Steel Institute, W., D.C. (2012). North American Standard for Cold-Formed Steel Framing – Truss Design, 2012 Edition. In (pp. 59).

Ardanuy, M., Claramunt, J., & Dias, R. (2015). Cellulosic fiber reinforced cement-based composites: A review of recent research. *Construction and Building Materials*, *79*, 115-128. https://doi.org/http://dx.doi.org/10.1016/j.conbuildmat.2015.01.035

Ariyanayagam, A. D., & Mahendran, M. (2019). Influence of cavity insulation on the fire resistance of light gauge steel framed walls. *Construction and Building Materials*, *203*, 687-710. https://doi.org/https://doi.org/10.1016/j.conbuildmat.2019.01.076

Australia, S. (2017). Gypsum linings-Application and finishing. In *AS/NZS 2589:2017*.

Australia, S. (2020). AS/NZS 2908.2 Cellulose-cement products. In *Part 2: Flat sheets*: Standards Australia and Standards New Zealand.

Baleshan, B. (2012). *Numerical and experimental studies of cold-formed steel floor systems under standard fire conditions* Queensland University of Technology].

Baleshan, B., & Mahendran, M. (2016). Numerical study of high strength LGS floor systems in fire. *Thin-Walled Structures*, *101*, 85-99.

Benichou, N., Sultan, M. A., MacCallum, C., & Hum, J. (2001). Thermal properties of wood, gypsum and insulation at elevated temperatures. *Internal Rep. IR-710, Institute for Research in Construction—National Research Council of Canada, Ottawa, Canada*.

de Seixas Leal, L. A. A., & de Miranda Batista, E. (2020). Experimental investigation of composite floor system with thin-walled steel trussed beams and partially prefabricated concrete slab [Article]. *Journal of Constructional Steel Research*, *172*, Article 106172. https://doi.org/10.1016/j.jcsr.2020.106172

Dias, Y., Keerthan, P. & Mahendran, M. Fire performance of steel and plasterboard sheathed non-load bearing LGS walls, Fire Safety J 103 (2019) 1–18.

Dizdar, Ç., Baran, E., & Topkaya, C. (2019). Strength and stiffness of floor trusses fabricated from cold-formed steel lipped channels [Article]. *Engineering Structures*, *181*, 437-457. https://doi.org/10.1016/j.engstruct.2018.12.041

Dodangoda, M.T. Improving the fire resistance of cold-formed steel frame wall systems using enhanced plasterboards, PhD thesis, Queensland University of Technology, Australia, 2018.

Dodangoda, M. T., Mahendran, M., Keerthan, P., & Frost, R. L. (2019). Developing a performance factor for fire rated boards used in LGS wall systems. *Fire Safety Journal*, *109*, 102872. https://doi.org/https://doi.org/10.1016/j.firesaf.2019.102872

Frangi, A., Schleifer, V., Fontana, M., & Hugi, E. (2008). Fire performance of gypsum plasterboards. Proceedings of the fifth International Conference Structures in Fire: SiF 2008, Nanyang Technological University, Singapore, 28-30 May, 2008,

Gardner, L., & Yun, X. (2018). Description of stress-strain curves for cold-formed steels. *Construction and Building Materials*, *189*, 527-538. https://doi.org/10.1016/j.conbuildmat.2018.08.195

Gnanachelvam, S., Ariyanayagam, A., Mahendran, M. (2019) Fire resistance of light gauge steel framed wall systems lined with PCMplasterboards, Fire Safety J 108, 102838 (2019).

Güldür, H., Baran, E., & Topkaya, C. (2021). Experimental and numerical analysis of cold-formed steel floor trusses with concrete filled compression chord. *Engineering Structures*, *234*, 111813. https://doi.org/https://doi.org/10.1016/j.engstruct.2020.111813

Gunalan, S. and Mahendran, M. (2013) Finite Element Modelling of Load Bearing Cold-formed Steel Wall Systems under Fire Conditions, Engineering Structures, Vol.56, pp.1007-1027.

Gunalan, S., Kolarkar, P., Mahendran, M. (2013) Experimental study of load bearing cold-formed steel wall systems under fire conditions, Thin Wall Struct 65 (2013) 72-92.

Hisham, F. (2025). *Fire Resistance of LGS Floor Systems Made of Lipped Channel Joists* Queensland University of Technology].

Jatheeshan, V. (2015). *Numerical and experimental studies of cold-formed steel floor systems made of hollow flange section joists in fire* Queensland University of Technology].
Jatheeshan, V., & Mahendran, M. (2015). Experimental Study of Cold-Formed Steel Floors Made of Hollow Flange Channel Section Joists under Fire Conditions. *Journal of Structural Engineering*, *142(2)*, 14.
Just, A. (2010). *Structural fire design of timber frame assemblies insulated by glass wool and covered by gypsum plasterboards*. TUT Press Minsk, Belarus.
Just, A., Schmid, J., & König, J. (2010). Gypsum plasterboards used as fire protection-Analysis of a database. In.
Kankanamge, N., & Mahendran, M. (2011). Mechanical properties of cold-formed steels at elevated temperatures. *Thin-Walled Structures*, *49*, 26-44. https://doi.org/10.1016/j.tws.2010.08.004
Karki, D., Far, H., & Nejadi, S. (2024). Structural Behavior of Prefabricated Composite Cold-Formed Steel and Timber Flooring Systems. *Journal of Structural Engineering*, *150*(7), 18. https://doi.org/ 10.1061/JSENDH.STENG-12382
Keerthan, P., & Mahendran, M. (2012). Numerical modelling of non-load-bearing light gauge cold-formed steel frame walls under fire conditions. *Journal of Fire Sciences*, *30*, 375-403. https://doi.org/10.1177/0734904112440688
Konig, J., & Walleij, L. (2000). Timber frame assemblies exposed to standard and parametric fires. *Part 2: A Design Model for Standard Fire Exposure*, 76-76.
Kraudok, K. (2015). Protective effect of gypsum plasterboards for the fire design of timber structures. In: Tallinn University of Technology, Tallinn, Estonia.
Kyvelou, P., Gardner, L., & Nethercot, D. A. (2018). Finite element modelling of composite cold-formed steel flooring systems. *Engineering Structures*, *158*, 28-42. https://doi.org/https://doi.org/10.1016/j.engstruct.2017.12.024
Lim, W. W. (2025). Moment capacity of cold-formed steel trusses with Howick Rivet Connectors: Tests, modelling and design. Engineering Structures, 322.
Limited, S. A. (2014). Methods for fire tests on building materials, components and structures. In *Part 4: Fire resistance tests for elements of construction*: Standards Australia.
LTD, S. A. (2018). AS/NZS 4600:2018. In *Cold formed steel structures* (pp. 196).
Magarabooshanam, H. (2020). *Fire Performance of Complex Light Gauge Steel Framed Wall Systems* Queensland University of Technology].
National Construction Code (NCC). (2022). (2.1 ed., Vol. 3).
Peiris, M., & Mahendran, M. (2022). Advanced numerical modelling of light-gauge steel framed walls subject to eccentric compression. *Engineering Structures*, *256*. https://doi.org/https://doi.org/10.1016/j.engstruct.2022.114063
Peiris, M., & Mahendran, M. (2023). Numerical modelling of LGS walls under combined compression and bending actions and fire conditions. *Thin-Walled Structures*, *182*(110132). https://doi.org/https://doi.org/10.1016/j.tws.2022.110132
Ranasinghe, G. (2025). *Behaviour and Design of LGS Truss Floor-Ceiling Systems under Ambient and Fire Conditions* Queensland University of Technology].
Ranasinghe, G., Mahendran, M., Ariyanayagam, A., & Vy, S. T. (2025). Experimental and numerical studies of LGS truss floor-ceiling systems under standard fire conditions. *Thin-Walled Structures*, *113883*.
Ranasinghe, G., Vy, S. T., Mahendran, M., & Ariyanayagam, A. (2025). Experimental study of LGS truss floor-ceiling systems made of top hat sections. *Thin-Walled Structures*, *212*.
Ranawaka, T., & Mahendran, M. (2009). Experimental study of the mechanical properties of light gauge cold-formed steels at elevated temperatures. *Fire Safety Journal*, *44*, 219-229.
Richardson, L. R. (2001). Thoughts and observations on fire-endurance tests of wood-frame assemblies protected by gypsum board. *Fire and materials*, *25*(6), 223-239.
Rokilan, M., & Mahendran, M. (2020). Elevated temperature mechanical properties of cold-rolled steel sheets and cold-formed steel sections *Journal of Constructional Steel Research*, *167*, 105851. https://doi.org/https://doi.org/10.1016/j.jcsr.2019.105851
Steau, E., & Mahendran, M. (2020a). Fire resistance behaviour of LGS floor-ceiling configurations. *Thin-Walled Structures*, *156*. https://doi.org/10.1016/j.tws.2020.106860

Steau, E., & Mahendran, M. (2020b). Thermal modelling of LGS floor-ceiling systems with varying configurations [Article]. *Fire Safety Journal*, *118*, Article 103227. https://doi.org/10.1016/j.firesaf.2020.103227

Steau, E., & Mahendran, M. (2021a). Elevated Temperature Thermal Properties of Fire Protective Boards and Insulation Materials for Light Steel Frame Systems. *Journal of Building Engineering*, *43*, 102571.

Steau, E., & Mahendran, M. (2021b). Elevated temperature thermal properties of fire protective boards and insulation materials for light steel frame systems. *Journal of Building Engineering*, *43*, 20. https://doi.org/https://doi.org/10.1016/j.jobe.2021.102571

Sultan, M. (2008). Gypsum Board Performance in Fire Rated Floor Assemblies. In. National Research Council, Canada.

Sultan, M., Latour, J., Leroux, P., Monette, R., Seguin, Y., & Henrie, J. (2005). *Results of Fire Resistance Tests on Full-Scale Floor Assemblies–Phase II*.

Sultan, M., Seguin, Y. P., & Leroux, P. (1998). *Results of Fire Resistance Tests on Full-Scale Floor Assemblies*.

Sultan, M. A. (2008). Fire Resistance of Wood Joist Floor Assemblies. *Fire Technology*, *44*(4), 383-417. https://doi.org/10.1007/s10694-007-0038-0

Sultan, M. A. (2015). Fire Resistance of Wood Truss Floor Assemblies. *Fire Technology*, *51*(6), 1371-1399. https://doi.org/10.1007/s10694-012-0311-8

Sultan, M. A., & Roy-Poirier, A. (2007). Gypsum Board Fall-Off Temperature in Floor Assemblies Exposed to Standard Fires. 11th InterNational fire science & engineering conference,

Sultan, M. A., Séguin, Y. P., & Leroux, P. (1998). *Results of Fire Resistance Tests on Full-Scale Floor Assemblies*.

Thomas, G. (2002). Thermal properties of gypsum plasterboard at high temperatures. *Fire and materials*, *26*(1), 37-45.

Tian, H. W., Li, Y. Q., & Yu, C. (2015). Testing of steel sheathed cold-formed steel trussed shear walls [Article]. *Thin-Walled Structures*, *94*, 280-292. https://doi.org/10.1016/j.tws.2015.04.009

Tian, L.-m., Kou, Y.-f., Hao, J.-p., & Zhao, L.-w. (2019). Flexural performance of a lightweight composite floor comprising coldformed steel trusses and a composite mortar slab. *Thin-Walled Structures*, *144*(106361). https://doi.org/https://doi.org/10.1016/j.tws.2019.106361

Vy, G. R. M. M. S. T., & Ariyanayagam, A. (2025). Numerical modelling of LGS truss floor-ceiling systems made of top hat sections. *Journal of Constructional Steel Research*, *234*.

Vy, S. T., Mahendran, M., & Ariyanayagam, A. (2024). Numerical modelling and investigation of CFS built-up stud walls in fire. *Fire Safety Journal*, *144*(104102), 0379-7112. https://doi.org/https://doi.org/10.1016/j.firesaf.2024.104102

Ye, J., Chen, W., & Wang, Z. (2017). Fire-Resistance Behavior of a Newly Developed Cold-Formed Steel Composite Floor. *Journal of Structural Engineering*, *143*(6), 04017018. https://doi.org/10.1061/(ASCE)ST.1943-541X.0001744

info@building40crc.org
www.building4pointzero.org
/building-4-0-crc